

Three-dimensional Stem Cell Aggregates for Cartilage Tissue Engineering

By

BanuPriya Sridharan

B. Tech., Bioengineering, SASTRA University, India, 2010

Submitted to the Bioengineering program and the
Graduate Faculty of the University of Kansas
in partial fulfillment of the requirements for the degree of
Doctor of Philosophy

Committee members

Dr. Michael Detamore, Committee Chair

Dr. Cory Berkland

Dr. Arghya Paul

Dr. Lisa Stehno-Bittel

Dr. Donna Pacicca

July 31, 2015

Date defended

The Dissertation Committee for BanuPriya Sridharan certifies that this is the approved version of the following dissertation:

Three-dimensional Stem Cell Aggregates for Cartilage Tissue Engineering

Committee chair

Dr. Michael Detamore, Committee Chair

July 31, 2015

Date approved

ABSTRACT

Osteoarthritis is the degradation of the knee cartilage within the joints that is often painful and can be debilitating and affect movement, thus impacting the overall quality of life. Current approved treatment methods include microfracture, autologous chondrocyte implantation (ACI) and osteochondral autograft transfer system (OATS). Tissue engineering approaches that are still under clinical trials include naturally derived or synthetic biocompatible scaffolds that possess good mechanical properties, or minimally manipulated devices like decellularized juvenile cartilage that are yet to demonstrate long-term benefits. Using the therapeutic potential of undifferentiated stem cells not only provides a sustainable and long-term approach but also promotes natural healing of the damaged cartilage through biochemical cues. The current thesis work describes the evaluation of 3D stem cell aggregates for the regeneration of the osteochondral interface to overcome some of the limitations posed by the above surgical techniques. *In vitro* and *in vivo* studies were completed to evaluate the performance of aggregates in both a hydrogel system and a rat *in vivo* system. Compared to conventional cell suspensions, aggregates had improved cellular response, biochemical content and higher chondroinductive gene expression. Furthermore, the chondrogenic nature of the aggregate was next investigated as a consequence of cellular media priming and substrate coating. Specifically, ‘raw materials’ such as chondroitin sulfate and aggrecan in the culture medium outperformed growth factors in chondroinductive gene expression and collagen production, thus producing chondromimetic cellular aggregates. *In vivo* studies

demonstrated the feasibility and efficacy of cellular aggregate technology with two different cell densities and combining them with fibrin at the defect site. In the Sprague-Dawley rat knee, implants with higher cell density aggregates received higher morphology scores, better immunohistochemistry staining, and demonstrated the best defect filling compared to the fibrin-alone group. Moreover, this thesis has taken the cell-aggregate technology from an *in vitro* proof of concept study to a translational *in vivo* animal model, thus opening new avenues of investigation for further refinement of the technology. The important next steps will be to characterize the mechanical properties of the scaffolds in an *in vivo* model, and further explore the regenerative-potential of the stem cell aggregates in a large animal model.

ACKNOWLEDGMENTS

I gratefully acknowledge funding from the National Institutes of Health (NIH R01 AR056347), the Kansas Rising Star Award and the State of Kansas Umbilical Cord Matrix Project, and The KU School of Engineering. I would like to acknowledge Drs. Michael Detamore, Cory Berkland, Donna Pacicca, Lisa Stehno-Bittel, and Arghya Paul for serving on my dissertation committee and providing constant guidance and support with my thesis research. I would like to acknowledge other people who helped me learn research methods and molded my technical skills necessary for project completion: Heather Shinogle and Prem Thapa for their training on Dual Beam, SEM, confocal microscopy, and Dr. Richard Galbraith for insightful training on histological techniques and analysis. I thank Dr. Aaron Scurto for access to his laboratory for CO₂-related research, Alan Walker for assistance with developing custom laboratory equipment. I would like to thank Drs., Nicholas Wischmeier, Jeremiah Easley, Ross Palmer, Donna Pacicca, and Vincent Key for their collaborative efforts during *in vivo* studies. A special recognition to the former and current staff at KU Animal Care facility, including Heidi and Allison, and Drs. William Hill and Keith Anderson for assisting with animal surgeries.

I would like to acknowledge all of the effort and assistance from all of the undergraduate research students whom I supervised: Jerrica Washburn, Staphany Lin, Alexander Hwu, Amy Laflin and Mike Holtz. I thank Drs. Lindsey Ott, A.J. Mellott, and Neethu Mohan who motivated me and patiently trained me in my first two years

in the lab. I also thank fellow lab mate Emily Beck for helping me with scientific writing and presentation skills.

I would like to acknowledge the current graduate students in my lab who have been encouraging, helpful and help maintain a great work environment. Special thanks to Peggy Keefe for being a very caring and efficient lab manager.

I am extremely lucky and grateful for having Dr. Michael Detamore as my academic advisor. I would be forever indebted, for his mentorship and guidance on all aspects of my growth and serving as one of the greatest role models on a professional and a personal front. I have had the great opportunity to be trained by him on varied aspects like experimental design, scientific writing, and undergraduate mentorship.

Finally, I want to thank my parents, Sridharan and Usha, my brother, Adhithyaa, my well-wishers, my extended family and friends for their unconditional love and support, throughout this academic journey.

TABLE OF CONTENTS

ACCEPTANCE PAGE	ii
ABSTRACT	iii
ACKNOWLEDGMENTS	v
TABLE OF CONTENTS	vii
LIST OF FIGURES	x
LIST OF TABLES	xii
CHAPTER 1: Introduction	1
CHAPTER 2: A Roadmap to Commercialization of Cartilage Therapy in the United States of America	5
ABSTRACT.....	5
INTRODUCTION	6
METHODS	8
SURGICAL TECHNIQUES	8
CHOICE OF COMPARATOR GROUP	11
CURRENT TRANSLATIONAL TECHNIQUES	12
Devices.....	14
Injectable drugs.....	16
Biologics	19
ANIMAL STUDY CONSIDERATIONS	24
Large and small animal studies.....	24
FEDERAL REGULATION.....	27
OTHER COMMERCIAL CONSIDERATIONS	31
CONCLUSION.....	32
CHAPTER 3: Short-term Characterization of Microsphere-Based Raw Material Encapsulated Scaffold	35
ABSTRACT.....	35
INTRODUCTION	36
MATERIALS AND METHODS.....	37
Microsphere Fabrication	37
Scaffold Assembly	38
SEM Analysis	39
Dry Weight Analysis	40
Retention of Chondroitin Sulfate in the CS Scaffolds.....	41
Retention of Calcium in the TCP Scaffolds.....	41

Statistical Analyses	42
RESULTS	43
Retention of Chondroitin Sulfate in the CS scaffolds.....	44
Retention of Calcium in the TCP scaffolds	44
Mechanical Testing.....	44
DISCUSSION	45
CONCLUSION.....	48

CHAPTER 4: Stem Cells in Aggregate Form to Enhance Chondrogenesis in

Hydrogels.....	50
ABSTRACT.....	51
INTRODUCTION	51
MATERIALS AND METHODS.....	52
Cell culture and expansion.....	54
Cell aggregate formation	54
Encapsulation of cells in hydrogels	55
Cell viability assay.....	56
Biochemical assay.....	57
Gene expression assay	58
Immunohistochemistry	59
RESULTS	60
Live-dead assay.....	60
DNA content	61
GAG assay	62
Collagen assay	63
Gene expression analysis	65
Immunohistochemistry	72
DISCUSSION.....	72
CONCLUSION.....	75

CHAPTER 5: Generating Chondromimetic Mesenchymal Stem Cell Spheroids by Regulating Media and Substrate Coating

ABSTRACT.....	77
INTRODUCTION	78
MATERIALS AND METHODS.....	79
Cell Expansion and Seeding	80
Cell aggregate formation (all the groups).....	81
Biochemical Analyses.....	83
Quantitative Polymerase Chain Reaction	84
Immunohistochemical Staining	85
Statistical Analyses	86
RESULTS	86
Cell viability of the aggregates at different time points.....	86
DNA content	87

GAG content	87
Collagen content	88
Gene expression analysis	89
Immunohistochemistry staining.....	92
DISCUSSION.....	93
CONCLUSION.....	96

CHAPTER 6: *In Vivo* Evaluation of Stem Cell Aggregates on Osteochondral

Regeneration.....	97
ABSTRACT.....	97
INTRODUCTION	98
MATERIALS AND METHODS.....	100
Cell harvest and cell culture.....	101
Cellular aggregate preparaion.....	102
Description of experimental groups.....	102
Surgical procedure	102
Post-surgical care.....	103
Morphological assessment of retrieved implants.....	103
Histological preparation and staining	104
Immunohistochemistry	105
Statistical analyses	106
RESULTS	107
Gross morphological observations.....	107
Histomorphometric observations	107
DISCUSSION	111
CONCLUSION.....	114

CHAPTER 7: Conclusion

APPENDIX A: Figures.....

APPENDIX B: Tables.....

LIST OF FIGURES

CHAPTER 1

No Figures

CHAPTER 2

Figure 2.1: Translation of devices & stem cell products 150

CHAPTER 3

Figure 3.1: SEM micrographs of the different groups 151

Figure 3.2: Dry weight and molecular weight of the scaffolds 152

Figure 3.3: CS and TCP retention in scaffolds 153

Figure 3.4: Compressive elastic moduli at different time points 154

CHAPTER 4

Figure 4.1: Schematic representation of the hanging drop approach 155

Figure 4.2: Cell viability of the rBMSC aggregates 156

Figure 4.3: Cell viability of the hWJC aggregates 157

Figure 4.4: DNA content for all of the scaffolds 158

Figure 4.5: GAG content for all of the scaffolds 159

Figure 4.6: Collagen content for all of the scaffolds 160

Figure 4.7: Gene expression for all of the rBMSC groups 162

Figure 4.8: Gene expression for all of the hWJC groups 164

Figure 4.9: Immunohistochemistry for all of the rBMSC groups 165

Figure 4.10: Immunohistochemistry for all of the hWJC groups 166

CHAPTER 5

Figure 5.1: Schematic representation of the experimental design 167

Figure 5.2: Cell viability of the aggregates at different time points 168

Figure 5.3: DNA content for all of the groups 169

Figure 5.4: Normalized GAG content for all of the groups 170

Figure 5.5: Normalized collagen content for all of the groups 171

Figure 5.6: Gene expression analysis for all of the groups 172

Figure 5.7: Representative IHC for the study 173

CHAPTER 6

Figure 6.1: Schematic representation of the surgical procedure 174

Figure 6.2: Experimental design and surgery photos 175

Figure 6.3: Gross morphological images of the different groups 176

Figure 6.4: Morphological assessment of the rat knees 177

Figure 6.5: Histology and IHC for Group A implants 178

Figure 6.6: Histological score distribution plots 179

Figure 6.7: Histology and IHC for Group B implants 180

Figure 6.8: Histology and IHC for the Fibrin-alone implants.. ..	181
Figure 6.9: Histology and IHC for the sham surgeries.. ..	182
Figure 6.10: Dual-beam microscopic image of the defect area.	183

CHAPTER 7

No Figures

LIST OF TABLES

CHAPTER 1

No Tables

CHAPTER 2

Table 2.1: List of abbreviations.	186
Table 2.2: List of devices under clinical trials	187
Table 2.3: List of biological products under clinical trials	188
Table 2.4: List of drug products under clinical trials.....	189
Table 2.5: Common inclusion and exclusion criteria for clinical trials	190
Table 2.6: FDA approval pathways	192

CHAPTER 3

Table 3.1: List of experimental groups and their abbreviations	193
--	-----

CHAPTER 4

Table 4.1: List of experimental groups used in the study	194
Table 4.2: Summary of the best performing groups	195

CHAPTER 5

Table 5.1: List of experimental groups	196
Table 5.2: Summary of the best performing groups for each assay	197
Table 5.3: List of antibodies and dilutions used for immunohistochemistry.....	198

CHAPTER 6

Table 6.1: List of primary antibodies.....	199
Table 6.2: Scoring card for morphological analysis	200
Table 6.3: Histology scoring parameters	201
Table 6.4: Animal ID and weight of each animal	202

CHAPTER 7

No Tables

CHAPTER 1: Introduction

The overall objective of my dissertation was to introduce and evaluate the cartilage regenerative potential of three dimensional mesenchymal stem cell aggregates. The overall plan was to start with a completely material-only approach, transition to hydrogel encapsulated cell aggregates that are further refined, and to finally test the aggregates with fibrin alone in a rat knee defect model. To look at both material-based strategies and also perform an in-depth analysis of the stem cell aggregates, the thesis design included three corresponding aims: (1) characterization of acellular microsphere-based scaffolds with raw materials encapsulated (2) biofabrication and *in vitro* analyses of stem cell aggregates encapsulated in hydrogels, further refined by media priming and substrate stiffness (3) preliminary *in vivo* testing of two different cell density aggregates in a rat trochlear knee defect model.

The first aim was to characterize the degradation of raw material encapsulated microsphere-based scaffolds fabricated by a well-established technology from the research group. The second aim was to develop a platform technology to fabricate stem cell aggregates from different cell sources, rat bone marrow mesenchymal stem cells (rBMSC) and human umbilical cord Wharton's Jelly cells (hWJC), encapsulate the aggregates in an agarose hydrogel model and test the chondrogenic properties over a period of three weeks. The second part of second aim was to further refine the aggregates alone by testing the chondroinductive properties of the rBMSC aggregates that are grown under different media formulation (growth factor and raw materials) and substrate stiffness induced by hyaluronic-acid coated plates. The third aim tested the feasibility of the aggregates sealed with fibrin, when implanted in a rat trochlear groove defect model. The progression of the chapters is as follows:

Chapter 2 provides a background on the current commercialization environment for cartilage tissue engineered products in the United States. This chapter covers the different treatment options, specific examples of devices, biologics, and injectable drugs and associated federal regulations. It provides a brief overview of animal models for cartilage regeneration and other considerations to keep in mind for establishment of clinical studies. The knowledge gained from Chapter 2 inspired the pursuit of both material-based (microsphere scaffolds) and cell-based (stem cell aggregates) approaches toward a common goal of osteochondral tissue engineering.

Chapter 3 addresses the first aim, i.e., the characterization of acellular homogenous raw material encapsulated microsphere-based scaffolds. Two different types of PLGA were encapsulated with chondroitin sulfate (CS) and β -tricalcium phosphate (TCP) and the scaffolds were characterized for dry weight, molecular weight, CS and TCP retention in scaffolds, and mechanical properties, over a period of four weeks. The results of this study provided insight into degradation properties of raw-material encapsulated scaffolds that can be utilized in the study design for future *in vivo* experiments.

Chapter 4 addresses the second aim by introducing the first full-scale study in which the cellular aggregates were fabricated from two different cell sources (rBMSCs and hWJCs). Secondly, the aggregates were encapsulated in a 3% agarose hydrogel system with different aggregates per scaffold and different cell density/aggregate and were compared to conventional cell suspension group. Testing parameters included cell viability, biochemical assays, gene expression and immunohistochemistry. The high cell density aggregates outperformed the cell suspension groups in terms of aggrecan gene expression and GAG production, thus providing insight into the differences between rBMSC and hWJC cell sources for aggregate applications.

The results from this study established a platform technology for aggregate fabrication and encouraged the idea behind the successive studies.

Chapter 5 further addresses the second aim with an objective to generate chondromimetic rBMSC cell spheroids that are cultured on surfaces with different stiffness and primed under varied media compositions for a period of one week. Cell viability, biochemical assays, gene expression, and immunohistochemistry data was evaluated as a function of aggregates under different growth factor and raw material-composed media and under different surface stiffness.

Chapter 6 addresses the third and final aim of evaluating the rBMSC aggregates in a rat *in vivo* model. Critical sized defects were created in the trochlear groove of Sprague-Dawley rats and implanted with aggregates of two different cell densities evaluated for a period of 8 weeks. After sacrificing the animal at 8 weeks, immunohistochemistry was performed to assess cartilage tissue regeneration.

Chapter 7 serves as a summary of my thesis work, and highlights common trends observed from the different projects. Recommendations for future experiments and studies are made based on informed observations from conducted studies. The work within this thesis proposes a novel approach for treating focal cartilage lesions, by means of presenting cells in a three-dimensional aggregate manner. Currently, autologous chondrocyte implantation (ACI) is the only FDA-approved cell-based therapy in the United States. Although there are several new upcoming approaches widely discussed in Chapter 2, the major limitations are multiple surgeries and the time taken from diagnosis to treatment. Utilizing allogeneic cellular aggregates is an attractive solution that addresses donor site morbidity and presents a readymade solution without a significant time delay. Throughout the thesis, the aggregate technology is constantly compared

with the conventional two dimensional cell suspensions approach to demonstrate relative performance.

CHAPTER 2: A Roadmap to Commercialization of Cartilage Therapy in the United States of America¹

ABSTRACT

Despite numerous efforts in cartilage regeneration, few products see the light of clinical translation, as the commercialization process is opaque, financially demanding, and require collaboration with people of varied skill sets. The aim of this review is to introduce, to an academic audience, the different paradigms involved in the commercialization of cartilage regeneration technology, elucidate the different hurdles associated with the use of cells and materials in developing new technologies, discuss potential commercialization strategies, and inform the reader about the current trends observed in both the clinical and laboratory setting for establishing clinical trials. Although there are review articles on articular cartilage tissue engineering, independent reports provided by the Food and Drug Administration (FDA), and separate review articles on animal models, this is the first review that encompasses all of these facets and is presented in a format favorable to the academic investigator interested in clinical translation from bench to bedside.

¹ In Press as **Sridharan B**, Sharma B, Detamore MS, “A roadmap to commercialization of cartilage therapy in the United States of America,” Tissue Engineering Part B, 2015

INTRODUCTION

Cartilage defects of the knee range from cartilage lesions and osteochondritis dissecans to debilitating grade III or IV osteoarthritis (OA; see Table 2.1 for listing of abbreviations), and result in more than 200,000 surgical procedures annually^{23, 50, 162}. Current surgical treatment paradigms range from microfracture for initial impact injuries to total knee replacement in advanced cases; however, there are no universally agreed-upon solutions that have unequivocally been shown to regenerate fully structural and functional cartilage^{28, 96, 204, 212, 233}. Specialized surgical treatments, such as autologous chondrocyte implantation (ACI), have emerged over the past few decades and have often been used among younger patients. However, ACI has not been as successful for long-term treatment of older patients^{53, 200}. Microfracture is the established standard of care for focal cartilage defect repair and is commonly used as a comparator group in clinical trials with devices and autologous grafts.^{90, 268} Academic tissue engineering solutions endeavoring to restore and repair cartilage have traditionally used the triad approach (cells, biomaterials, and bioactive factors) with common materials such as polycaprolactone (PCL), poly(ethylene glycol) (PEG)-based materials, poly(lactic-co-glycolic acid) (PLGA), agarose, chitosan, collagen, and hyaluronic acid, which have all been employed in other products that have been FDA approved.^{36, 89, 148} Different sources of cells, such as chondrocytes, bone marrow mesenchymal stem cells, adipose-derived stem cells, and cells derived from the umbilical cord have been employed in efforts to differentiate these cells toward a chondrocyte-like phenotype using polymeric substrate adherence, novel cell culture media, growth factors, and/or gene therapy.^{92, 103, 199, 206} Over the years, biomaterials strategies have evolved from a single polymeric substrate to superior hierarchical matrices that mimic the native tissue and attempt to enable directed differentiation²²². Recently, ‘raw materials’²⁰⁹ such as cartilage matrix^{42, 88, 240} (including

decellularized cartilage (DCC)^{238, 242}) and demineralized bone matrix (DBM) have been used directly or combined with other biomaterials to create hybrid materials that provide biochemical and mechanical cues for the cells to differentiate.^{224, 241, 245} Some of the current products that employ this technology are DeNovo NT from Zimmer^{77, 78} and DeNovo® ET (Engineered Tissue Graft) from ISTO technologies, which obtained special rights and permission from Zimmer^{107, 247}. Both products employ juvenile decellularized cartilage with a combination of cells and materials to treat cartilage lesions. BioCartilage from Arthrex¹ employs micronized allogeneic cartilage to treat osteochondral lesions.

Despite so many new innovative approaches and technologies that address articular cartilage regeneration, there are very few FDA approved products and only a handful of products currently in clinical trials¹⁵⁵ (Tables 2.2, 2.3, and 2.4). Unfortunately, academic training does not typically provide a clear picture of the various steps involved in therapeutic product design, development, registration, and launch³⁹. A thorough understanding of the challenges in translation, restrictions due to government regulations, funding opportunities, and overall study design is of paramount importance to help academics think about product development while designing hypothesis-driven research, proposing innovative and novel strategies, designing animal studies with the final clinical study in mind, and understanding the cost-benefit ratio in every step of the process to enable a smoother transition from pre-clinical animal studies to human clinical studies. Review papers have done an excellent job in covering various facets of cartilage regeneration in depth, such as animal models^{49, 111, 151}, FDA regulations^{141, 166} osteochondral scaffolds for cartilage tissue engineering^{39, 196, 201, 223, 250} challenges of stem cell technology,^{53, 121, 123, 199} product legislation in other countries,²⁰⁵ hurdles and general trends in

biomaterial commercialization.^{20, 58, 84, 87, 144, 263} However, the current review endeavors to classify the different categories of tissue-engineered products and their relative benefits and challenges associated with specific product examples. Secondly, we also discuss different animal models, inclusion and exclusion criteria for clinical studies, primary and secondary endpoint analyses, and a standard set of FDA recommendations. Thirdly, we aim to give the reader a brief introduction into other commercialization considerations to keep in mind before launching into translation. Finally, the current review aims to introduce a product development-based perspective to the academic investigator in anticipation of future healthcare commercialization. Therefore, building on other outstanding reviews, the current review fills a gap in the literature to provide a roadmap to commercialization for academic investigators to translate their cartilage regeneration technologies.

METHODS

A review of all of the tissue engineered and industrial products, inclusion and exclusion criteria, and FDA approval status was performed using clinicaltrials.gov with the search terms “articular cartilage” and “osteoarthritis” in March 2015 to determine the current status of active clinical trials for cartilage repair treatments. Additionally, the corresponding company’s website was also reviewed for additional product information. FDA guidance documents, clinical trial recommendations by the International Cartilage Repair Society (ICRS), and large animal study manuscripts for cartilage repair were reviewed and cited accordingly.

SURGICAL TECHNIQUES

Three common surgical procedures are utilized to address OA or cartilage degeneration. The first procedure, microfracture, is a marrow stimulation technique, whereby a full thickness chondral defect is created, including removal of calcified cartilage, followed by puncturing the underlying subchondral bone with a drill or awl to create small holes for bone marrow constituents, including MSCs, to fill the defect.^{8, 118} The resulting tissue is less durable, less organized, and has a higher quantity of collagen type I than normal articular cartilage.¹⁹² Poor clinical outcomes from microfracture have been associated with inadequate filling of defect with repair tissue and osseous overgrowth.^{29, 176} Good outcomes are typically limited to young patients (<40 years with small lesions (<2 cm²), low body mass indexes, and acute onset of symptoms.¹⁷⁸ Otherwise, clinical results are highly variable. Approaches to improve the repair process initiated by microfracture are being actively explored. BioCartilage from Arthrex (Naples, FL), employed frequently with platelet rich plasma (PRP),¹ and another approach by Milano *et al.* from Catholic University (Rome)¹⁷³ have both employed microfracture in combination with their scaffold and are comparing that with a scaffold-only approach (i.e., without microfracture) to evaluate the complementary effect of microfracture. The final data from the BioCartilage study are expected to be available in June 2016. The importance of microfracture as an emerging comparator group in clinical studies will be discussed in the next section.

The second procedure is mosaicplasty, or osteochondral autograft transfer, which involves surgical transfer of mature autologous or cadaveric tissue from a non-load-bearing region to a cartilage defect.^{104, 248} While this relatively inexpensive reparative technique has helped to serve the growing need for cartilage repair, grafting is a suitable option only for small (< 2 cm²) to

medium-sized (3-5 cm²) defects;^{82, 105} with time, patients seem to develop symptoms attributable to the donor area, thus reducing the overall effectiveness of this technique.¹⁰⁵ In addition to donor-site morbidity, the technically challenging autologous procedure adds complexity for the surgeon and requires longer operating times.

The third and most widely used procedure is autologous chondrocyte implantation (ACI). ACI is a two-step procedure wherein chondrocytes are harvested arthroscopically from healthy cartilage and expanded *in vitro* before reimplantation through a second, more invasive surgery that requires a periosteal flap to be harvested from the patient that must be sutured to the cartilage surface to keep the cells in place. ACI is technically challenging, costly, requires two surgeries, must receive health insurance approval, and has been associated with high reoperation rates.^{16, 133} Several modifications to ACI have been introduced. The most popular is the matrix-induced ACI (MACI), which involves implantation of *in vitro* expanded chondrocytes in a suitable matrix, which is then fixed in the defect area using fibrin glue and/or sutures.⁹¹ This does not refer to the Sanofi biosurgery registered MACI® product. Several papers have evaluated side-by-side performance of ACI, microfracture, and mosaicplasty over long periods^{65, 96, 170} and have produced recommendations factoring in the age and nature of cartilage injury (stage of OA and size of the lesion). In one study, both MF and OATS showed encouraging clinical results for athletes under the age of 40 with the OATS group producing slightly increased results over MF, assessed over a period of 37.1 months.⁹⁷ Gudas *et al.*⁵ compared the effect of MF, OATS, ACI, and debridement in articular cartilage lesions associated with ACL injuries and a 3-year follow-up. Pain scores revealed that intact articular cartilage during ACL reconstruction yields more favorable IKDC subjective scores compared with any other articular cartilage surgery type.⁹⁶

However, if an articular defect is present, the subjective IKDC scores are significantly better for OATS versus microfracture or debridement after a mean period of 3 years.⁹⁶

The choice of the comparator group is largely dictated by the regulatory requirement for the specific type product. For cell-based products, ACI is the most commonly employed comparator group. The use of ACI as a comparator group is challenging, as it is expensive and logistically demanding, and, consequently, has not been widely adopted. On the other hand, microfracture is a more straightforward procedure and is the most commonly used first-line procedure for cartilage regeneration; it has therefore been a popular choice as a comparator group in clinical trials. However, the defect type and disease state of the joint must be considered to be within the clinical indication for microfracture.

CHOICE OF COMPARATOR GROUP IN CLINICAL TRIALS

Comparator groups for cartilage therapy change according to the treatment modality and include placebo and standard of care groups. FDA guidelines require that experimental groups demonstrate statistically superior primary endpoints of treatment over a current comparator group such as microfracture, debridement, mosaicplasty, and ACI.^{166, 177} Microfracture is the most commonly used comparator group for late-phase clinical trials, as it is inexpensive compared to ACI, easier to perform, and is widely performed throughout the world. However, FDA Guidance also allows ACI as a control group for large defects (greater than 5-7 cm² lesions) where microfracture may not be indicated.^{177, 252} In summary, choosing a comparator group depends on the nature of the defect, the “standard” treatment for the defect type and

disease state of the joint, results of existing or previous clinical studies, and guidance-from FDA/consultants. It is important to note that the recent literature suggests that, for most focal defects of the knee cartilage and small-sized lesions due to impact injuries, microfracture is emerging to be a superior comparator group in light of effective repair tissue formation and availability of uniform instruments with which to perform the surgery throughout the country.

CURRENT TRANSLATIONAL TECHNOLOGIES IN CARTILAGE REPAIR

The following sections will highlight the FDA classification scheme and briefly cover the different approaches (i.e., devices, drugs, and biologics) with current examples in clinical trials and, finally, provide summary of these translational technologies as well as their relative benefits and limitations.

FDA Classification of Cartilage Repair Therapies

Within the FDA, the Center for Devices and Radiological Health (CDRH), the Center for Biologics Evaluation and Research (CBER), and the Center for Drug Evaluation and Research (CDER) are responsible for devices, biologics, and drugs, respectively.¹⁶⁶ The type of classification impacts the number of subjects enrolled, the nature of primary and secondary endpoints, and the implementation period to the market. The duration of a study is also impacted by the nature of control groups, recovery periods, long-term pain evaluation, device performance tracking, and post-market surveillance. Tables 2.2, 2.3, and 2.4 list all of the products either currently in the process of seeking FDA approval, which are classified as device, drug, biologic, or a combination of any of these three, along with a brief product description and their current status.

Most of the devices, biologics, and drugs are classified under section 351 or 361 of the Public Health Service (PHS) Act.⁴⁴ Scaffolds, polymeric constructs, and injectable pastes are likely to fall under the device classification, while stem cell technologies, combinatorial products that employ cells and materials, and incorporation of protein molecules like amino acids and growth factors are most likely going to be treated as a drug or biologic. Given that some cartilage tissue engineering technologies may be considered combination products, any ambiguity in classification can be directed to the Office of Combination Products (OCP). A company must submit a Request for Designation (RFD) to the FDA, which enables the FDA to determine the primary mode of action and to thus decide (within 60 days of RFD filing) the lead agency (CDRH, CBER, or CDER) for premarket review and regulation.

Before using any product for clinical trials, the FDA must approve an investigational device exemption (IDE) for devices or an investigational new drug (IND) for drugs and biologics. It must be noted that CBER may also regulate some devices (e.g., cellular products), in which case the IDE route is followed. In addition to FDA's IDE or IND approval, institutional review board (IRB) approval must be obtained prior to clinical trials, and one should expect that their IRB(s) would require FDA involvement before merely allowing a pilot clinical study. The clinical safety and efficacy data collected with IDE approval for devices are then used for either a Premarket Notification (510(k)) or Premarket Approval (PMA) application, which, if approved, allows the company to sell their device in the United States. The PMA is a longer, more complex, and more costly process than the 510(k). A 510(k) pathway requires that the device to be marketed is "substantially equivalent" (i.e., at least as safe and effective) to a predicate device, which

includes a device that was legally marketed in the US before May 28, 1976, a device that has cleared through the 510(k) process, or devices that have been down-classified from Class III to Class II or Class I. The necessary proof of safety and efficacy is determined predominantly via preclinical studies, though in some cases a clinical study is required. Nearly all Class III medical devices, which include most cartilage repair technologies, require a PMA, which is the most stringent type of device marketing application required by FDA. Unlike a 510(k), a PMA requires clinical studies that will need to demonstrate either non-inferiority or superiority against a control group, the determination of which depends on risk-benefit considerations posed by the product. In some rare cases, evaluation against an objective performance goal or criteria, rather than an active control group, may be appropriate. Clinical trials for PMAs typically consist of a small feasibility/pilot study to determine safety, and a pivotal study to demonstrate efficacy in addition to safety. There are no predicate devices (Class I and II) for most cartilage repair products, therefore, a PMA is required to legally market them. Some devices indirectly related to cartilage repair may be amenable to the 510(k) pathway. In contrast to devices, clinical safety and efficacy data collected with IND approval for biologics and drugs then lead to either a Biologics License Application (BLA) (via CBER) or a New Drug Application (NDA) (via CBER or CDER), respectively, which if approved allow the company to sell their product in the United States.

DEVICES

The CDRH is responsible for the approval of cartilage repair devices including biodegradable scaffolds, osteochondral plugs, and injectable substances that can fill defects. Depending on an RFD, the CDRH may also serve as the lead agency for combination products if the FDA

determines that the primary mode of action is as a device. The two primary routes to acquire FDA approval for medical devices are through a 510(k) or PMA; each of which has different requirements for approval.^{110, 166, 232}

It is important to note that most devices for cartilage application that are currently in clinical trials are from non-US-based companies and/or universities. Notable among them are HYTOP® from TRB Chemida (Germany), Agili C Biphasic Implant from CartiHeal (EU), and BST-CarGel from Piramal Healthcare (Canada).^{78, 134, 225, 232}

According to information found at clinicaltrials.gov, DePuy's Cartilage Autograft Implantation System (CAIS) is a kit of devices that employs morselized autologous cartilage harvested arthroscopically from a non-weight-bearing region, affixed onto a synthetic resorbable implant using fibrin sealant, and implanted in a single surgical procedure. CAIS has just completed Phase 2 clinical trials with microfracture as the comparator group.⁷⁷

HYTOP® is a two-layer bioresorbable matrix consisting of an upper layer of highly purified porcine splint skin and a lower layer of purified collagen fleece containing hyaluronan (HA). The primary working hypothesis is that HYTOP® is safe and suitable as a cell-free matrix to support hemostasis, as a cover for the cartilage lesion and eventually to enhance cartilage regeneration in a one-step surgical procedure. TRB Chemida AG, a German company that is sponsoring the study, utilizes the scaffold in conjunction with cartilage debridement and/or microfracture of the subchondral bone.

The Agili C Biphasic Implant™ is an off-the-shelf cell-free biphasic plug and is CartiHeal's trademarked product used in the treatment of focal articular cartilage and osteochondral defects. The biphasic implant is composed of calcium carbonate in the aragonite crystal form and composed of modified aragonite and hyaluronic acid in the cartilage phase. Holes are drilled into the bottom phase, comprised of coral material, through which the top phase material (hyaluronic acid) is gradually added to initially form a gradient, followed by a controlled deposition to form the desired height.¹³⁵ The product has currently secured approval for use in the European Union market and is running a multi-center post-marketing clinical study (phase IV). As of 2015, the company secured four patents (three in the U.S. and one in Japan) for its proprietary cell-free, off-the-shelf cartilage regeneration technology for patients with injuries to the articular surface of joints.¹³⁴ The product is not currently commercially available in the U.S.

BST-CarGel is a Canadian Piramal Healthcare product that is prepared by mixing chitosan and a buffer to form a liquid-like gel that has scientific evidence for biocompatibility and adherence to tissue. The BST-CarGel, which is fabricated under Canada's certified GMP protocol, is mixed with a patient's own blood and implanted into the surgically prepared defect lesion site. BST-CarGel was found to be safe and effective according to multi-center randomized controlled clinical trials.^{210, 236} According to the company's website, the safety was assessed to be similar to that of microfracture, and results demonstrate greater quantity and quality of repair cartilage.

INJECTABLE DRUGS

According to CDER at the FDA, current cartilage treatments that fall under the "Drugs" category include any modality that delivers compounds that elicit a repair response by a patient's own

joint tissue.¹⁶⁶ By definition, compounds that address cartilage repair and are metabolized, are classified as drugs and injectable forms are also therefore considered a drug.⁴ It should be noted that viscosupplements, such as hyaluronic acid, are considered devices rather than drugs, since their primary mode of action is viscosupplementation and not cartilage repair or metabolic mechanisms.²⁶⁰ Approval of a drug requires a phased approach with separate dosing (phase I), assessment of small-scale safety and effectiveness (phase II), and assessment of large-scale randomized safety and effectiveness (phase III); it therefore imposes more financial and clinical expenditure than the device route. Most of the cases that consult drug treatment are advanced OA and are usually not treatable by the device or biologic paradigm due to the condition of the joint or other reasons. Thus in most cases, drugs represent a palliative treatment paradigm and are usually used to treat advanced OA.

Examples of approved drugs include injectable Synvisc by Genzyme, topical NSAID cream Pennsaid by Nuvo Research, and other steroid-based painkillers that address inflammation, such as Supartz by Smith and Nephew and Mobic by Boehringer Ingelheim. A few drugs in phase III clinical trials include Condrosan by Bioiberica and dextrose injection by Universidad Nacional de Rosario. Condrosan is a prescription drug containing highly purified chondroitin 4- and 6-sulfate of bovine origin in a concentration of not less than 98%. It has an average molecular weight of about 15–16 kDa, and an intrinsic viscosity of about 0.02–0.06 m³/kg, and it has been approved as a prescription treatment for OA in many European countries.²⁶² Some other notable drug treatments include TPX-100 from USA, Condrosan from Spain and Canada, and AS902330 from Geneva.

TPX-100: According to the company's (OrthoTrophix) website, TPX-100 is a 23 amino acid peptide derived from matrix extracellular phosphoglycoprotein (MEPE) and has shown success in cartilage regeneration in large animal models through regulation of hard tissue and phosphate metabolism. TPX-100 is delivered via intra-articular injection, and has shown success in phase I and II trials for dentin regeneration. It is currently under randomized double blind, placebo controlled, multidose phase II trials for treating grade ICRS grade 3,4 bilateral OA with focal defects no greater than 1 cm. There have been no adverse events from previous clinical and non-clinical studies.¹²⁸ Specific cartilage or bone tissue regeneration, lack of ectopic bone formation, promotion of chondroprogenitor cells, and a long-term pharmacodynamics effect make TRX-100 a viable drug option for treating OA.¹⁷¹

Condrosan is a hard capsule of chondroitin sulfate marketed by Bioiberica in Canada and Spain. Publication and clinical studies revealed that Condrosan was found to perform better than Celecoxib, an anti-inflammatory steroid-based pain killer drug,^{202, 262} and reduced cartilage volume loss and marrow lesions in the knee as early as six months after administration.²⁰² Condrosan represents a symptomatic treatment, and future long-term analysis (phase IV) will help to determine efficiency of pain relief for arthritic patients.

AS902330 is a recombinant form of fibroblast growth factor 18 (rhFGF-18) currently in phase II clinical trials, sponsored by Merck KGaA from Geneva. The drug is delivered intra-articularly in the knees of patients with primary OA^{159, 274} and measured for safety, efficacy, and residual AS902330 in blood compared against a placebo. Depicting superior performance over

microfracture for clinically diagnosed stage I OA would be the next step in comparing drug treatment with standard of care.

In summary, drugs vary from steroid injection to anti-inflammatory drugs to hyaluronic acid injections. Since these treatments are mainly pain relieving either directly or indirectly, they often require multiple injections and life-long treatment and can be prohibitively expensive for the retired and elderly population. The drug route through the FDA is typically a longer process to demonstrate safety and efficacy in a large cohort, often with multiple comparator groups.

BIOLOGICS

Products that use growth factors and/or extracellular matrix in conjunction with cells to repair defects typically fall under the biologics or combination product category according to the CBER.¹⁶⁶ Similar to the drug criteria, biologics testing require dosing, safety and efficacy, and large-scale randomized safety and efficacy studies (phase I, II, and III), with each phase requiring an IND approval for commencement in the United States. After phase III, a BLA is submitted to the CBER for review and approval.

Autologous cellular products

Utilizing a patient's own cells to repair osteochondral defects is achieved by an initial biopsy or cell isolation, in which cells are expanded *in vitro* and re-implanted into the defect area.²⁷ Genzyme's Carticel, one of the pioneers that paved the way for this technology, is also FDA-approved and has been used to treat patients since 1995, according to the company's website.¹⁹¹ Briefly, autologous chondrocytes are harvested from two full thickness biopsies (5 x 8 mm) from

the patient from a lesser weight-bearing, non-articulating surface and transported to Genzyme via a Genzyme Biopsy Cartilage Transport Kit. After about 6 weeks, the cells are transported back to the medical center and implantation is performed by a trained CARTICEL® surgeon. The defect region is prepared by damaged tissue debridement and procurement of a periosteal flap. After confirming homeostasis, the cells are re-suspended to the defect region via a catheter and the defect is covered and sutured with fibrin glue and the aforementioned periosteal flap. In general, ACI has favorable reports of regeneration predominantly for a younger population (up to 40 years),^{30, 109} whereas chondroplasty and microfracture are more common and routinely performed with the older age groups (< 40 years).¹⁸⁴

Most cellular products under the biologics designation employ MSCs from bone marrow, adipose tissue, or umbilical cord with a combination of material and/or PRP and are delivered as a patch or injection.^{98, 116} Notable among them are adipose-derived stem cells (ASC) that are isolated from a patient's own fat pad, which can be processed by medium selection and seeded on a collagen dermal matrix with fibrin glue. Such a study is currently recruiting participants in a phase I clinical trial sponsored by Stanford University, with microfracture as the comparator group.^{132, 158}

The University of Marseille in France conducted a pilot (phase 0) study to evaluate the efficacy and safety of scaffolds composed of fresh non-expanded autologous bone marrow-derived mesenchymal mononuclear stem cells, stimulated with a protein matrix and mixed in a collagen hydroxyapatite scaffold. This cellular paste was then transplanted in the prepared defect arthroscopically, with injection of PRP.⁷

Investigators at the University Hospital of Basel in Switzerland, in collaboration with a non-profit organization situated in Germany called Deutsche Arthrose-Hilfe, are currently in phase I clinical trials conducted in Switzerland for evaluating the safety and feasibility of implanting an engineered cartilage graft in the femoral condyle or trochlea of the knee after a traumatic injury with one or two symptomatic lesion(s) of grade III, IV and a defect area between 2 and 8 cm². The graft is obtained by culturing expanded autologous nasal chondrocytes within a collagen type I/III membrane (Chondro-Gide®) into the cartilage defect on the femoral condyle and/or trochlea of the knee after a traumatic injury.²⁰³ According to clinicaltrials.gov, it was found that the current study was a phase I, prospective, uncontrolled, investigator-initiated clinical trial involving 25 patients.

Allogeneic cellular products

Allogeneic products use human donor cells and tissues to repair damaged cartilage, thereby reducing the need for a primary biopsy, reducing donor site morbidity, and allowing for a one-step procedure. Allogeneic products include morselized tissue and transgenic cells engineered to secrete growth factors,^{18, 165} although some of the donor tissues, which are minimally manipulated, are regulated as an organ transplant and not as a biologic.

CARTISTEM®, a product developed by Medipost Co. Ltd., has currently completed phase III clinical trials in the United States, and was approved for clinical use by the Korean FDA (KFDA). According to the company's website, CARTISTEM® contains selectively grown MSCs from allogeneic umbilical cord blood, mixed with sodium hyaluronate, and delivered at

the cartilage defect region, although it is unclear from available sources how the solution stays in the defect. The inclusion criteria for the study include patients with cartilage lesions between 2 and 9 cm² in area. The intervention by allogeneic treatment is being compared in clinical trials with microfracture. The Korean's government approved the usage of CARTISTEM® as an off-the-shelf, stem cell drug manufactured according to GMP standards.^{261, 266} The long-term efficacy of the drug treatment is the next question the company will be addressing through phase IV clinical trials.

TG-C, sponsored by TissueGene, Inc., is currently in phase II clinical trials in the United States and in phase IIb in Korea. Delivered through a local injection, TG-C offers a non-invasive therapy that treats the symptoms and causes of osteoarthritis. Allogeneic human donor chondrocytes are transfected by viral vector to produce TGF-β1 and are called the modified cells. The product is composed of a 3:1 ratio of unmodified to modified chondrocytes, delivered as an intra-articular injection to patients with grade 3 chronic degenerative joint disease of the knee, and compared against placebo normal saline injection.¹⁰¹ Before injecting the cells, synovial fluid is removed from superolateral portal region of the joint and the knee is laid out straight in the supine position for two hours during the course of slow injection to obtain a dependent position and avoid shear while injecting.¹⁰²

According to the company's website, TissueGene's allogeneic cells (i.e., donor cells) are mass cultured and mass packaged in DMEM media and are delivered in a ready-to-inject, off-the-shelf form to any patient.¹⁰²

Revaflex, used for the treatment of ICRS Grade III and IV articular cartilage lesions of the knee, is marketed by ISTO Technologies, and has currently proceeded to conduct phase III clinical trials to evaluate safety and efficacy of the graft versus the microfracture technique.⁷⁹ The engineered tissue implant consists of living cartilage tissue grown in the laboratory, cultured using human cartilage cells. The scaffold is surgically inserted into the subchondral bone using fibrin glue for patients with cartilage defects.

Geographically independent companies like CARTISTEM® from Korea, Chondrogen from Osiris, and RepliCart from Australia have marketed products in their respective countries and are currently in the regulatory space for product approval in the United States. Closely following the companies' clinical trials, outcome measures and learning along the way will reduce both cost and time for future applicants and introduce both the investigator and the FDA to a niche treatment modality.

Compared to cell-based products, allogeneic treatments such as MSCs offer the option of tissue storage, commercial opportunity via tissue banking and also reduces a patient's time in the hospital, thus reducing overall healthcare costs.

Summary of the Cartilage Treatment Technologies

For cartilage repair technologies, devices, drugs, and biologics are the three main pathways to secure US regulatory approval for licensing and marketing. On one hand, devices currently have yet to show long-term successful cartilage regeneration, but they have adequately been shown to be safe and represent a faster approval route. Drug treatments, on the other hand, currently treat

late-term OA symptoms although many approaches are currently underway to treat early symptoms, and results are yet to show long-term successful treatment of osteoarthritis. Cell therapies present challenges for choosing animals for pre-clinical models. It is the responsibility of the investigators to ensure close mimicking of the human system; hence, choosing between allogeneic versus autologous cells becomes important. Moreover, choosing the right cellular phenotype, ensuring GMP standard of practice, evaluating the effect of immunosuppressants on overall health, and efficiency of the surgical procedure on older populations must be evaluated even at the pre-clinical step by using alternatives, such as older animal populations and carefully drafted assay procedures. Some of the major challenges of autologous cell-based techniques are the need for two or more surgeries in addition to production and facility expenses. Additionally, cost to the patient, healthcare expenses, and insurance reimbursement are major role players in determining the route of treatment and availability throughout the country. The principal investigator(s) may save a lot of time, money, and effort if pre-clinical data that are submitted to the FDA demonstrate durability, safety, and efficacy of the product/treatment/technique. Of special significance is the design of the large animal study and its clinical endpoints, as it sets the stage for upcoming human clinical trials. Adequate physician and surgeon training for consistent device delivery into the defect region and employing uniform surgical practices for a given device/biologic dictate the overall power as well as aid in increasing the power of the experimental design.

ANIMAL STUDIES FOR CLINICAL TRIALS

Small and Large animal study

Several parameters to consider when choosing between small and large animals for cartilage repair are clearly outlined by Stannard *et al.*,⁴⁹ Chu *et al.*,⁴⁵ Ebihara *et al.*,⁷⁵ and Hang *et al.*⁴⁰

They provided extensive information and aid in understanding the balancing factors to leverage the translational potential of an animal model for cartilage repair, and employed the information to outline repair strategies and to further refine control groups and outcome measures.

Outcome assessments of typical small animal models (e.g., rodent, rabbit) are mechanical testing, histology, immunohistochemistry, imaging, and gross morphological scoring. Outcome measures in induced defect live-animal models such as sheep, dogs, and horses include arthroscopic scoring, computed tomography (CT), radiograph, visual analog scale (VAS) for pain assessment, range of motion, muscle mass around the defect area, kinematics, and India ink staining for select biopsied tissue in addition to the ones described above.^{35, 111} Immunohistochemistry is specifically relevant for large animal studies for elucidation of collagen II and aggrecan content and distribution.^{111, 161} Specifically, please refer to Table 2.5 in Stannard *et al.*,⁴⁹ entitled “Comparison of common used animals models for cartilage regeneration,” which outlines the benefits and challenges of using different animal models for demonstrating cartilage repair. The specific columns entitled “cartilage thickness” and “primary use” clearly correlate with each other, and outline the data one can obtain from using a specific animal model, thus enabling the investigators to have an informed decision and understand the capability of the outcome measures. Additionally, the testing paradigms and measurement criteria are similar in both induced defect and animals with natural ailments. The FDA Guidance to Industry¹¹⁵ indicates that they consider goats, sheep, and horses as acceptable pre-clinical models. The articular cartilage thickness in the horse is closest to that in humans. However, goats and sheep are recommended given that horses have much larger joints and forces, and are not necessarily a relevant model for the veterinary market as patients, nor are they an ethically preferable animal model for induced defects and sacrifice. For goats and sheep as pre-clinical

models, establishment of an appropriate control comparator group is required, preferably microfracture. Additionally, while employing pluripotent stem cells, issues such as ethical concerns, long-term stability, tumorigenesis and mutagenesis must also be considered.

However, the challenge with microfracture in sheep and goats is mimicking the continuous passive motion (CPM) and restricted weight bearing rehabilitation protocol used with human patients, which lasts several weeks. Although no model will be perfect for mimicking the restricted weight bearing period, investigators may consider limited activity, for example, being kept in smaller pens for a period of several weeks before returning to normal activity. Two important documents for preclinical cartilage repair studies are the *Standard Guide for in vivo Assessment of Implantable Devices Intended to Repair or Regenerate Articular Cartilage*³⁵, by the American Society for Testing and Materials (ASTM), and the FDA Guidance for Industry.¹¹⁵ These documents convey the requirements for the approval of drugs, biologics, devices, or combination products intended to repair or replace cartilage in the knee, and serve as a “roadmap” for gaining clinical approval. It is beyond the scope of the current review to delve into FDA and ASTM guidelines, but several reviews and letters have covered the topic. Two important documents for preclinical cartilage repair studies are the *Standard Guide for in vivo Assessment of Implantable Devices Intended to Repair or Regenerate Articular Cartilage*³⁵, by the American Society for Testing and Materials (ASTM), and the FDA Guidance for Industry.¹¹⁵ These documents convey the requirements for the approval of drugs, biologics, devices, or combination products intended to repair or replace cartilage in the knee, and serve as a “roadmap” for gaining clinical approval. It is beyond the scope of the current review to delve into FDA and ASTM guidelines, but several reviews and letters have covered the topic

extensively, which the reader is encouraged to read.^{177, 195, 215} Based on the requirements of a typical clinical study, it can be said that a team of a biostatistician, an FDA regulatory consultant, a veterinarian, a biomedical engineer, an experienced orthopedic surgeon, and experts in biomechanical testing, musculoskeletal histology, and diagnostic imaging is necessary to overcome the challenges associated with clinical trials.

Preclinical and simultaneous veterinary market approach

Figure 2.1, adapted from Lee *et al.*,¹⁴⁴ shows a logical progression from lab-based research to clinical trials, where stage 2 of research and development branches out to two animal-based applications: preclinical data and veterinary medicine. The numerous approaches to cartilage therapy have increased the veterinary market population. Pre-clinical studies conducted in domestic animals such as dogs have facilitated rapid translation into veterinary medicine,⁴⁹ closing a gap between the human and veterinary markets. Transparent publication of methods and results by the scientists who conduct large animal studies will help to establish a unified protocol, useful for future investigators. The existing use of cartilage therapy in veterinary medicine creates an exciting opportunity for collaboration between veterinarians and physicians to advance the treatment of injury and disease in both human and animal patients.

FEDERAL REGULATIONS AND CLINICAL STUDY CONSIDERATIONS

The only cell-based FDA-approved product in the United States is Genzyme's Carticel®, a 510(k) approved mixing and delivery system by Arthroflex, and 361 HTC/P approved product

DeNovo® ET by Zimmer.²⁷³ The FDA in the USA has issued specific IND/IDE guidelines on cartilage therapy, and, depending upon the nature of the product, they are classified into different categories and accordingly handled by the designated control centers.¹⁶⁶

Overall, careful design of the clinical study, selection of intervention and comparator group, patient population, factors affecting enrollment and clinical endpoints, choosing appropriate investigators and medical clinic(s), and allocation of proper funds is crucial for the success of any clinical trial. Special emphasis is laid on choosing the appropriate patient population that targets the appropriate indication, as it is crucial to demonstrate efficacy of the drug/product in disease treatment. In addition to careful selection, clinical endpoint determination must be formulated in reference to previous successful and unsuccessful clinical trials, collaboration with research scientists, orthopedic surgeons, regulatory personnel, and technicians to ensure standardization of testing procedures in the event of a multi-center study. Additionally, the FDA considers post-surgery follow-up a significant concern; obtaining more than 85% short and long-term follow-up data on pain, functional testing, and quality of life questionnaires is of great importance.¹⁶⁶

Clinical endpoints

Cartilage repair therapies include primary and secondary outcome measures, which measure pain and/or function using well-defined scales¹⁷⁷ determined by the FDA. Apart from including robust primary and secondary outcome measures, including too many individual measurements in a primary endpoint can be limiting financially and prove detrimental to the overall success of both the treatment and control groups. Primary evaluation endpoints are based on pain and function and since it is qualitative, the results depend on the actual success of the repair procedures and

the patient population,¹⁸⁷ and enrollment numbers for statistical considerations. The endpoints for the purpose of clarity are divided into pain scoring and function scoring, and are typically comprised of:

Pain-based:

- I. Knee Injury and Osteoarthritis Outcome Score (KOOS)
- II. International Knee Documentation Committee (IKDC) Subjective Knee Evaluation Form
- III. Symptom Rating Form
- IV. Western Ontario and McMaster University Osteoarthritis Index (WOMAC)
- V. Knee Society Score (KSS)

Function-based:

- I. Cincinnati Knee Rating System
- II. Structural changes (MRI & MOCART)

The recommended primary and secondary tests included criteria for advanced stage arthritis and for sports-related injuries²¹³ with recommendations from the International Cartilage Repair Society (ICRS). Pain is an important measurement, crucial to the success of the product, and is usually examined as an addition to the primary endpoints (WOMAC/KOOS pain analysis) or as a questionnaire to assess the nature and quality of pain.⁴⁸

For most devices, tissue remodeling of the cartilage repair are typically measured non-invasively using magnetic resonance imaging (MRI) and magnetic resonance observation of cartilage repair tissue (MOCART), and information regarding device and defect location, cartilage thickness,

volume loss, and repair tissue characteristics are all considered as crucial secondary endpoints that demonstrate product efficacy, which further require standardization and validation across several instruments.^{24, 93} However, for specific drugs that delay the onset of cartilage degradation, they are FDA-approved to employ IND studies with the use of X-rays or MRI.²⁴

Once again, the emphasis lies on selecting important primary and secondary endpoints and ensuring the elimination of redundant data sets. Maintaining uniform measurements throughout the study and throughout all of the campuses in cases of multi-center trials is of paramount importance, as this uniformity affects the overall quality of the data. Standard protocols, uniform time points, and diligent reporting of any aberrant information ensure hassle-free and expedited review of the data. In addition, clinical measurements including general health data, reimbursement outcomes, and overall quality of life can be collected and positively used to obtain for the product in the market.

The primary outcome measures in clinical studies, namely pain and function, are different from preclinical studies, where the emphasis is on an objective analysis of cartilage morphology/structure. This difference can pose challenges in designing the clinical study and selecting outcome measures that will demonstrate the advantages of the therapy in a practical/feasible manner for clinical investigators and patients. Clinical studies of ACI vs. microfracture, in which repair tissue was biopsied and evaluated histologically, did not find an association between better structural repair and improved clinical outcomes (pain and function) at 1-2 years follow up.¹³⁰ Studies of ACI using a characterized cell therapy (termed Characterized Chondrocyte Implantation, CCI), where patients were followed long term, did not

demonstrate superior clinical outcomes over microfracture until 3 years post-surgery;²¹⁶ the clinical outcomes were again comparable between the two groups at 5 years, except for a cohort of patients that were treated early (<3 years from onset of symptoms) who did experience clinical benefits with CCI.²⁵¹ This finding suggests that the clinical benefits of producing more hyaline-like repair tissue may take many years to translate into improved clinical outcomes, and may be restricted to certain patients/injuries. Consequently, clinical trials for cartilage repair technologies may require long-term follow up and careful enrollment to reach endpoints, thereby increasing the financial burden of product development. Ongoing work in the development and validation of new biomarkers for cartilage repair and joint preservation will be valuable for the translation of cartilage repair technologies, especially if biomarker(s) can be used at early time points to predict long term outcomes.

OTHER COMMERCIALIZATION CONSIDERATIONS

It is important to note that FDA approval of a cartilage repair therapeutic, regardless of the specific regulatory pathway, depends not only on completion of a successful clinical trial, but also on establishment of design control, GMP manufacturing processes, and quality control systems to ensure safety and efficacy of drug/device products. FDA clearance of a device/drug and medical need do not guarantee coverage by insurance companies. Therefore, a reimbursement strategy is often critical to the commercial viability of a cartilage repair product. While the FDA focuses on safety and efficacy, insurance companies focus on superiority of the product relative to the gold standard, and economic evaluation (eg. cost per quality adjusted life year).¹⁷⁵ To determine coverage, it is possible that insurance companies may require data beyond those provided to the FDA for clearance to determine drug/device value and impact on patient

care, depending on if/how the clinical study was conducted. It may be advantageous to consider the requirements for FDA approval and reimbursement simultaneously in designing the clinical efficacy study.

CONCLUSIONS

Although there are several surgical and tissue engineering-based treatments that treat osteoarthritis and other cartilage disorders of the knee that have achieved differential success rates for both short and long terms, a successful product line recommended uniformly across all healthcare facilities does not exist. While many upcoming products are at different stages in their FDA trials, there is still an unmet need for a translational technology for cartilage tissue engineering.

Common tissue engineering approaches for cartilage regeneration can be broadly divided into cell-based and material-based strategies. Cell-based strategies include autologous or allogeneic chondrocytes, bone-marrow mesenchymal stem cells, and adipose-derived stem cells. Currently, under the FDA, the only cell-based therapy is Carticel from Genzyme. While cell-based therapies offer great potential for regeneration, they require two surgeries (if autologous) and can be costly. Allogeneic treatments offer greater convenience, but carry additional risks of infection, immune rejection or graft-versus-host-disease, which makes the cell-based therapy system financially demanding, and a long path to FDA approval.

Material-based strategies such as osteochondral plugs and injectable paste-like materials offer a one-step solution, which is financially appealing, and may ensure uniform treatment across several institutions without worrying about device implantation and contamination. However,

long-term efficacy in terms of cartilage repair and functional restoration of a device system has not yet been demonstrated. Currently, Zimmer Orthobiologics is in the final stages of obtaining FDA clearance and around five other products from different companies based in other countries are in phase 3 or 4 clinical trials in the brink of securing approval to use in respective countries.

Drugs, on the other hand, consist of predominantly intra-articular injection or oral capsules taken by the patient at regular time intervals, although demonstrating efficacy with these approaches for treating large defects or advanced stage osteoarthritis has proven to be difficult. Such injections are expensive and are mostly focused on relieving pain. While such approaches may in general not be considered regenerative medicine strategies, they reduce pain and restore daily function for a finite period of time.

The time period from commencing feasibility (i.e., phase 0) clinical trials to actual product sales in the market is dependent on several factors, such as success of the clinical trials, selection of primary and secondary endpoints for the clinical study, establishment of approved protocols, creation of a manufacturing process to meet GMP standards, and working with a fine team to address concerns. One important factor to consider is the selection of a proper comparator group (i.e., control, standard of care). The information from clinicaltrials.gov suggests that ACI, OATS, and microfracture are commonly used as comparators for most devices and biologics, with a trend toward using microfracture for late phase clinical trials. Owing to being the most common surgical treatment for cartilage injury, and having zero product cost, microfracture is the gold standard of comparison that orthopedic surgeons will need to see a product surpass if a company wants to convince the surgeons to adopt their product. Microfracture has thus emerged as a

preferred control group for clinical trials, and we recommended it as the comparator for pre-clinical and even small animal cartilage repair studies as well.

It is worth emphasizing that microfracture may also be a desirable first step for certain cartilage repair devices. For example, a porous chondral-only (as opposed to osteochondral) device approach could leverage the infiltrating cells from the marrow for cartilage regeneration as opposed to requiring exogenously seeded cells prior to the surgery.

In addition to selecting an appropriate comparator, other important factors that need to be emphasized for running successful clinical trials include knowledge of common inclusion and exclusion criteria, strategies to improve the power of the clinical trial, ensuring successful enrollment, choosing the right geographic location, and establishing uniform data collection in the case of multicenter trials. As already mentioned, adequate care must be taken to include pain measurement and important primary and secondary endpoints that can also be used for future funding agencies.

In general, the route taken to achieve federal regulatory approval may seem daunting, but with multi-disciplinary expertise, an understanding of the dynamic regulations, and lessons learned from animal studies, we can expect to formulate better study design aimed toward translational goals.

CHAPTER 3: Short-term Characterization of Microsphere-Based Raw Material Encapsulated Scaffold²

ABSTRACT

“Raw materials,” or materials capable of serving both as building blocks and as signals, which are often but not always natural materials, are taking center stage in biomaterials for contemporary regenerative medicine. In osteochondral tissue engineering, a field leveraging the underlying bone to facilitate cartilage regeneration, common raw materials include chondroitin sulfate (CS) for cartilage and β -tricalcium phosphate (TCP) for bone. Building on our previous work with gradient scaffolds based on microspheres, here we delved deeper into the characterization of individual components. In the current study, the release of CS and TCP from poly(D,L-lactic-co-glycolic acid) (PLGA) microsphere-based scaffolds was evaluated over a time period of 4 weeks. Raw material encapsulated groups were compared to ‘blank’ groups and evaluated for surface topology, molecular weight, and mechanical performance as a function of time. The CS group may have led to increased surface porosity, and the addition of CS improved the mechanical performance of the scaffold. The finding that CS was completely released into the surrounding media by 4 weeks has a significant impact on future *in vivo* studies, given rapid bioavailability. The addition of TCP seemed to contribute to the rough external appearance of the scaffold. The current study provides an introduction to degradation patterns of homogenous raw material encapsulated scaffolds, providing crucial characterization data to advance the field of microsphere-based scaffolds in tissue engineering.

² Resubmitted as **Sridharan B**, Mohan N, Berkland CJ, Detamore MS, “Short-term Characterization of Microsphere-based Raw Material Encapsulated Scaffold,” *Material Science and Engineering C*, 2015

INTRODUCTION

Biphasic and gradient scaffold fabrication are attractive approaches for interface tissue engineering applications,⁶⁹ demonstrating that microspheres can offer spatial patterning with different microsphere layers possessing different degradation kinetics. New methods to incorporate raw materials in biodegradable scaffolds are constantly being explored as they enhance regeneration.^{43, 147, 182} Raw material encapsulation in turn alters degradation rate and the associated polymer composition that eventually leads to a potential to fabricate desirable degradation rate for improved regeneration. Polymer selection, encapsulation of bioactive factors, and alterations in porosity are some of the key techniques employed to tune the degradation rate of biodegradable scaffolds to best coincide with the rate of tissue regeneration.

With respect to *in vivo* osteochondral applications, it would be highly desirable to have a gradient pattern, where for example the cartilage section of the scaffolds have a faster degradation rate to allow faster access for released chondroinductive signals, and correspondingly a slightly slower degrading section for the bone region to provide better mechanical support. Particularly, the changes in the degradation rate in the first month impacts the initial cellular differentiation and sets the stage for downstream regeneration processes. In view of the imminent translational applications, we chose the polymer formulation that was employed in a Coulter Foundation-funded sheep study¹⁸¹ and input from regulatory consultants.

The goal of the current study was to fabricate microsphere-based scaffolds with different raw materials, and to observe the material properties over time using scanning electron microscopy (SEM), size exclusion chromatography (SEC), and measuring retention of raw materials through

biochemical assays.⁷⁰ Polymeric scaffolds were fabricated using biodegradable PLGA microspheres that encapsulated TCP or CS as the raw materials.¹⁸² These unique microspheres were fabricated and characterized for degradation in an acellular environment over a period of 4 weeks. Throughout the study, the raw material encapsulated groups were compared to their respective control groups, which were composed solely of the polymer.

MATERIALS AND METHODS

Materials

Faster degrading poly(D,L-lactic-co-glycolic-acid) (PLGA) (50:50 lactic acid:glycolic acid, ester end group, $M_w = 106$ kDa) of intrinsic viscosity 0.6-0.8 dL/g, and slower degrading PLGA (75:25 lactic acid:glycolic acid, ester end group, $M_w = 112$ kDa) of intrinsic viscosity 0.6-0.8 dL/g were purchased from Evonik Industries (Birmingham, AL). The raw materials were chondroitin sulfate A sodium salt (CS) and β -tricalcium phosphate (TCP), which were obtained from Sigma (St. Louis, MO). All reagents and organic solvents utilized were of cell culture or ACS grade.

Microsphere fabrication

Four different types of microspheres were fabricated. The microspheres for the study groups were CS microspheres (50:50 PLGA+CS+NaHCO₃, 77.5:20:2.5 by weight) and TCP microspheres (75:25 PLGA+TCP, 90:10 by weight). The microspheres for the control groups were “CS control” (50:50 PLGA+NaHCO₃, 97.5:2.5 by weight) and a “TCP control” (75:25 PLGA) microspheres. The CS microspheres were fabricated by adding 20% w/v CS and 2.5%

w/v NaHCO₃ to 77.5% w/v PLGA (50:50 lactic acid:glycolic acid, ester end group) with intrinsic viscosity 0.6-0.8 dL/g dissolved in dichloromethane (DCM) (20% w/v) (Sigma-Aldrich). NaHCO₃ was dissolved in 0.5 mL deionized water (DI), to which CS powder was added; it was then vortexed for 15 minutes to obtain a uniform viscous solution that was subsequently mixed with PLGA, dissolved in DCM (20% w/v), and sonicated for 2 minutes. TCP group microspheres were fabricated by adding TCP (10% w/v) to PLGA (75:25; 90% w/v) in DCM (20% w/v). The TCP powder was added to PLGA, dissolved in DCM, and sonicated for 2 minutes.

Monodisperse microspheres¹⁰⁰ were prepared according to our previously reported technology^{71, 99, 181, 227, 229}. Briefly, the polymer stream was broken into uniform polymer droplets by exposing the stream to acoustic excitation. An annular carrier non-solvent stream (0.5%-2% w/v polyvinyl alcohol (PVA) in DI) surrounding the droplets was produced using a nozzle coaxial to the needle. The polymer/carrier streams flowed into a beaker containing the non-solvent. The polymer droplets were stirred via magnetic stir bar and plated for 3-4 h to allow solvent evaporation. Afterward, the polymer droplets were filtered and rinsed in DI to remove residual PVA, further lyophilized for 48 h, and stored at -20°C until further use.

Scaffold assembly

The microspheres were assembled into a mold (3.5 mm in diameter and 4.5 mm in height) and fabricated into scaffolds following an hour sintering with an 95% ethanol-5% acetone solvent process as previously reported [5]. All scaffolds in this study were 3.5 mm in diameter and 4 mm in height. For all individual analyses, a sample size of n = 4 or 5 was used.

Scanning electron microscopy (SEM)

At 1, 2, 3, and 4 weeks, the PLGA scaffolds were collected, freeze-dried overnight, sliced into small sections, and set up for sputter coating. The sectioned and dried scaffolds were mounted on 10 mm aluminum SEM stubs (Ted Pella Inc., Redding, CA) and sputter coated with gold at 30 mA for 46 seconds in a chamber purged with argon gas. After sputter coating, the samples were imaged using a LEO 1550 field emission scanning electron microscope under an acceleration of 5 kV and high vacuum.

Description of experimental groups

For the entire study, four different groups were investigated: (i) homogenous microsphere scaffolds composed of only 50:50 PLGA+NaHCO₃ (ester functional group with intrinsic viscosity 0.6-0.8 dL/g), acting as "CS control" (ii) "CS group" microsphere scaffolds composed of (50:50 PLGA+CS+NaHCO₃) (iii) microsphere scaffolds made of 75:25 PLGA, acting as "TCP control" and (iv) "TCP group" microsphere scaffolds composed of 75:25 PLGA encapsulated with 20% w/v TCP. Please refer to Table 3.1 for the entire list of experimental groups and their abbreviations.

Sample collection

The microsphere-based scaffolds of all the experimental groups were put in 24 well-plates and incubated in sterile phosphate buffered saline (PBS) (ThermoFisher) that was stored at 37°C and 5% CO₂ jacket controlled incubator with access to fresh air. The PBS was changed every other day and samples were collected at corresponding time points.

Dry weight analyses

At weeks 0, 1, 2, 3, and 4, the scaffolds and release media were collected and filtered. The recovered microspheres were freeze-dried, weighed [dry weight (t)], and stored at 4°C for further analysis.

The relative dry weight of the scaffold at time t was calculated as follows:

$$\text{Dry weight}(\%)(t) = \frac{\text{Dry weight}(t)}{\text{Dry weight}(t = 0)} \cdot 100\%$$

Where dry weight (t = 0) denotes the initial dry weight of the microsphere scaffolds (before exposure to PBS).

Molecular weight determination

The molecular weight of the polymeric scaffolds (n = 4) at specific time points (weeks 0, 1, 2, 3, and 4) was determined using a Shimadzu LC-20AB HPLC pump equipped with a Shimadzu RID-10A refractive index detector (Shimadzu Scientific Instruments, Columbia, MD). Briefly, lyophilized scaffolds were dissolved in chloroform to form a final concentration of 0.5% polymer and passed through a 0.22 µm syringe filter (BD Biosciences, San Jose, CA) to remove any insoluble components. After a brief centrifugation at 5,000 rpm for 10 minutes, the supernatant was collected for further analysis. Chloroform was used as the mobile phase with a flow rate of 1 mL/min and a column temperature of 40 °C. The molecular weight of the polymers was determined relative to the molecular weight of the polystyrene standards (Viscotek, Malvern, UK), and weight average molecular weight was calculated from the HPLC plots.

Chondroitin sulfate in CS group scaffolds

As previously reported, the amount of CS retained within the scaffold was measured by dissolving the polymeric constructs in 1 mL of DCM. To each polymeric construct, 0.5 mL of DI was added to extract the CS into the aqueous phase. The quantity of CS retained in the scaffold (n=4) was measured by the Blyscan dimethylmethylene blue (DMMB) assay (Biocolor, Newtownabbey, Northern Ireland).

Calcium in TCP group scaffolds

TCP group scaffolds were dissolved in 1 mL of DCM (dichloromethane) followed by the addition of 0.5 mL of DI to precipitate the calcium ions into the aqueous phase. After a brief centrifugation at 5,000 rpm for 10 minutes, the calcium content was measured via the QuantiChrom™ calcium assay kit (DICA-500; Hayward, CA) according to the manufacturer's instructions. The final values were read using a UV microplate reader (Thermo Electron Corporation, Waltham, MA), measured at 620 nm.

Mechanical Testing

Unconfined compression was performed using a uniaxial testing apparatus (Instron Model 5848, Canton, MA, 50 N load cell) according to our previously reported method. Briefly, following a tare load (0.05 N), scaffolds were compressed to 15% strain at a rate of 1% per second under PBS at 37 °C, similar to our previous testing.²²⁷ The elastic moduli were obtained from the linear regions of the stress–strain curves. Stress was defined as the ratio of the load to the initial cross sectional area, and strain was defined as the ratio of the change in the length to the original length. Mechanical testing was performed for all of the scaffolds at weeks 0 (i.e., 24 h), 1, 2, 3, and 4.

Statistical Analyses

Statistical analyses were performed using a one-way analysis of variance (ANOVA) with Minitab 17.0 software (Minitab Incorporated, State College, PA), in conjunction with a Tukey's post hoc comparison test for repeated measurements. The statistical significance threshold was set at $\alpha = 0.05$ for all tests (with $p < 0.05$). All quantitative results were expressed as the mean \pm standard deviation.

RESULTS

SEM characterization of scaffolds

The fabricated microspheres were uniform in size and overall were porous in nature (Fig. 3.1). The PLGA-only scaffolds exhibited a smooth surface topology; an effect observed due to the ethanol acetone sintering,²³⁰ while the CS group displayed minute pores on the microsphere surface. TCP group exhibited rough patches on the surface compared to its control group. Over the period of 4 weeks, both the CS group and CS control group displayed macroporous degradation, with the CS control group losing complete structural integrity by week 3 and becoming paste-like by week 4. The CS group microspheres, on the other hand, retained their macroporous shape until week 4. The TCP control microspheres retained their original shape and showed little to no degradation, macroscopically, even at week 4. Conversely, the TCP group showed increased surface area roughness and did not degrade macroscopically until week 4.

Dry weight and Molecular weight analysis

Figure 3.2a represents the percentage dry weight of all of the microsphere-based scaffolds over a period of 4 weeks. The CS control group did not have any significant change in weight from week 0 to week 2, but decreased by 13.4% from week 0 to week 3 ($p < 0.05$). By week 4, the CS control group had a significant 99.6% decrease from week 0 ($p < 0.05$). The CS group also did not show any significant difference in dry weight content from week 0 to week 2, but decreased by 52% from week 0 to week 3, and by 97.1% from week 0 to week 4 ($p < 0.05$). In comparing the CS group to its control, at week 3, we observed that the CS control had a 1.9-fold higher dry weight than the CS group ($p < 0.05$). However, there was no statistically significant difference between these two groups at other time points. There were no statistically significant changes in dry weight over time, or between the groups, for the TCP group and its control.

Figure 2b represents the weight-average molecular weight (M_w) of all of the microsphere-based scaffolds over the period of 4 weeks. The CS control group was measured to have a starting M_w of 339 ± 9 kDa and there was no significant change in M_w over the period of 4 weeks. The CS group had a starting M_w of 342 ± 11 kDa, and there was a 9.2% decrease in M_w from week 0 to week 4 ($p < 0.05$). The TCP control group did not have any statistically significant change in M_w over time, however the TCP group had a 12.3% decrease in M_w from week 0 to week 4 ($p < 0.05$). In comparing the CS and TCP group, the CS group had a 10.5% higher M_w than the TCP group only at week 4 ($p < 0.05$).

Retention of chondroitin sulfate in the CS group scaffolds

The total chondroitin sulfate retained by the CS group scaffolds from week 0 (24 hours) to week 4 is represented in Figure 3.3a. The GAG value measured from the scaffolds represents the CS entrapped within the CS group polymer matrix at the different time points. At week 0, the CS scaffolds had an average CS amount of 273 ± 78 μg , which decreased by 59.3% at week 1 ($p <$

0.05). There was a further 74.7% and 64.2% decrease from week 1 to week 2 and from week 2 to week 3 ($p < 0.05$), respectively. By week 4, there was no detectable CS retained in any of the scaffolds.

Retention of calcium in the TCP group scaffolds

The total calcium retained by the TCP group scaffolds from week 0 (24 hours) to week 4 is represented in Figure 3.3b. At 24 hours, the TCP group had an average calcium content of $432 \pm 18 \mu\text{g}$ in the scaffolds, which decreased by 31% at week 1 ($p < 0.05$). The calcium content in the scaffolds decreased by 36.3% from week 0 to week 2 and 59.4% from week 0 to week 3 ($p < 0.05$). Finally, there was a 77.3% calcium content decrease in the TCP scaffolds from week 0 to week 4 ($p < 0.05$).

Mechanical testing

There was no significant change in the elastic modulus of the CS control group from week 0 to week 2. However, beyond week 2, these samples became too unstable to be loaded into the instrument's sample holder. The CS group on the other hand had a significant 75.1% decrease in elastic moduli only from week 0 to week 3 and 77.2% decrease from week 0 to week 4 ($p < 0.05$). There was no significant change in moduli from week 0 to week 2. There was no sample at week 4 to make any comparisons. There were no significant differences in the moduli between CS control and CS group at the time points where the CS control had available data. The TCP control group had a statistically significant 73.6% decrease in elastic modulus from week 0 to week 3 ($p < 0.05$) and no significant change from week 0 to week 2, or from week 0 to week 4. However, there was a 2.1-fold higher modulus for the TCP control at week 4 compared to week

2 ($p < 0.05$). With regard to the TCP group, there was a 43.9% increase in the elastic modulus from week 0 to week 3 and a 2.8-fold higher modulus at week 4 compared to week 0 ($p < 0.05$). In comparing the TCP control and the TCP group, we observed that there was a 5.3-fold higher compressive elastic modulus for the TCP control group compared to the TCP group ($p < 0.05$) at week 0. In addition, there were 3.1-fold and 1.9-fold higher moduli for the TCP control group compared to the TCP group at week 2 and week 4, respectively ($p < 0.05$).

DISCUSSION

The current study demonstrated, for the first time, the degradation pattern of nanocomposite microsphere-based scaffolds. The gradient capability that we have demonstrated with microsphere-based scaffolds allows for CS and TCP to be encapsulated in opposing gradients within a single biomaterial construct.^{99, 181} For the first time, we have an understanding of the mechanics and the raw material retention within these scaffolds over the crucial first month, from which we can quantitatively infer gradients not only in initial material composition, but also in mechanics and degradation and release rate.

We are the first group to vigorously investigate the potential of TCP as a viable raw material for microsphere-encapsulation for osteochondral applications. Although other groups have used hydroxyapatite-sintered microspheres and carbon-nanotube reinforced scaffolds, no studies have fully characterized homogenous TCP-encapsulated, microsphere-based scaffold degradation in comparison to the polymer alone.^{54, 157, 172}

The SEM images depicted an overall porous nature of the microsphere-based scaffolds with interconnected pores and were in agreement with our previous findings with low molecular weight PLGA.²³⁰ The CS microspheres had a porous surface that could be the effect of CS

embedding and subsequent removal during the scaffold fabrication step, which was consistent with our previous publications.^{100, 183} Although the current paper did not measure porosity, information can be obtained from our previous manuscripts that use similar formulation.¹⁰⁰ The TCP group on the other hand did not possess porous but had a rough external surface instead. The surface characteristics of the raw material encapsulated may have great implications for cell anchorage, cell migration and nutrient diffusion.

The dry weight data were in accordance with the SEM analysis. While both the low molecular weight PLGA lost its dry weight completely by week 4, the TCP scaffolds did not have any significant change in mass even after week 4. Thus, using a higher molecular weight PLGA that had a higher percentage of lactic acid not only delayed degradation on the surface, but also maintained its overall mass percentage.

The GAG and calcium release assay that evaluated the raw material content in the scaffolds were consistent with the SEM observations. The starting values of GAG and calcium at week 0 do not represent their loading value. This may be attributed to loss during the lyophilization and the solvent sintering step. About 60% of the CS was released at week 1 into the surrounding media. The relatively high bioavailability of CS within the first week and complete release within one month may be highly desirable for initiating a bioactive chondrogenic response *in vivo* during the crucial period of regeneration.

Mechanical testing results demonstrated the compressive moduli of microsphere-based scaffolds to be of similar order of magnitude relative to articular cartilage (0.1–0.9 MPa) and within an order of magnitude of the moduli for cancellous bone (0.01–2 GPa).^{5, 19, 100, 126} The elastic modulus of the TCP group at week 0 was in agreement with the moduli of calcium phosphates as observed by Ly *et al.*⁵⁶, thus confirming that the addition of TCP enhances the elastic moduli.

Although the starting modulus of the PLGA groups in the current study are comparable to our previous studies, over a period of 4 weeks, there was a an order of magnitude increase in modulus for the gradient groups, which may be the combined effect of two types of PLGA and the stiffness contributed by cellular differentiation.^{72, 100} In another previous study from our team, which employed raw material-encapsulated scaffolds compressed at strain rate of 1 mm/min, we observed that the elastic moduli was generally lower than the moduli reported in the current study.¹⁸³ However, the previous study employed rat bone marrow mesenchymal stem cells (rBMSCs) and gradient scaffolds with a low-molecular weight PLGA. In the current study, while the moduli of the TCP control scaffolds did not show any significant change over time, the TCP group had a 91.5% increase from week 2 to week 4 ($p < 0.05$) an observation consistent with our previous paper.²²⁸ Both the CS control and CS groups showed a decline in elastic modulus that may be explained by the low molecular weight nature and the high glycolic content of the polymer.³ PLGA microspheres are known to degrade via bulk erosion where the rate-limiting step is the diffusion of water molecules into the microsphere core. CS microspheres, because of their porous nature and the hydrophilic nature of CS, may have allowed faster diffusion of the water molecules into their core, thereby initiating the polymer degradation more quickly than in the other three groups, as evidenced by a significantly greater mass loss by 3 weeks. However, the structural integrity of the CS constructs was superior to the CS control through the 4 week duration. Additionally, swelling caused by penetration of water inside of the microspheres may have also played a role in the drop in elastic modulus of CS scaffolds.¹⁸³ Moreover, the polymer composition (75:25 PLGA) and microsphere morphology (absence of minute pores on surface) may have allowed the TCP scaffolds to further retain their mechanical properties. The imminent next step would be to test the impact of cells on known mechanical properties of the scaffolds

and independently correlate the effect of cells versus the effect of raw materials and thus results from such studies would be valuable in designing scaffolds for future large animal models.

Findings from the current study necessitate the need to refine the technology by parameters like adjusting raw material and polymer concentration that in turn would modify the degradation rate. Since the polymer degradation and the raw material released plays a major role for *in vivo* studies, there is a pressing need to reach a suitable selection of polymer and raw material concentration for specific applications. The scaffold selected to treat small animals like rats and rabbit may not match the need of a large animal model. Moreover other factors like bone stiffness, cartilage thickness must also be considered for enhanced scaffold design. The current study attempted to characterize homogenous microsphere-based scaffolds to provide a basis for analyzing degradation patterns that in turn would enable multilayered and gradient scaffold fabrication. In addition to just altering the degradation kinetics, raw materials can also provide beneficial signals to the surrounding cells guiding the differentiation and neo-tissue regeneration.

CONCLUSIONS

The current study evaluated the degradation properties of raw material encapsulated microsphere-based scaffolds over a period of 4 weeks. Overall, the results demonstrated that the incorporation of CS with 50:50 PLGA may have increased surface porosity and enhanced the structural stability over 4 weeks compared to the polymer without CS. More importantly, about 60% of the CS encapsulated was released at week 1 and 100% of the CS was released by 4 weeks. The current finding might have significant implications for the design of future *in vivo* microsphere-based scaffolds for chondrogenesis. The TCP incorporation with 75:25 PLGA also

avored a better mechanical response over time and retention of an overall rough surface topology even at 4 weeks compared to the TCP control group. Such a complementary nature of the encapsulated raw material adds value to the polymer selection, thus aiding the fabrication of gradient or multilayered scaffolds with informed decision about degradation. Future studies will benefit from expanded analyses to further elucidate the effects of the raw materials on the degradation and mechanics of the scaffolding materials over time.

As an example, for *in vivo* interface tissue engineering applications that need different degradation rates to match the properties of the native tissue, the current study provides a means to evaluate the individual parameters involved in assessing the degradation pattern under an *in vitro* setting. The degradation pattern according to this platform can be tailored by polymer selection, nature of raw materials that are encapsulated and the concentration of both to manufacture the final scaffold. Additionally, the current study also employed a set of raw materials (CS & TCP) combined with two specific types of PLGA, and emphasized that the raw material content, along with the PLGA composition, are important parameters for controlling degradation and mechanics over time.

CHAPTER 4: Stem Cells in Aggregate Form to Enhance Chondrogenesis in Hydrogels³**ABSTRACT**

There are a variety of exciting hydrogel technologies being explored for cartilage regenerative medicine. Our overall goal is to explore whether using stem cells in an aggregate form may be advantageous in these applications. 3D stem cell aggregates hold great promise as they may recapitulate the *in vivo* skeletal tissue condensation, a property that is not typically observed in 2D culture. We considered two different stem cell sources, human umbilical cord Wharton's jelly cells (hWJCs, currently being used in clinical trials) and rat bone marrow-derived mesenchymal stem cells (rBMSCs). The objective of the current study was to compare the influence of cell phenotype, aggregate size, and aggregate number on chondrogenic differentiation in a generic hydrogel (agarose) platform. Despite being differing cell sources, both rBMSC and hWJC aggregates were consistent in outperforming cell suspension control groups in biosynthesis and chondrogenesis. Higher cell density impacted biosynthesis favorably, and the number of aggregates positively influenced chondrogenesis. Therefore, we recommend that investigators employing hydrogels consider using cells in an aggregate form for enhanced chondrogenic performance.

³ Resubmitted as **Sridharan B**, Lin SM, Hwu AT, Laflin AD, Detamore MS, "Stem Cells in Aggregate Form to Enhance Chondrogenesis in Hydrogels," PLOS ONE, 2015

INTRODUCTION

The Wharton's jelly of the human umbilical cord is believed to contain mesenchymal progenitor cells¹¹. Wharton's jelly cells (WJCs), when cultured in chondrogenic medium, have been shown to produce elevated expression of cartilage specific genes such as SOX9, collagen II, and aggrecan²¹⁴. Human WJCs (hWJCs) were first introduced to the 3D musculoskeletal tissue engineering literature in 2007⁹, and have since emerged as a promising alternate source of cells due to desirable properties such as ease of collection, immunocompatibility, superior tropism, and differentiation potential^{59, 63, 125, 152, 256, 258, 259}.

When chondrocytes are plated in monolayer culture, after several passages they lose their native phenotype and express collagen I, which is absent in articular cartilage¹¹⁴. The standard method for culturing cells for chondrogenesis has been pellet culture, in which chondrogenic differentiation is facilitated by the direct cell-cell interaction available in the 3D pellet. Our global hypothesis is that multiple aggregates of cells will be able to provide the benefit of cell-cell interaction relative to non-aggregated cells. Others have reported that microencapsulation of aggregates in a hydrogel has resulted in improved chondrogenic differentiation^{81, 150}. 3D embryonic stem cell (ESC) aggregates have been shown to initiate chondrogenic differentiation⁵¹. Condensation of cells by reduction in intercellular spaces is favorable for chondrogenesis²⁰⁸, and inhibition of cell aggregation delays chondrogenic differentiation²⁶⁵.

Several studies have explored the use of rat and human stem cell aggregates for musculoskeletal applications. In particular, Goude et al.⁹⁴ reported that MSC spheroids composed of 500-1,000 cells maintained a structure analogous to cartilage condensation, and the effect of chondroitin sulfate encapsulation in MSC spheroids also resulted in increased gene expression of collagen II

and aggrecan. Lei et al.¹⁴⁵ reported that MSC spheroids had the therapeutic potential to treat repaired cartilage tissue. When grown as spheroids and supplemented with TGF- β 1-encapsulated gelatin microspheres⁵⁷, human adipose-derived stem cells (hADSC) were shown to differentiate toward the chondrogenic differentiation pathway, thus exploring large sized aggregates for clinical application⁸⁰.

To the best of our knowledge, never before have hWJC aggregates been fabricated in a 3D platform, much less been explored for cartilage tissue engineering applications. Moreover, no other study has compared cell suspension and aggregates side by side with two different cell types. Our overall hypothesis for the current study was that the aggregate groups would outperform the cell suspension (CS) groups in chondrogenesis. We further hypothesized that the effect of the aggregate model on chondrogenesis would be dependent on the number of cells per aggregate.

MATERIALS AND METHODS

Cell culture and expansion

hWJC were isolated from Wharton's jelly of five human umbilical cords obtained from the Lawrence Memorial Hospital with informed consent (Institutional Review Board Lawrence Memorial Hospital Protocol# 08-2, University of Kansas Institutional Review Board, Protocol# 15402), with all births at full term and under normal delivery conditions. Written consent was obtained from the patient and the consent method and cord-harvest for approved for this study by the IRB committee. The cord collection and cell harvest was approved by the IRB specifically for this study. We isolated hWJC according to our previous published protocol^{64, 169}. Briefly, the

cells were cultured in hWJC media, which was composed of 10% MSC qualified fetal bovine serum (FBS) (Invitrogen Life Technologies, Carlsbad, CA) and 1% Penicillin-Streptomycin (Invitrogen Life Technologies, Carlsbad, CA) in low glucose DMEM (Life Technologies, Grand Island, NY). The medium was changed every other day, and hWJCs were maintained at 37°C with 5% CO₂ in a cell culture grade incubator. At 80% to 90% confluence, hWJCs were trypsinized with 0.05% Trypsin-EDTA (Life Technologies) and expanded in this fashion up to passage 4 (P4). Cells at P4 from all five cords were pooled into one tube.

Rat bone marrow-derived mesenchymal stem cells (rBMSC) were harvested from the femurs of seven young male Sprague–Dawley rats (200–250 g, Charles River) following a University of Kansas approved IACUC protocol for cellular harvest protocol# 175–08. The femur harvest and cell isolation was approved specifically for this study. The cells were isolated according to a protocol previously reported by our lab⁹. Briefly, isolated cells were cultured in rBMSC media (α MEM supplemented with 10% MSC qualified FBS (Life Technologies, Grand Island, NY) 1% Penicillin-Streptomycin (Invitrogen Life Technologies, Carlsbad, CA) and passaged at 80% confluence until P4. All cells from different femurs were pooled together at P4, and used for the study.

The rationale for use of rat BMSCs instead of human BMSCs is for reproducibility, i.e., the opportunity to procure rats of the same strain, age and gender, thus removing the inherent variability associated with adult human BMSC donors. With umbilical cords all coming from patients of the same age (i.e., birth), this concern of age variation that applies to BMSCs does not apply to WJCs. The objective of the study was not to make broad general conclusions about WJCs versus BMSCs, but to rather to explore whether the aggregate method may lead to

different results when different sources of mesenchymal cells are used, including their respective different species and culture medium compositions prior to encapsulation in agarose.

Cellular aggregate formation

Aggregates for the current study were generated by the hanging drop technique.²⁴³ Cellular suspensions (hWJC & rBMSC) were prepared at two concentrations, either 10.0×10^6 or 20.0×10^6 cells/mL, in respective media. Droplets of cell suspensions at a controlled volume of 10 μ L that had 10,000 or 20,000 cells, respectively, were pipetted in an array onto the inside surface of a petri dish lid using a 10 μ L pipette (Eppendorf, Hauppauge, NY), making sure that the droplets had a safe distance between each other to prevent collision. The cells were allowed to aggregate overnight, aided by gravity when the petri dish was reversed (Fig. 1). The petri dish bottom was then filled with PBS to prevent drying of these droplets. After 24 hours, the cell aggregates were collected from the dish with a 1 mL pipette and then encapsulated in agarose hydrogels as described below.

Encapsulation of cells in agarose hydrogels

Phosphate-buffered saline and low temperature gelling agarose (Type VII- A#A0701) were purchased from Sigma-Aldrich (St. Louis, MO). All other chemical reagents and solvents were of analytical reagent grade. Agarose was prepared according to a previously reported protocol⁶¹. Briefly, 0.3 grams of agarose was added to 10 mL of PBS and autoclaved for 30 minutes to create a 3% (w/v) agarose solution. The agarose solution was cooled to 39 °C after autoclaving. Next, CS or aggregates were pipetted into the agarose solution accordingly. Table 4.1 gives a comprehensive list of all of the groups, controls, and the respective time points for analysis. For

the “low aggregate number” group, one to four aggregates were encapsulated in a single agarose hydrogel, and for the “higher aggregate number” group, five to seven aggregates were encapsulated in a single agarose gel. The aggregates were pipetted into the agarose solution gels very quickly, thus giving only a few seconds of working time and so a few aggregates were always lost in the micropipette tip. To account for the loss in pipetting, a range of numbers (1-4): LA and (5-7): HA was denoted. Using the same number of cells per hydrogel, corresponding controls (cell suspension) were fabricated. For the CS groups, the required amount of cells was pipetted into the agarose solution at 37°C and pipetted gently up and down, then poured into sterile airtight silicone molds (5 mm diameter x 1.9 mm height) and refrigerated at 4°C for 3-4 minutes. The molds were then retrieved, and the constructs were punched out into a 24 well plate (Sigma-Aldrich, St. Louis, MO) and incubated with medium composed of high glucose DMEM (Invitrogen, Carlsbad, CA) with 4.5 g/L D-glucose supplemented with 10% MSC fetal bovine serum (FBS), 1% non-essential amino acids, 1% sodium pyruvate, 50 µg/mL ascorbic acid, 0.25 mg/mL penicillin-streptomycin-fungicide and 100 ng/mL human transforming growth factor (TGF)-β3 (PeproTech Inc., Rocky Hill, NJ) at 37°C and 5% CO₂. All of the aggregate groups had corresponding controls except hWJC 20M HA, which did not have 20M HA CS, as there were not enough cells to make the control groups. Medium was made fresh every other day to avoid freeze-thaw cycles and thus to preserve the bioactivity of TGF-β3, and changed every other day.

Cell viability assay

To check the viability of the encapsulated cells and aggregates on agarose scaffolds, a fluorescent live/dead viability staining kit (Invitrogen, Carlsbad, CA) was used at days 0 and 21.

The samples were washed once with PBS and incubated in live/dead staining solution (0.5 μ L calcein and 2.0 μ L ethidium homodimer-1 (ETH) diluted in 1 mL DPBS) for 10 min (37°C, 5% CO₂). The samples were once again washed with PBS prior to imaging using an inverted epifluorescent microscope (Zeiss-LSM 710, Thornwood, NY). Live and dead cells were respectively stained green and red, and the process was repeated on the study groups (aggregates) and the control groups (cell suspensions).

Biochemical analysis

DNA analysis:

Constructs were removed from culture in a sterile manner, crushed manually using pipette tips, and incubated in a papain digestion solution consisting of 125 mg/mL papain, 5 mL N-acetyl cysteine, 5 mL ethylenediaminetetraacetic acid, and 100 mL PBS (all reagents from Sigma-Aldrich, St Louis, MO) in distilled water overnight in a 60°C water bath. The next day, sample digests were centrifuged for 5 minutes and stored at -20 °C until further use. DNA content was quantified for all samples utilizing a PicoGreen kit (Molecular Probes, Eugene, OR) according to the manufacturer's instructions. Previous studies²⁵⁷ from our lab established a conversion factor of 8.5 pg/cell that may be used to convert DNA content to cell number for human cells. For the rat species, the conversion factor of 7.7 pg/cell has been used to convert DNA content to cell number.^{72, 169}

Collagen assay:

For quantifying collagen production, a Sircol soluble collagen assay kit and manufacturer's protocol were used (Biocolor, Belfast, U.K.). Briefly, samples, standards and blanks (distilled

water) were incubated in pepsin solution (Sigma-Aldrich) and stored overnight at -4°C . The kit provided standards, and distilled water was used as the blank. 1.0 mL of Sircol dye reagent and 100 μL of each sample were mixed slowly for 30 minutes. Solutions were centrifuged at 12,000 rpm for 10 minutes, and the resulting supernatant was discarded, keeping the pellet intact. The previous step was repeated after the addition of 750 μL of ice-cold acid salt wash. The pellet was resuspended, and 250 μL of alkali reagent was added. Solutions were then vortexed thoroughly and 200 μL of the solution was transferred to a 96-well plate and read at 555 nm in a Multiscan Ascent microplate reader (Thermoelectron Corporation, Waltham, MA). The exact same procedure was repeated for standards and blanks, and all biochemical assays were done in triplicate.

Glycosaminoglycan assay:

GAG content was measured with the Sircol DMMB assay kit and manufacturer's protocol (Biocolor B1000 Belfast, U.K.) was followed. Constructs were homogenized with the aforementioned papain digesting solution and left in a 60°C water bath overnight prior to measuring increase in glycosaminoglycan (GAG) content. A chondroitin sulfate standard was provided with the kit, and distilled water was again used as the blank. 1.0 mL of dimethylmethylene blue dye solution was added to 100 μL of sample, standard, and blank. Solutions were mixed slowly for 30 minutes and centrifuged for 10 minutes. The supernatant was discarded, the pellet was resuspended, and 1.0 mL of dissociation solution was added. The solutions were vortexed and transferred to a 96-wellplate and run at 656 nm in a microplate reader.

Gene expression analysis

Real-time reverse transcriptase polymerase chain reaction (RT-PCR) was used to assess gene expression levels for collagen types I, X; aggrecan; SOX9; GADPH; and Runx2. Collagen II primer was not considered due to high variability in results even after multiple trials. To each sample, 1.0 mL of lysis buffer (Qiagen, Germantown, MD) was added, and after 1 hour, the solutions were homogenized with a QIAshredder column (Qiagen 79656, Germantown, MD) to extract messenger RNA (mRNA) in accordance with the RNEasy Plus Mini Handbook. A high capacity cDNA reverse transcription kit (Applied Biosystems 4368814, Foster City, CA) allowed reverse transcription of mRNA to complementary DNA (cDNA). 10 μ L of the master mix and RNA samples were combined in a 96-well plate, which was then loaded into an Eppendorf Realplex Mastercycler (Eppendorf, Hamburg, Germany). cDNA concentrations were normalized with DNASE-free water, and a Taqman gene expression assay kit (Applied Biosystems) provided the seven primers for the above-mentioned genes (Table 4.2). 1 μ L of cDNA from each sample, 10 μ L of universal fast master mix (2x), and 1 μ L of a specific primer were mixed in a 96-well plate. RT-PCR reactions were then run in an Eppendorf Realplex Mastercycler.

Immunohistochemistry

Frozen hWJC and rBMSC scaffolds were embedded in Optimal Temperature Cutting (OCT) medium (TedPella Inc, Redding, CA) overnight at 37°C and frozen at -20°C until further use. 10 μ m sections were generated using a cryostat (MICROM HM 550, Thermo-Fisher, Carlsbad, CA). The sectioned aggregates taken at week 0, week 2, and week 3 time points for both 10M and 20M samples were kept frozen at -20°C prior to staining. Thawed samples were fixed with 5% formalin for 10 minutes, immersed in xylene, rehydrated in graded ethanol, and submerged

in 0.1% triton X for 5 minutes (all reagents from Sigma-Aldrich, St. Louis, MO). The sections were exposed to 3% hydrogen peroxide in methanol for 10 minutes to suppress endogenous peroxidase activity, and the slides were immediately incubated in proteinase K (IHCWORLD IW-1101, Woodstock, MD) at 37°C for 10 minutes. Sections were blocked with 3% blocking serum (Vector Laboratories S-2012, Burlingame, CA) for 30 minutes preceding primary antibody incubation for collagen I, collagen II, and aggrecan for 30 minutes (Table 4.1). Following primary antibody (Lifetechnologies, Carlsbad, CA) incubation where all of the primary antibodies were rabbit IgG, slides were exposed to biotinylated secondary antibody (horse anti-rabbit IgG) and ABC reagent (Vectastain ABC kit PK-6200, Burlingame, CA) for 30 minutes each. Lastly, the ABC reagent was added to the sections after washing with PBS and incubated for 30 minutes and then washed again. Visualization was accomplished with ImmPact DAB peroxidase substrate (Vector laboratories SK-4105, Burlingame, CA) before rinsing with distilled water and counter stained with VECTOR hematoxylin QS stain. Following staining, slides were rinsed in tap water; dehydrated in ethanol, cleared in xylene for mounting (Permount SP15-500 Fair Lawn, NJ), and viewed under an upright microscope (Zeiss, Axiomanager 2.0, Thornswood, NY). Negative controls for IHC consisted of isotype IgG controls (Life Technologies) being added instead of the primary antibody.

Statistical analyses

All data are expressed as average \pm standard deviation. Statistical analyses were performed using one-way ANOVA (Minitab 15, Minitab Incorporated, State College, PA), followed by a Tukey's post hoc comparison test for repeated measurements. The statistical significance threshold was set at 0.05 for all tests (with $p < 0.05$)

RESULTS

Live-dead assay

3.1.1 rBMSC

Cell viability overall was quite high. Compared to the 20M aggregate groups, the 10M LA and 10M HA groups had relatively higher densities of live cells at week 3 than at week 0 (Fig. 2). 20M aggregates exhibited some cell death right from week 0, and all of the HA groups had more visible dead cells than the LA groups for both 10M and 20M at week 3 compared to week 0. Among the aggregate groups, 20M HA, 10M HA, and 20M LA had condensed regions of cell death at the aggregate periphery at week 0, whereas cell death was distributed throughout the aggregate at week 3. There was no noticeable increase in aggregate diameter over the 3 weeks for any of the groups. There was increased cell death in week 3 in 20M HA CS compared to week 0, but lesser cell death compared to aggregates.

3.1.2 hWJC

The 10M LA CS group showed higher cell viability at week 3 compared to week 0; and 10M HA CS exhibited its highest cell death rate at week 3 (Fig. 3). 10M LA and HA maintained consistent cell viability; however, similar to the rBMSC group, the 20M groups experienced relatively more cell death than 10M groups at the week 3 time point. It is also important to note that the 10M HA aggregates displayed a tightly condensed aggregate compared to the LA aggregates. Week 3 images visibly demonstrated an apparent decrease in aggregate diameter and an increase in cell death for 20M LA aggregates. Among the CS groups, the 20M HA and CS groups experienced significant cell death at both week 0 and week 3 compared to the LA CS groups, owing to increased cellular density. Compared to the rBMSC groups, hWJC groups

displayed higher viabilities and 20M LA groups were hollow and spherical compared to rBMSC aggregates.

DNA content

rBMSC

The 10M LA CS and 10M HA CS groups increased in DNA content by 2.6% and 2.3%, respectively, from week 0 to week 3 ($p < 0.05$). All other CS groups did not display any statistically significant difference in DNA content with respect to time (Figure 4.4 A&B). Among the aggregate groups, the DNA content of the 10M LA group decreased by 1.9% from week 0 to week 2 with no significant difference at week 3, and the 20M HA group displayed a 2.5% decrease from week 2 to week 3 ($p < 0.05$). There were no other significant changes in DNA content over time for the other aggregate groups. In comparing the aggregate and corresponding CS groups, we saw that at week 0, the DNA content of 10M LA aggregates was 2.7-fold greater than the 10M LA CS ($p < 0.05$), but differences were not significant at other time points.

The differences in DNA contents between the 20M LA and 20M LA CS groups were not statistically significant at any time point.

Among the LA groups, the 10M LA and 20M LA groups did not exhibit any statistically significant differences in DNA content from each other at any time point. On the other hand, the 20M HA group at week 2 had the highest DNA content (18.1 μg) among all of the sample groups ($p < 0.05$). At week 0, the 20M LA CS group had 1.7% more DNA content than the 10M LA CS group, but there were no significant differences in their values at other time points ($p < 0.05$).

hWJC

Among the CS groups (Figure 4.4 C&D), the 10M LA CS, 10M HA CS, 20M LA CS and 20M HA CS groups did not display any significant changes in DNA content over the 3 week period. However among the aggregate groups, only the 10M LA group (Figure 4.4C) exhibited a statistically significant change over time, with a 1.4% increase in DNA content from week 0 to week 2 ($p < 0.05$). In comparing the aggregate and corresponding CS groups, the 10M LA group DNA content was 1.6-fold higher at week 2 compared to its 10M LA CS control group, and at week 3 the DNA content of the 10M HA group was 2.6 times higher than that of its 10M HA CS control group ($p < 0.05$). A comparison between the 10M and 20M groups did not show any significant differences at any time point.

GAG assay

rBMSC

All values are reported on a normalized (to DNA) basis. Among the CS groups, the 10M LA CS group (Figure 4.5A) had a 23% increase in GAG/DNA from week 0 to week 2 ($p < 0.05$) and no significant increase from week 2 to week 3. The 20M LA CS group experienced a 21% increase in DNA content from week 0 to week 2 ($p < 0.05$), and no other significant differences from week 2 to week 3. The 10M HA CS group had a 43% increase in GAG/DNA content from week 0 to week 2, and similarly the 20M HA CS group had a 60% increase in GAG/DNA content from week 0 to week 2 and no statistically significant increase at week 3 ($p < 0.05$). Among the aggregate groups, the 10M LA group had a 26% increase in GAG/DNA content from week 0 to week 2 ($p < 0.05$), but no significant increase from week 2 to week 3. The 20M LA group had a 73% increase at week 2 and 81% increase at week 3 in GAG/DNA content, both relative to week

0 ($p < 0.05$). The 10M HA group (Figure 4.5B) had a 43% increase in GAG/DNA content from week 0 to week 2, and the 20M HA group had an 85% increase in GAG/DNA at week 3 compared to week 0 ($p < 0.05$), although other differences over time for the HA groups were not significant. Comparing the aggregate and corresponding CS control groups, the 20M LA group had a 4.2-fold higher GAG/DNA content compared to its 20M LA CS control group at week 3, and the DNA/GAG content for the 20M HA group was 2.5-fold higher than its 20M HA CS control group at week 3 ($p < 0.05$). In comparing the 10M vs. 20M groups, 10M HA had 2.7-fold higher GAG/DNA content than 20M HA at week 3 ($p < 0.05$). Similarly, in comparing the LA vs. corresponding HA groups, the 20M HA group had a 2.3-fold higher GAG/DNA content than the 20M LA group at week 3 ($p < 0.05$). The 10M LA vs. 10M HA did not display significant differences at any of the time points.

hWJC

None of the CS groups (Figure 4.5 C&D) showed a statistically significant difference in the GAG/DNA content. Except for the 10M HA group, which had a 21% increase in GAG/DNA at week 2 compared to week 0, no other aggregate group experienced any significant changes over time ($p < 0.05$). In comparing the control and aggregate groups, only the 10M HA group had a 2.3-fold higher GAG/DNA compared to the control 10M HA CS at week 2 ($p < 0.01$). All other comparisons, including 10M vs. 20M and LA vs. HA, were statistically insignificant.

Collagen assay

rBMSC

All of the reported values represent collagen content that is normalized to DNA. Among the rBMSC CS groups, only the 10M LA CS group (Figure 4.6 A&B) had a significant change in

collagen content over time, with a 75% decrease in collagen/DNA from week 0 to week 2 ($p < 0.05$). Among the aggregate groups, there were two statistically significant changes over time. First, at week 3, the 20M LA group had a 3.8-fold higher collagen/DNA than at week 0, and the 20M HA group had an 8.5-fold higher collagen/DNA content at week 3 than at week 0 ($p < 0.05$). In comparing the aggregate and corresponding CS control groups, at week 3 only the 20M LA and 20M HA were significantly higher, with 2-fold and 4.6-fold higher collagen/DNA contents relative to their respective CS controls ($p < 0.05$). In comparing the LA vs. HA groups, the 10M HA group exhibited an 8.7-fold higher and 72% higher collagen/DNA content than the 10M LA group, at weeks 0 and 3, respectively ($p < 0.05$). Similarly, at week 3, the 20M HA group had a 4.8-fold higher collagen/DNA content compared to the 20M LA group ($p < 0.05$). Lastly, comparing the 10M vs. 20M groups, we observed that the 20M LA group had a 2.8-fold and 2.3-fold higher collagen/DNA content compared to 10M LA group at weeks 2 and 3, respectively ($p < 0.05$). At week 3 alone, the 20M HA group had 5.6-fold higher collagen/DNA than the 10M HA ($p < 0.05$).

hWJC

Among the hWJC CS groups (Figure 4.6 C&D), only the 10M HA CS group experienced a significant change over time, with a 2.3-fold increase in collagen/DNA content from week 0 to week 2 ($p < 0.05$). Among the aggregate groups, there were two statistically significant changes over time. First, the 10M LA group at week 3 had a 37% increase in collagen/DNA from week 0 to week 3, and the 10M HA group had a 4.9-fold increase in collagen/DNA content from week 0 to week 3 ($p < 0.05$). No other groups had a significant increase over time. In comparing the aggregate groups to their respective CS controls, there were four statistically significant

differences over the period of 3 weeks. First, the 10M LA group at week 3 alone had a 2.7-fold higher collagen/DNA content than its 10M LA CS group ($p < 0.05$). Secondly, the 20M LA group at week 3 alone had a 3.1-fold higher collagen/DNA content than its 20M LA CS control group ($p < 0.05$). In addition, the 10M HA group at week 3 alone had a 2.3-fold higher collagen/DNA content than its 10M HA CS control group ($p < 0.05$). Finally, the 20M HA group at week 0 had a 63% higher collagen/DNA content compared to its 10M HA CS control group ($p < 0.05$).

In comparing LA vs. HA, we observed that only at week 3 the 10M HA group had a 2.7-fold higher collagen/DNA content compared to the 10M LA group ($p < 0.05$). There were no other statistically significant changes over time for any other group. In comparing the 10M vs. 20M groups, there was only one significant difference. At week 0, the 20M HA group had a 7.5-fold higher collagen/DNA content than the 10M HA group, but, at week 3, the 20M HA had a 74% lower collagen/DNA than the 10M HA group ($p < 0.05$).

Gene Expression

rBMSC

Collagen I:

The 10M LA CS group (Figure 4.7 A&B) had a 3.5-fold increase in expression in collagen I gene expression from week 0 to week 2, and the 20M LA CS group had a 10.2-fold increase in collagen I expression from week 0 to week 3 ($p < 0.05$). The 10M HA CS group did not show any significant increase in gene expression over time, but the 20M HA CS group had a 97.5% increase in gene expression from week 0 to week 2 ($p < 0.05$). Among the aggregate groups, there were two significant changes in gene expression over time. First, the 20M LA group had a

5.6-fold increase at week 2 compared to week 0 and no significant increase at week 3 ($p < 0.05$). Second, the 10M HA group had a 3.6-fold increase in gene expression at week 2 compared to week 0 and no significant increase at week 3 ($p < 0.05$). The other aggregate groups (10M LA and 20M HA) did not show statistically significant changes over time. In comparing the aggregate and corresponding CS control groups, at week 3, the 10M HA group had a 1.7-fold higher collagen I expression compared to its respective CS control group ($p < 0.05$).

In comparing the 10M vs. 20M groups, we observed that only at week 0, the 20M LA group had 83% lesser collagen I gene expression than the 10M LA group ($p < 0.05$). In comparing the LA vs. HA groups, we observed only one significant difference. At week 3, the 10M HA group had a 2.2-fold higher collagen I gene expression than the 10M LA group ($p < 0.05$). No other differences were significant.

SOX9:

The 10M HA CS group (Figure 4.7 C&D) had a 3.1-fold increase in SOX9 expression from week 0 to week 2, and the 20M HA CS group had a 57% decrease in expression from week 0 to week 2 ($p < 0.05$). Among the aggregate groups, the 10M LA group had a 4.5-fold increase in SOX9 gene expression from week 2 to week 3, and the 20M LA group at week 2 had a 34% increase in SOX9 expression compared to week 0 ($p < 0.05$). Additionally, the 10 HA group also had a 27% increase in SOX9 gene expression from week 2 to week 3 ($p < 0.05$). In comparing aggregate and control groups, we observed that at week 2, the 10M LA group had a 2.8-fold higher SOX9 expression compared to its CS control group ($p < 0.05$). At week 2 and week 3, the 20M HA group had a 4.1-fold and 3.8-fold higher SOX9 expression compared to its CS control

($p < 0.05$), and the 10M HA group had a 1.4-fold higher SOX9 gene expression compared to its CS control group ($p < 0.05$).

In comparing the 10M vs. 20M groups, we observed only one statistically significant difference. At week 3, the 20M HA group had a 2.6-fold higher SOX9 gene expression than the 10M HA group ($p < 0.05$). In comparing the LA vs. HA groups, we observed that at week 0, the 10M LA group had a 3.6-fold higher SOX9 expression than the 10M HA group, but at week 3 the 10M HA group had a 5.4-fold higher expression than 10M LA group ($p < 0.05$).

Aggrecan:

At week 2, the 10M HA CS and 20M HA CS groups (Figure 4.7 E&F) exhibited a 4.0-fold increase and 47% decrease, respectively, in aggrecan gene expression compared to week 0 ($p < 0.05$), although no changes were significant at week 3. There were no other significant differences in expression by the CS groups at any other time point. Among the aggregate groups, the 20M LA group at week 3 had a 9.0-fold increase in aggrecan expression from week 0 to week 3 ($p < 0.01$). At week 3, the 20M HA group had a 54% decrease in expression from week 0 ($p < 0.05$). In comparing the aggregate and respective control groups, the 10M and 20M LA group had a 3.0-fold higher and 2.5-fold higher aggrecan gene expression than their CS control groups ($p < 0.05$). Similarly, the aggrecan expression in the 20M HA aggregates were 8.3-fold, 2.6-fold, and 3.1-fold higher than the respective CS control group at weeks 0, 2 and 3, respectively ($p < 0.05$).

In comparing the 10M vs. 20M groups, we observed only one significant difference. At week 0, the 20M HA group had a 8.3-fold higher aggrecan gene expression than the 10M HA group ($p < 0.05$). In comparing the LA vs. HA groups, we observed that there were two statistically significant differences. First, at week 3, the 10M LA group had a 4.4-fold higher aggrecan gene

expression than the 10M HA group ($p < 0.05$). Lastly, at week 0, the 20M HA group had a 8.6-fold higher aggrecan gene expression than the 10M HA group ($p < 0.05$). The Collagen X and Runx2 gene expression data were not reported for the rBMSC cell line because the primers led to highly variable results that were not reliable in allowing for comparisons to be made, and thus the data were discarded from the manuscript.

hWJC

Collagen I:

The CS groups (Figure 4.8A) did not have any significant changes in gene expression over the 3-week period. Among the aggregate groups, the 10M HA group had an 8.7-fold increase in collagen I gene expression from week 0 to week 3 ($p < 0.05$). The 20M LA group had a 4.0-fold and 5.5-fold increase in gene expression at week 2 and week 3, respectively, relative to week 0 ($p < 0.05$). In addition, the 10M HA group had a 3.5-fold increase in collagen I gene expression from week 0 to week 3 ($p < 0.05$). In comparing the aggregates to their CS controls, we discovered only one significant difference: at week 3, the 10M LA group had a 10-fold higher collagen I gene expression compared to its CS control ($p < 0.05$).

In comparing the 10M vs. 20M groups, we observed that at week 2, the 20M LA group had a 2.3-fold higher collagen I expression than the 10M LA group ($p < 0.05$). However, at week 3, the 10M LA group had a 3.3-fold higher collagen I gene expression than the 20M LA group ($p < 0.05$). In comparing the LA vs. HA groups, it was seen that only at week 3, the 10M LA group had a 4.8-fold higher collagen I gene expression than 10M HA group ($p < 0.05$). The comparisons between the 20M LA and 20M HA groups were not significant.

SOX9:

Among the CS groups (Figure 8B), there was a 4.9-fold increase in SOX9 gene expression from week 0 to week 3 for the 20M LA CS group ($p < 0.05$). The 10M HA CS group had a 2.2-fold increase in SOX9 gene expression from week 2 to week 3 ($p < 0.05$). Among the aggregate groups, the 10M LA group had a 5.0-fold higher expression from week 0 to week 3, and the 20M LA group had a 5.6-fold expression from week 2 to week 3 ($p < 0.05$). In comparing the CS and aggregates we discovered that the 20M LA aggregates had a 2.3-fold expression at week 3, compared to the control group ($p < 0.05$).

In comparing the 10M vs. 20M groups, the 20M LA group had a 4.2-fold and a 2.3-fold higher SOX9 gene expression than 10M LA group at week 2 and week 3, respectively ($p < 0.05$). The 10M HA group had a 5.8-fold and a 7.3-fold higher expression in SOX9 compared to 20M HA at week 2 and week 3, respectively ($p < 0.05$). In comparing the LA vs. HA groups we observed that there were no significant difference in expression between 10M LA and 10M HA at any time point. However, the 20M LA group had a 5.5-fold and a 7.2-fold higher gene expression than the 20M HA group at week 2 and week 3, respectively ($p < 0.05$).

Aggrecan:

Among the CS groups (Figure 8C), the 10M LA CS group had a 5.8-fold increase in aggrecan gene expression only from week 0 to week 3 ($p < 0.05$). The other groups (10M HA CS, 20M LA CS, 20M HA CS) did not show any significant changes over time. Among the aggregate groups, the 10M HA group had a 9.3-fold increase in aggrecan expression from week 2 to week 3, and the 20M LA group had a 6.1-fold increase in aggrecan expression from week 0 to week 3

($p < 0.05$). Finally, the 10M HA and 20M HA groups had 4.4-fold and 3.7-fold increases, respectively, in aggrecan gene expression from week 0 to week 3 ($p < 0.05$).

In comparing the aggregate and control groups, there was only one significant difference. At week 3, the 20M HA group had a 2.1-fold higher aggrecan expression than its CS control ($p < 0.05$). No other comparisons between the aggrecan expressions of aggregate and CS were statistically significant.

In comparing the 10M vs. 20M groups, we observed that at week 2, the 10M LA group had 3.1-fold and 2.7-fold higher aggrecan expression than the 20M LA group at weeks 2 and 3, respectively ($p < 0.05$). In contrast, for the HA groups, the 20M HA group had a 3.3-fold higher aggrecan gene expression than 10M HA group at week 3 ($p < 0.05$). In comparing the LA vs. HA groups, the 10M HA group had a 4.5-fold higher aggrecan gene expression than the 10M LA group at week 0 ($p < 0.05$), but no significant differences at weeks 2 or 3. The 20M HA group had 2.7-fold and 13.1-fold higher aggrecan gene expression than the 20M LA group at weeks 0 and 3, respectively ($p < 0.05$).

Collagen X:

Among the CS groups (Figure 8D), only the 10M HA CS group displayed a significant change over time, with a 7.5-fold increase in collagen X gene expression from week 0 to week 3 ($p < 0.05$). The other CS groups (10M LA CS, 20M LA CS, and 20M HA CS) did not display significant changes in expression over time. Coming to the aggregate groups, there was only one significant change in expression. The 10M LA group had 8.3-fold and 2.2-fold increases in collagen X expression from week 0 to week 2, and week 0 to week 3, respectively ($p < 0.05$). Comparing the aggregate and CS groups, the 10M LA group had 3.5-fold and 10.3-fold higher

collagen X gene expression at weeks 2 and 3, respectively, compared to its CS control group ($p < 0.05$). Moreover, the 20M HA group had a 3.8-fold higher collagen X expression than its CS control group ($p < 0.05$).

In comparing the 10M and 20M groups, at week 3 alone, the 10M LA group had a 5.4-fold higher collagen X gene expression compared to the 20M LA group ($p < 0.05$). In addition, the 20M HA group had 8.6-fold and a 2.9-fold higher collagen X gene expression compared to the 10M HA group at weeks 0 and 3, respectively ($p < 0.05$). In comparing the LA vs. HA groups, we observed that the 10M LA group had a 5.8-fold and a 7.8-fold higher collagen X expression than the 10M HA group at weeks 2 and 3, respectively ($p < 0.05$). The 20M HA group had a 4.7-fold and a 6.3-fold higher collagen X gene expression than the 20M LA group at weeks 0 and 2, respectively ($p < 0.05$).

Runx2:

The 10M HA CS group (Figure 4.8E) had a 2.5-fold increase in Runx2 expression from week 0 to week 2, but no statistically significant increase at week 3 ($p < 0.05$). The 10M HA CS group had a 6.0-fold increase in Runx2 gene expression only from week 0 to week 3 ($p < 0.05$). Among the aggregate groups, the 20M HA group had a 97% decrease in Runx2 expression from week 0 to week 3 and the 10M HA group had a 5.6-fold increase from week 0 to week 3 ($p < 0.05$). In comparing the aggregates and CS control groups, we observed only one statistically significant difference. At week 0, the 20M HA group had a 5.6-fold higher gene expression than its CS control group ($p < 0.05$).

In comparing the 10M vs. 20M groups, we observed that at week 3 alone, the 10M LA group had a 8.3-fold higher Runx2 expression than 20M HA group ($p < 0.05$). In comparing the LA vs. HA

groups, we observed that at week 3 alone, the 10M HA group in turn had a 3.5-fold higher expression than 10M LA group ($p < 0.05$).

Immunohistochemistry

rBMSC

IHC staining of the rBMSC aggregates revealed that the diameter of the aggregates decreased over the 3-week period, specifically the 10M HA (Figure 4.9) and 20M LA aggregates. In contrast, the 20M HA aggregates increased in size from week 0 to week 3. Except for the 10M HA group that showed increased collagen I staining at week 2 compared to week 0, collagen I staining did not increase with time for any other group. Collagen II and aggrecan staining were more intense in the 20M group for LA (especially at 2 weeks), but more intense in the 10M group for HA (especially at 3 weeks).

hWJC

Collagen I stain was prominent in the center of the aggregate for the 20M LA group at week 3 (Figure 4.10). Collagen I did not increase in staining intensity over the 3 week period except for the 10M LA and 20M LA group, where the collagen I staining was highest at week 3. 20M HA showed highest collagen II staining at week 3. Aggrecan presented a very interesting staining pattern in the 10M LA and 20M HA groups, as both of these groups had starting aggrecan staining at week 0 to be the most intense (throughout the aggregate) and at week 3, staining was localized to specific patches near the center (10M LA) and around the periphery (20M HA). The 20M LA group were also striking for its intense aggrecan staining at week 3.

DISCUSSION

This is the first attempt to explore the potential of hWJC aggregates, and also the first to compare hWJC and rBMSC aggregates with CS in the context of chondrogenesis. Cell-based approaches have been recently explored to regenerate several organ types, serve as a model for drug testing and routinely used in high throughput screening applications.^{60, 112, 186, 272} The use of stem cell aggregates for differentiation into the cartilage phenotype is a promising avenue for cartilage regeneration because of the ability to mimic mesenchymal condensation and provision of favorable microenvironment for cell differentiation. Hydrogel-based strategies are especially well poised to capitalize on these advantages by moving away from suspensions of individual cells to aggregate based strategies.

Successful cell-based approaches have been reported using methods such as cell sheet technology, employing human embryonic stem cell aggregates and bioprinting cell-laden microcarriers, and have reported different results with respect to matrix biosynthesis and chondrogenesis.^{22, 57, 68, 146} Cell-sheet technology has broadly been used in the sense of cell-based approaches, although attempts are now being made to classify them into more refined ways.⁷⁴ A few other groups looked into rat and mammalian stem cell aggregates, but did not employ the bone marrow or Wharton's jelly cell type and the specific aggregate sizes used in the current study was not considered,^{185, 211, 243} as well. Our group has published several reports on hWJC cells for multiple applications, including chondrogenesis,^{10, 167, 258} and we are pleased to report that by far, the current aggregate system has produced the highest aggrecan and SOX9 gene expression and corresponding staining for aggrecan IHC compared to our previous studies.

The current study further attempted to understand the influence of the number of aggregates per hydrogel, the number of cells per aggregate, and compared and contrasted the results with the

conventional CS approach (Table 4.2). Lastly, the study served as a great opportunity to compare the chondrogenic performance of hWJC compared to rBMSC, a well-established cell source for musculoskeletal tissue engineering applications.^{168, 256} Although the current study may not be able to conclusively prove the mechanisms by which the aggregates consistently outperformed the CS groups, it might be possible that the presentation of cells in a condensed manner allows better intercellular communication and such a high cell to cell interaction may be the basis for chondrogenesis.

The cell viability and DNA content of all rBMSC aggregates had a higher starting DNA content (Figure 4.3 and 4.4) at week 0, however, at week 3, the CS and aggregate groups had comparable DNA content, perhaps due to a lack of adequate nutrient supply and space to proliferate. All of the hWJC aggregates followed a similar pattern with the aggregates having a higher starting DNA content compared to the CS controls at week 0, and at week 3 both groups (CS and aggregates) had comparable DNA content (Figure 4.4). For the rBMSC group, both LA and HA groups had the same starting GAG/DNA content at week 0. But at week 3, the 20M HA group had a 3 fold increase compared to 20M LA suggesting that the aggregate number had an impact on GAG/DNA biosynthesis. However, the hWJC aggregates did not have any statistically significant increase in GAG biosynthesis compared to the control groups at any time point. On a per DNA basis for the rBMSC group, the 20M LA and 20M HA groups had the highest collagen content (Figure 4.6) at week 3 compared to their control groups. Taken together, findings reveal that on a per cell basis, both rBMSC and hWJCs did better in matrix biosynthesis and chondrogenesis when in aggregates than in free cell suspension. Secondly, the cell density seemed to impact the biosynthesis (i.e., 20M better than 10M) than for chondrogenesis (i.e., both

20M and 10M groups did well). Moreover, the number of aggregates also mattered more for biosynthesis (i.e., HA outperformed LA) than for chondrogenesis. In the future, it will be necessary to explore which parameter values and aggregate formation methods are most supportive of chondrogenesis, but at least here we have demonstrated that the concept of aggregates to enhance chondrogenesis in hydrogels, with two different stem cell sources, is worth exploring, and that manipulation of parameters can impact the level of improvement.

Some of the limitations in the current study extended to spatial and temporal control of aggregate placement in the agarose gels that may be addressed by a fully automated system that can direct aggregate placement. In the current study, agarose was used merely as a proof of concept method to demonstrate the impact of aggregation on cellular differentiation. In this sense, future studies could use cellular aggregates in conjunction with bioactive hydrogel materials such as functionalized poly(ethylene glycol), hyaluronic acid and other ECM-derived hydrogels to name a few.^{17, 21, 231} For the current study, it should also be noted that aggregates were directly harvested from the petri-dish and encapsulated into the agarose gels instead of chondrogenically inducing the aggregates. Recently, it has been reported that exposure of aggregates to chondroinductive media prior to encapsulation provides an extremely favorable environment for the aggregates to be “primed,” which drives chondrogenic differentiation.^{38, 83, 217} According to our data, further optimization of differentiation media, aggregate priming, and a longer duration of the study, will be required to achieve a molecular phenotype similar to that of a healthy articular cartilage, as is desired for cartilage tissue engineering.

CONCLUSIONS

In the current study, we successfully designed and fabricated aggregate-encapsulated agarose hydrogels with varied cell concentration and aggregate numbers, resulting in improved GAG content, DNA content, collagen content with increased gene expression of collagen II and aggrecan, and darker IHC staining for collagen and aggrecan compared to the CS control groups. Additionally, significant improvement in performance compared to the cell suspension control groups suggested that the aggregate approach could be a new way of looking at cells used for cartilage regeneration. The aggregate technique presents a simple, robust method of presenting cells as clusters, which, due to inherent interaction and cell-cell communication, and may prove to be a better choice than the conventional cell-suspension-in-hydrogel approach for cell-encapsulated hydrogel approaches for cartilage tissue engineering in the future.

CHAPTER 5: Generating Chondromimetic Mesenchymal Stem Cell Spheroids by Regulating Media Composition and Substrate Coating⁴

ABSTRACT

Spheroids of mesenchymal stem cells (MSCs) in cartilage tissue engineering have been shown to enhance regenerative potential owing to their 3D structure. In the current study, rat bone marrow-derived MSCs were organized into cell spheroids by the hanging drop technique and subsequently cultured on hyaluronic acid (HA) coated or non-coated well plates under different cell media conditions. We demonstrated that for chondrogenic applications, MSC spheroids derived on HA-coated surfaces outperformed the non-coated spheroids in matrix synthesis and gene expression of chondrogenic markers. In particular, spheroids on HA-coated surfaces gave rise to the highest collagen and glycosaminoglycan production when primed with medium containing insulin-like growth factor (IGF) for a period of one week. The current study suggested that inductive surfaces and growth factors might influence the chondrogenesis at different time points suggesting the importance of a long-term study in the future. Such tailored bioactivity of the stem cell spheroids may give rise to a platform technology that may eventually produce spheroids capable of chondrogenesis achieved by surface coating and media manipulation over time.

⁴ Under preparation as **Sridharan B.**, Laflin AD., Detamore M.S., “Generating Chondromimetic Mesenchymal Stem Cell Spheroids by Regulating Media Composition and Substrate Coating” Cellular and Molecular Engineering, 2015.

INTRODUCTION

Autologous chondrocytes are a limited resource due to donor site availability, tissue morbidity, and waiting period for expansion in culture. Several studies have illustrated the promise that multipotential mesenchymal stem cells (MSCs) hold for chondrogenesis, osteogenesis, adipogenesis and other musculoskeletal applications, including current clinical trials.^{13, 120, 137, 198}

Often the regenerative benefits are lost after successive passaging and expansion of cells *in vitro*, which relies on culturing them a non-physiologic monolayer.^{189, 226} 3D culture overcomes some of the limitations presented by the monolayer culture system. For example, assembly of MSCs as cell spheroids by the pellet culture technique has long been employed for increasing the chondrogenic potential under *in vitro* conditions.^{6, 265, 270} Forming 3D cell spheroids by the conventional hanging drop method has been suggested as a means to enhance the therapeutic potential and has been shown to elicit anti-inflammatory effect of MSCs.^{14, 15, 136, 269} Recent reports have demonstrated that the use of MSC spheroids formed by hanging drop or suspension culture enhanced their therapeutic potential for cartilage regeneration *in vivo*.^{80, 136, 163} Similarly, growing MSCs on surfaces with different surface stiffness have also yielded viable spheroids with great stemness and differentiation capabilities.^{139, 153, 253}

Hyaluronic acid (HA) is a linear anionic polysaccharide composed of long chains of repeating disaccharide units of D-glucuronic acid and *N*-acetyl-D-glucosamine.^{76, 244} In cartilage extracellular matrix (ECM), HA is the backbone of aggrecan superstructure complexes,³² and it is commonly employed as a biomaterial for cartilage tissue engineering. For the current study,

we explored the potential of HA as a surface coating agent to evaluate its impact on MSC spheroid differentiation.

We hypothesized that MSCs that were formed into 3D spheroids, cultured in HA-coated well-plates and primed under different medium compositions would exhibit increased survival and chondrogenic gene expression compared to spheroids in control medium under non-coated conditions. To test this hypothesis, we examined the chondrogenic potential of MSC spheroids that were first subjected to either HA-coated or non-coated conditions. To further explore the influence of raw materials and growth factor under culture conditions, the spheroids were subjected to serum-rich or serum free medium with either transforming growth factor (TGF)- β_3 , insulin-like growth factor (IGF)-1, chondroitin sulfate (CS), and aggrecan. Lastly, an additional group was added where the medium was changed from TGF- β_3 to IGF-1 after 3 days of culture (TGF \Rightarrow IGF). The experimental group and controls were tested for cell viability and chondrogenic applications through gene expression, immunohistochemistry and matrix content.

MATERIALS AND METHODS

Cell culture and expansion

Rat bone marrow-derived mesenchymal stem cells (rBMSCs) were harvested from the femurs of seven young male Sprague–Dawley rats (176–200 g, Charles River) following a University of Kansas approved IACUC protocol (175–08). The IACUC protocol approved the cellular harvest procedure and usage of cells for this particular study. The cells were isolated according to a previously reported protocol.¹⁶⁹ Briefly, isolated cells were cultured in control medium (α MEM supplemented with 10% Certified FBS and 1% Penicillin-Streptomycin (Pen-Strep)) (Invitrogen

Life Technologies, Carlsbad, CA) and passaged at 80% confluence until passage 4 (P4). As reported earlier, all of the cells from 14 different femurs were pooled together at P4 for use in the study.

Preparation of HA-coated well plates

HA sodium salt of medical grade (Lifecore Biomedical, Chaska, MN, USA) was obtained as a dry powder. According to the information from the supplier, the HA molecular weight was between 200-350 kDa. Well plates were coated with HA according to a previously reported protocol.¹³⁹ Briefly, polylysine-coated 96-well plates (Sigma-Aldrich) were cleaned ultrasonically in acetone and then rinsed with ethanol. A deionized water rinse was used to remove liquid chemicals followed by a nitrogen purge. 300 μ L of 1 mg/mL aqueous solution of HA was pipetted into a single well of a 96-well plate and air-dried in a sterile environment for 3 days at 25 °C to prepare the HA-coated surfaces.

Cellular aggregate formation

Spheroids were generated by the hanging drop technique according to a previously reported protocol.^{15, 267} Cellular suspensions (rBMSC) were prepared at concentration of 10×10^6 cells/mL in medium. Droplets of cell suspensions (cells with corresponding medium, see below) at a volume of 10 μ L were pipetted onto the inside surface of a sterile petri dish lid in an array using a 10 μ L pipette (Eppendorf, Hauppauge, NY), making sure that the droplets have a safe distance between each other to prevent mixing. The cells were allowed to aggregate overnight, with the help of gravity when the petri dish lid was reversed (Fig. 1). The sterile petri dish bottom was then filled with PBS to prevent drying of these droplets. After 24 h, the cell spheroids were

collected from the dish with the help of a 1 mL pipette and placed into well plates (1 spheroid per well) and cultured in the same medium composition in which the spheroids were formed.

Spheroids were created in one of six different types of medium, including control medium, and then placed on either a coated or non-coated surface, where the spheroids then continued in the same medium in which they were formed (Fig. 1). The one exception was the TGF/IGF group, where spheroids were formed in TGF medium, then cultured in TGF medium for 3 days before being switched to a different medium (i.e., IGF medium). The spheroids were harvested after 24 h, and were either processed directly for different assays (i.e., the week 0, or “hanging drop” time point), or placed in well plates for additional culture. In the well plates, one set of spheroids were placed in HA-coated well plates, where the medium was changed every other day and samples were collected at 24 h and 7 days (to evaluate changes over time for the experimental coating surface). The other set of spheroids were placed under regular 96 well plates that were not coated with HA, where the medium was changed every other day and samples were collected at 7 days (providing a control surface comparison for the experimental coating surface at the final time point).

The six medium groups used for aggregate formation and culture were as follows (Fig. 1):

Control group: The control medium consisted of α MEM, 10% FBS and 1% Pen-Strep.

TGF group: TGF medium consisted of low glucose DMEM, 1% Pen-Strep, and 5 ng/mL TGF- β_3 (PeproTech, Rocky Hill, NJ).

IGF group: IGF medium consisted of low glucose DMEM, 1% Pen-Strep, and 100 ng/mL IGF-1 (PeproTech, Rocky Hill, NJ).

CS group: CS medium consisted of low glucose DMEM, 1% Pen-Strep, and 40 μ g/mL CS (Catalog number: C3788, Sigma-Aldrich).

Aggrecan group: Aggrecan medium consisted of low glucose DMEM, 1% Pen-Strep, and 40 µg/mL aggrecan (Catalog number: A1960, Sigma-Aldrich).

TGF ⇒ IGF group: Spheroids were formed in TGF medium, and then conditioned with the TGF medium in well plates for the first 3 days. After medium removal at the end of day 3, IGF was added to the spheroids for 4 additional days. Given that this group was identical to the TGF group at the hanging drop and 24 h time points, only the 7 day time point was run for this group (only coated).

Cell viability assay

To check the viability of the spheroids, a fluorescent live/dead viability staining kit (Invitrogen, Carlsbad, CA) was used at day 0 and 7 days. The samples (n = 3) were washed once with phosphate-buffered saline (PBS) and incubated in live/dead staining solution (0.5 µL calcein and 2.0 µL ethidium homodimer (ETH) diluted in 1 mL PBS) for 10 min (37°C, 5% CO₂). The samples were once again washed with PBS prior to imaging using an inverted epifluorescent microscope (Zeiss-LSM 710, Thornwood, NY). Live and dead cells were stained green and red, respectively.

DNA analysis

Spheroids were placed in a papain digestion solution consisting of 125 mg/mL papain, 5 mL N-acetyl cysteine, 5 mL ethylenediaminetetraacetic acid and 100 mL PBS (all reagents from Sigma-Aldrich, St. Louis, MO) in distilled water overnight in a 60°C water bath. On the following day, sample digests (n = 5) were centrifuged for 5 minutes and stored at -20 °C until further use. DNA content was quantified for all samples utilizing a PicoGreen kit (Life

technologies) according to the manufacturer's instructions. Previous studies from our group (unpublished) established a conversion factor of 7.7 pg/cell that may be used to convert DNA content to cell number.

Glycosaminoglycan assay

Spheroids (n = 5) were digested with the aforementioned papain digesting solution and left in a 60°C water bath overnight prior to measuring glycosaminoglycan (GAG) content. GAG content was measured with a Sircol DMMB assay kit and the manufacturer's protocol (Biocolor B1000, Belfast, U.K.) was followed. 1.0 mL of dimethylmethylene blue dye solution was added to 100 µL of sample, standards provided in the kit (Chondroitin sulfate, Sigma-Aldrich), and blank. Solutions were mixed slowly for 30 minutes and centrifuged for 10 minutes. The supernatant was discarded and the pellet was resuspended, and 1.0 mL of dissociation solution was added. The solutions were vortexed and transferred to a 96-well plate and ran at 656 nm in a microplate reader.

Collagen assay

For quantifying collagen production, a Sircol soluble collagen assay kit and manufacturer's protocol were used (Biocolor, s5000, Belfast, U.K.). Briefly, samples (n = 4) were incubated in .1 mg/mL pepsin in 0.5 M acetic acid (Sigma-Aldrich P7012) and placed overnight at 4°C. 1.0 mL of Sircol dye reagent and 100 µL of each standard (collagen standards provided by the manufacturer) and sample were mixed slowly for 30 minutes. Solutions were centrifuged at 12,000 rpm for 10 minutes and the resulting supernatant discarded, keeping the pellet intact. The previous step was repeated after the addition of 750 µL of ice-cold acid salt wash. The pellet was

resuspended and to this 250 μL of alkali reagent was added. Solutions were then vortexed thoroughly and 200 μL of the solution was transferred to a 96-well plate and ran at 555 nm in a microplate reader.

Gene expression analysis

Real-time reverse transcriptase polymerase chain reaction (RT-PCR) was used to assess gene expression levels for collagen types I, II, SOX9, and aggrecan ($n = 5$). To each sample 1.0 mL of lysis buffer (Qiagen, Germantown, MD) was added, and after 1 hour, the solutions were passed through a QIAshredder column (Qiagen 79656, Germantown, MD) to extract messenger RNA (mRNA) in accordance with the RNEasy Plus Mini Handbook (Qiagen 74136, Germantown, MD) ($n = 4$). A high capacity cDNA reverse transcription kit (Applied Biosystems 4368814, Foster City, CA) allowed reverse transcription of mRNA to complementary DNA (cDNA); 2x RT Master Mix was prepared using the kit's protocol. 10 μL of the master mix and RNA samples were combined in a 96-well plate. The well plate was then loaded into an Eppendorf Realplex Mastercycle (Eppendorff, 5345 Hauppauge, NY). cDNA concentrations were normalized with DNASE-free water, and a Taqman gene expression assay kit (Applied Biosystems 1325810, Foster City, CA) provided the primers for the above-mentioned genes. 1 μL of cDNA from each sample, 10 μL of universal fast master mix (2x), and 1 μL of a specific primer were mixed in a 96-well plate. RT-PCR reactions were run in an Eppendorff Realplex system.

Immunohistochemistry

Spheroids were fixed, cleared in xylene, dehydrated and embedded in paraffin blocks until further use. The sections were generated using a microtome and sectioned to a thickness of 4 μm . Sections ($n = 3$) were immersed in xylene; rehydrated in graded ethanol and rehydrated in deionized water for 5 minutes (all reagents from Sigma-Aldrich). The sections were exposed to 3% hydrogen peroxide in methanol for 10 minutes to suppress endogenous peroxidase activity and immediately the slides were incubated in proteinase K (IHCWORLD IW-1101, Woodstock, MD) at 37°C for 10 minutes. Sections were blocked with 3% blocking serum (Vector Laboratories S-2012, Burlingame, CA) for 30 minutes preceding primary antibody/ isotype (IgG) control antibodies incubation for collagen I, collagen II, and aggrecan for 60 minutes (Table 3). Following primary antibody incubation, slides were exposed to biotinylated secondary antibody and ABC reagent (Vectastain ABC kit PK-6200 Vector laboratories) for 30 minutes each. Lastly, the ABC reagent was added to the sections after washing with PBS and incubated for 30 minutes and then washed again. Tissue staining was accomplished with ImmPact DAB peroxidase substrate (Vector laboratories SK-4105) before rinsing with distilled water and counter stained with VECTOR hematoxylin QS stain (Vector laboratories H-3404). Following staining, slides were rinsed in tap water; dehydrated in ethanol; cleared in xylene for mounting (Permount SP15-500 Fair Lawn, NJ) and viewed under an upright microscope (Zeiss, Imager A2).

Statistical analyses

All data were expressed as mean \pm standard deviation. Statistical analyses were performed using one-way ANOVA (Minitab 15, Minitab Incorporated, State College, PA) followed by a Tukey's post hoc comparison test for repeated measurements. The statistical significance threshold was set at 0.05 for all tests (with $p < 0.05$).

RESULTS

Cell viability assay

Cell viability was high overall for the spheroids that were isolated right after the hanging drop procedure (Fig. 2). When the spheroids were placed in HA-coated plates, there was an apparent decrease in spheroid diameter. By 7 days, the coated groups had roughly half the cell viability for the aggrecan, IGF, and the TGF \Rightarrow IGF group. In fact, the IGF and CS groups lost their spherical shape and only spheroid fragments were stained. Similarly, in the 7-day non-coated groups, only the TGF group maintained its spherical morphology. The control medium group (10% FBS) completely disintegrated, and the spheroids in the aggrecan and CS group were disintegrated.

DNA Content

Within each given medium group, DNA content differences over time were statistically significant between the hanging drop time point (Fig. 3) (i.e., $t = 0$, prior to placing on any surface) and the 7 day time points, for both the coated and uncoated surfaces. The control medium group DNA content dropped by 43.7% and 61.4% from $t = 0$ to day 7 for the coated and non-coated surfaces, respectively ($p < 0.05$). The TGF group DNA content dropped by 40.6% and 44.9% from $t = 0$ to day 7 for the coated and non-coated surfaces, respectively ($p < 0.05$). The IGF group DNA content dropped by 56.4% and 95.3% from $t = 0$ to day 7 for the coated and non-coated surfaces, respectively ($p < 0.05$). The CS group DNA content dropped by 97.2% and 84.5% lower DNA content from $t = 0$ to day 7 for the coated and non-coated surfaces, respectively ($p < 0.05$).

The aggrecan group DNA content dropped by 81.7% and 32.6% from $t = 0$ to day 7 for the coated and non-coated surfaces, respectively ($p < 0.05$). The TGF \Rightarrow IGF group DNA content

dropped by 93.2% from $t = 0$ to day 7 for the coated surface ($p < 0.05$). No statistically significant differences in DNA content were noted among groups at $t = 0$, 24 h or on either surface at 7 days.

GAG content

Statistically significant increases in GAG/DNA content were observed in all six groups (including control) for both surfaces by 7 days, but only the control group had a significant increase by the 24 hour time point. The control medium group had 5.0-fold and 6.8-fold increases in GAG/DNA content (Fig. 4) from $t = 0$ to 24 h and 7 days on the non-coated surface, respectively ($p < 0.05$). The TGF group had 2.7-fold and 2.4-fold increases in GAG/DNA content from $t = 0$ to day 7 for the coated and non-coated surfaces, respectively ($p < 0.05$). The IGF group had a 9.3-fold increases in GAG/DNA content from $t = 0$ to day 7 for non-coated surface ($p < 0.05$). The CS group had 3.3-fold and 7.5-fold increases in GAG/DNA content from $t = 0$ to day 7 for coated and non-coated surface, respectively ($p < 0.05$). The aggrecan group had 3.4-fold and 1.4-fold increases in GAG/DNA content from $t = 0$ to day 7 for the coated and non-coated surfaces, respectively ($p < 0.05$). Among the groups on the HA-coated surface at day 7, the TGF and IGF groups had 1.6 and 1.1 times higher GAG/DNA contents compared to the control group, respectively ($p < 0.05$), with no other statistically significant differences. Finally, the aggrecan group had a 23.5% lower GAG/DNA content from $t = 0$ to day 7 for non-coated surface ($p < 0.05$).

Collagen content

There were no statistically significant increases in collagen content for any group from the hanging drop ($t = 0$) point to the 24 hour time point, although the following significant increases

were noted by 7 days. First, the control group had 5.3-fold and 5.1-fold increases in collagen/DNA content (Fig. 5) from $t = 0$ to day 7 for the coated and non-coated surfaces, respectively ($p < 0.05$). The TGF group had a 6.3-fold increase in collagen/DNA content from $t = 0$ to day 7 for the coated surface ($p < 0.05$). The IGF group had 11.7-fold and 26.1-fold increases in collagen/DNA content from $t = 0$ to day 7 for the coated and non-coated surfaces, respectively ($p < 0.05$). The CS group had 16.5-fold and 11.8-fold increases in collagen/DNA content from $t = 0$ to day 7 for the coated and non-coated surfaces, respectively ($p < 0.05$). The aggrecan group had a 2.7-fold increase in collagen/DNA content from $t = 0$ to day 7 for the non-coated surface ($p < 0.05$). Finally, the TGF \Rightarrow IGF group had a 13.9-fold increase in collagen/DNA content from $t = 0$ to day 7 for the coated surface ($p < 0.05$). In comparing the collagen/DNA values between the control group and each of the other groups at the same time point, there were two statistically significant differences. At day 7 on the coated surface, the CS group had a 3.3-fold higher collagen/DNA content than the control group ($p < 0.05$). At day 7 on the non-coated surface, the IGF group had a 6.7-fold higher collagen/DNA content compared to the control media group ($p < 0.05$).

Gene expression analysis

Aggrecan:

There was no statistically significant change in aggrecan gene expression (Fig. 7) for the control group over time. Coming to the TGF group, there were 23.4%, 68.9%, and 37.4% decreases in aggrecan gene expression from $t = 0$ to 24 h and day 7 for the coated and non-coated surfaces, respectively ($p < 0.05$). For the IGF group, there were 35.6%, 85.4% and 98.5% decreases in gene expressions from $t = 0$ to 24 h and day 7 for the coated and non-coated surfaces,

respectively ($p < 0.05$). The CS group had 76.4%, 79.2%, and 71.3% decreases in gene expression from $t = 0$ to 24 h and day 7 for the coated and non-coated surfaces, respectively ($p < 0.05$). The aggrecan group also had decreases of 45.7%, 38.4%, and 54.4% in aggrecan gene expression from $t = 0$ to 24 h and day 7 for the coated and non-coated surfaces, respectively ($p < 0.05$). The TGF \Rightarrow IGF group alone had a 1.55-fold higher aggrecan gene expression from $t = 0$ to day 7 coated surface ($p < 0.05$).

In comparing between the groups at the same time point, we observed that at $t = 0$, all of the medium compositions had a significantly higher aggrecan gene expression than the control group. However, there were no significant differences in gene expression between the control group and other groups at 24 h or at day 7 on the coated surface. For the $t = 0$ time point and day 7 non-coated surface, there was a 3.8-fold higher aggrecan gene expression for the TGF group and a 3.7-fold higher expression for the aggrecan group, ($p < 0.05$).

SOX-9:

The control group had a 2.9-fold higher SOX-9 gene expression from $t = 0$ to 24 h for the coated surface ($p < 0.05$). There was no statistically significant difference in SOX-9 expression over time for the TGF group. The IGF group had a 8.6-fold higher gene expression from $t = 0$ to day 7 for the non-coated surface ($p < 0.05$). The CS group on the other hand had a 11.2-fold, 6.4-fold, and 5.5-fold higher SOX9 gene expression from $t = 0$ to 24 h coated and day 7 for the coated and non-coated surfaces, respectively ($p < 0.05$). The TGF \Rightarrow IGF group had a 11.1-fold higher SOX-9 gene expression from $t = 0$ to day 7 coated surface ($p < 0.05$).

In comparing the different media compositions at the same time point, we observed that the CS group had a 6.5-fold higher expression at $t = 0$, compared to the control media group ($p < 0.05$). The CS group also had a 7.3-fold higher expression at $t=0$ compared to the control media group ($p < 0.05$). The IGF group had a 4.8-fold higher expression for the 24 h coated surface compared to the control group ($p < 0.05$). Lastly, the aggrecan medium at day 7 non-coated surface had a 7.1-fold higher gene expression compared to the control media group ($p < 0.05$).

Collagen II:

The control, IGF, and TGF \Rightarrow IGF groups did not have a significant change in gene expression over the 7 day time period. The TGF group had a 3.1-fold higher gene expression only from $t = 0$ to day 7 non-coated surface ($p < 0.05$) and not at any other time point. The CS group had a 10.6-fold higher collagen II gene expression from $t = 0$ to day 7 non-coated surface ($p < 0.05$). The aggrecan group had a 4.3-fold higher collagen II gene expression from $t = 0$ to 24 h coated surface ($p < 0.05$).

In comparing between the different media groups at the same time point we observed that all the media groups had a significantly higher gene expression compared to the control media group at the $t=0$ time point. There was no significant difference for the 24 h coated surface for any media groups. Coming to the 7 days coated surface, the TGF, IGF, CS, and aggrecan group had a 0.7-fold, 0.5-fold and 0.4-fold lower collagen II gene expression compared to the control media group ($p < 0.05$). At the 7 day non-coated surface, only the CS group had a 6.8-fold higher collagen II gene expression compared to the control media group ($p < 0.05$).

Collagen I:

The control media group had 2.7-fold, 2.1-fold and 1.9-fold higher collagen I gene expressions from $t = 0$ to 24 h coated and day 7 for the coated and non-coated surfaces, respectively ($p < 0.05$). The TGF group had a 15.6% and 42.8% decrease in collagen I gene expressions from $t = 0$ to 24 h coated and day 7 non-coated surfaces, respectively ($p < 0.05$). The IGF group had a 3.2-fold higher expression from $t = 0$ to day 7 coated surface, respectively ($p < 0.05$). It also had a 34.7% lower gene expression from $t = 0$ to day 7 non-coated group ($p < 0.05$). The CS group had 23.6% and 56.8% lower gene expressions from $t = 0$ to day 7 coated and non-coated surfaces, respectively ($p < 0.05$). The aggrecan group had 38.5% and 67.2% lower gene expression from $t = 0$ to day 7 coated and non-coated surfaces, respectively ($p < 0.05$).

In comparing the difference in expression between different media groups over the same time point we observed that the all the media groups (TGF, IGF, CS, aggrecan, and TGF \Rightarrow IGF) had a significant difference compared to the control media groups for the 24 h coated, day 7 coated and non-coated groups ($p < 0.05$).

Immunohistochemistry

IHC staining of the control media spheroids revealed that the diameter of the spheroids decreased over the one-week period, specifically from the hanging drop time point to the 7 day time point on the non-coated surface. Figure 7a represents the collagen I immunostaining for representative groups. The hanging drop time point showed the highest collagen I staining intensity followed by the CS and TGF groups at 24 h. The 7 day HA-coated (TGF) aggregate started to show disintegration and the 7 day HA-coated IGF showed complete degradation in spheroid morphology. Figure 7b represents the collagen II immunostaining for select groups. The spheroid

diameter apparently decreased from hanging drop group to the 24 h coated group. The hanging drop group with CS medium showed highly intense staining for collagen II compared to the TGF and aggrecan medium. Figure 7c shows aggrecan immunostaining for representative groups. TGF primed medium stained after hanging drop and after 24 h in coated plate showed intense aggrecan staining. Though the 24 h coated control media primed spheroid showed negligible staining, by day 7 it stained intensely throughout the spheroid.

DISCUSSION

MSCs are a promising source for cell-based therapies because of their multipotent regenerative capabilities. One way of exploiting MSCs is organizing them into 3D stem cell spheroids or spheroids that have shown good regeneration and anti-inflammatory properties. Spheroids have recently shown to be more effective than single cells for defect filling and better cartilage regeneration.^{108, 142}

Previous *in vitro* studies have shown that microenvironment and surface stiffness plays an important role in shaping the cell migration and eventual differentiation of the MSC spheroids.^{12, 153} Specifically, HA is a commonly explored chondroinductive ECM component used both as a surface and as a scaffolding agent.^{33, 129} Other studies have looked into using HA to coat well-plates where the molecular weight of the HA alters the stiffness.^{139, 140} For the current study, we used a M_w of 360 kDa that accounted for intermediate range of stiffness. Compared to the previous studies, we have for the first time use MSC spheroids of this cell density directed at chondrogenic applications. The effect of HA can clearly been seen in the GAG and collagen content of the spheroids, however the long-term effects cannot be elucidated from the current study. The HA-coated groups primed under different media conditions had a much higher GAG

and collagen content compared to the hanging drop group. Although the average size of the spheroids varied among the groups, from live-dead assay (Figure 2) we can infer that the spheroids harvested from the hanging drop petri dishes possessed the highest diameter compared to the spheroids after 24 h and 7 day culture. Due to a shortage of cells, we prioritized on the HA-coated group and did not include the 24 h non-coated group for the current study. The significant difference in the properties of the spheroids thus seemed to be associated with the overall spheroid size that will need further exploration. Furthermore, other polymers apart from HA such as chitosan, alginate, poly ethylene glycol with different molecular weights may yield exciting results on how surface stiffness affects differentiation.

New medium recipes are constantly being explored to enable provision of the best culture conditions for cellular differentiation. In particular, growth factors and bioactive peptides as medium supplements are being extensively researched for musculoskeletal applications.^{131, 193, 264} Several studies have shown the therapeutic advantages of using TGF in the medium composition and since been utilized in scaffold fabrication for controlled release over time.^{34 95} During the last decade, IGF had also gained a lot of interest as it has shown to be misregulated playing an anabolic role in cartilage degeneration.^{174, 234} Several approaches have thus employed IGF in their scaffold design and the media composition for regenerating cartilage.^{119, 254, 255} In comparing the results from the current study to previously published studies from our lab, we observed that for the same cell density, spheroids primed under IGF medium surpassed all other previous SOX9 and collagen I gene expression.²⁵⁴ At the hanging drop time point, the DNA content of the IGF group was higher than what we have seen so far²⁵⁵, thus reiterating the importance of cellular presentation as three-dimensional spheroids compared to cellular suspensions. Of particular interest was the TGF⇒IGF group where for the coated spheroids, the

spheroids were primed with TGF the first three days and changed to IGF for the last 4 days. This additional group was specifically included to observe the effect of IGF on late stage differentiation, as observed before.²⁵⁵ The IGF medium primed 7 day non-coated group, exhibited the highest GAG/DNA content. Although several groups have explored IGF for chondrogenesis,^{52, 160} this is the first time that IGF has been tested as a priming formulation for use in stem cell spheroids. One of the main directions of our lab has been to explore the chondroinductive properties of raw materials, and so far we have assessed raw materials like aggrecan, CS, decellularized cartilage, bioactive glass in scaffold fabrication. To take it one step further, in the current study we directly added CS and aggrecan in the medium at concentrations reported favorably earlier.^{100, 117} Although the concentrations are different under *in vivo* conditions, premature priming of the spheroids to raw materials may preemptively induce GAG and collagen production that can be complemented when placed in the body. In the current study, we found that the CS medium primed at the hanging drop stage showed the highest SOX-9 gene expression and at 7 days non-coated conditions showed the highest collagen II expression. This is an important implication as it opens a new path to look at medium formulations as raw materials so far are exclusively used only for scaffold fabrication. If the addition of CS in medium could yield comparable results with that of growth factors, it is an easy and efficient approach from a financial and federal regulation standpoint and cannot be ignored for future applications. Although there has been several studies that have independently explored surface stiffness on spheroid properties, and others that have looked into different media formulations, there is a complete lack of approaches that employ conjointly explore both the parameters on spheroid differentiation.

Although spheroids present several advantages over single cell suspensions, the main drawback

when it comes for clinical applications is the time required for spheroid formation. Secondly, there was a genuine attempt to vigorously perform immunohistochemistry testing for all the groups but the spheroids are extremely small after one week of culture and in many cases disintegrated and hence lost in sample processing. Future studies that focus on better spheroid retention in paraffin molds and look at the regeneration from a different testing paradigm may benefit the entire field. Finally, one week is too short a time to evaluate cartilage regeneration. The experiment presented here only serves as a preliminary *in vitro* approach to support the different capacities of the spheroids subjected to different surface stiffness and medium compositions.

Upon establishment of the benefits of spheroid priming, future studies could look at other media raw material/growth factor combination to find a winning formulation for cartilage-like tissue spheroids. The next step along the way is spheroid implantation into animal models and exploring flexible biomaterials for aggregate encapsulation would also be worthwhile.

CONCLUSIONS

In the current study, we successfully primed the spheroids under different medium conditions with exposure to HA coated or non-coated well plates and observed the chondrogenesis of the spheroids. We observed that exposure to HA-coated well plates resulted in overall retention of spherical morphology and increased viability compared to the non-coated groups. Moreover, the hanging drop time point demonstrated a high cell viability and aggrecan gene expression compared to the other time points. Additionally, raw materials (i.e., CS and aggrecan) alone had the capability to induce SOX-9 and collagen II gene expression compared the growth factor-

primed groups suggesting that raw material addition in the medium could be a new economic and efficient way of looking at medium formulation for chondrogenic applications. The priming exercise gave new insights in to 3D spheroid behavior under a diverse microenvironment, suggesting the close interplay between surface modification and medium composition. The consideration of control media spheroids, exclusion of serum and growth factors and inclusion of raw materials in the medium may be a promising path to generate chondromimetic tissue for cartilage regeneration in the future.

CHAPTER 6: *In Vivo* Evaluation of Stem Cell Aggregates on Osteochondral Regeneration⁵

ABSTRACT

To date, many osteochondral regenerative approaches have utilized varying combinations of biocompatible materials and cells to engineer cartilage. Even in cell-based approaches, to date, no study has utilized stem cell aggregates alone for regenerating articular cartilage. The purpose of this study was thus to evaluate the performance of a novel stem cell-based aggregate approach in a fibrin carrier to regenerate osteochondral defects in the Sprague-Dawley rat trochlear groove model. Two different densities of rat bone marrow mesenchymal stem cell (rBMSC) aggregates were fabricated by the hanging drop technique. At 8 weeks, the cell aggregates supported the defects and served as a catalyst for neo-cartilage synthesis, and the experimental groups may have been beneficial for bone and cartilage regeneration compared to the fibrin-only control and sham groups, as evidenced by histology. The cell density of rBMSC aggregates may thus directly impact chondrogenesis. The usage of cell aggregates with fibrin as a cell-based technology is a promising and translational new treatment strategy for defect repair of cartilage defects.

⁵ Submitted as **Sridharan B.**, Laflin A.D., Holtz M.A., Pacicca D.M., Wischmeier N.K., Detamore M.S. “*In Vivo* Evaluation of Stem Cell Aggregates on Osteochondral Regeneration,” Tissue Engineering Part A, 2015.

INTRODUCTION

In the United States, trauma-related cartilage damage and aging-related cartilage degeneration alone have cost several millions of dollars.^{26, 31, 235} There is thus an unmet need to develop substantial cost-effective treatments for osteoarthritis. Over the last couple of decades, numerous strategies have been developed in an effort to regenerate the osteochondral interface^{73, 156, 180, 201} that employ autologous cell suspensions of either differentiated chondrocytes or undifferentiated bone marrow-derived mesenchymal stem cells (BMSCs).^{37, 149} Several review papers discuss various types of cell-based approaches and the relative advantages they impose compared to other material-based strategies.^{67, 198, 237} Despite the success of cell-based techniques, clinical outcomes are significantly affected by the formation of fibrocartilage after long-term implantation, thus requiring multiple surgeries that in turn may give rise to donor site morbidity and increase the overall cost of healthcare.^{122, 179} To overcome the above listed disadvantages, investigators have resorted to employing cells in combination with biocompatible natural materials such as alginate, agarose, collagen, and silk fibroin, and polymers such as polylactic-co-glycolic acid, polyglycolic acid, and polycaprolactone, which under certain fabrication conditions may possess mechanical properties similar to the native cartilage.^{17, 66} However, a cell-based system based on both natural materials and cells may hold advantages in quality of regeneration, although translational limitations must be overcome.

While there have been several advances for *in vivo* approaches for cartilage tissue engineering using cell-based strategies, the number of cell aggregate approaches are limited.^{154, 207, 218, 219} Cell aggregates or spheroids are clusters of cells that are closely packed, enabling increased cell-to-

cell contact. Commonly, aggregates have been explored for pancreatic islet regeneration, targeted drug delivery approaches for cancer therapy, and in general they serve as a great three-dimensional cellular model for drug testing.^{86, 106, 127, 271} Translating the aggregate technology to regenerate articular cartilage is starting to gain interest.^{164, 221, 271}

Looking at material-based approaches in rat models, a steady number of studies use external chemical stimuli such as raw materials, growth factors and other bioactive molecules in their scaffolds. In this regard, transforming growth factors (TGFs) and bone morphogenetic proteins (BMPs) have been shown to stimulate stem cell differentiation into cartilage and bone, respectively. Specifically, TGF- β_1 and TGF- β_3 are known to promote chondrogenesis and BMP-2 and BMP-7 are known to promote osteogenesis.^{25, 85, 190} While the addition of these external stimuli may lead to quality tissue regeneration, it can be quite expensive, may have side effects, and lead to a more involved regulatory process. Cellular aggregates employed in the current study, however, provide a more translational approach by exploiting known intercellular communication from cell pellet cultures in chondrogenesis as an inherent cue to differentiate MSCs toward the cartilage phenotype. Based on a rationale of potentially possessing a greater extent of intercellular communication, our hypothesis was that within 8 weeks, dense cellular aggregate group would outperform the fibrin group and sham surgeries in histological and gross morphological assessment.

Small animal model such as rodents are considered valid as proof of concept and preliminary research models.^{2, 49} Since this is the first time we are looking to employ cell aggregates with

fibrin for articular cartilage regeneration, a critical sized defect of the trochlear groove was selected as a reasonable defect area based on established precedent in the literature.^{49, 138, 246} The current study investigated cartilage regeneration in a critical sized trochlear groove defect in Sprague-Dawley rats with cell aggregates of different densities, and compared the performance with a fibrin-only control group and a sham negative control. The induced defect size was approximately 2.0 mm in diameter and 2.0 mm in depth. Regeneration was evaluated at 8 weeks with gross morphological scoring and histological staining. The goal of this pilot study was to determine whether the cell aggregates would facilitate neo-cartilage formation in the rat trochlear groove as a foundation for future *in vivo* studies.

MATERIALS AND METHODS

Cell harvest and culture

Rat bone marrow-derived mesenchymal stem cells (rBMSC) were harvested from the femurs of five young male Sprague–Dawley rats (200–250 g, Charles River) following a University of Kansas approved IACUC protocol (175–08). The IACUC approved the use of rBMSC cells for use in this particular study. The cells were isolated according to our previously reported protocol.^{9, 239} Briefly, isolated cells were cultured in rBMSC media (α MEM supplemented with 10% MSC-qualified FBS and 1% Penicillin-Streptomycin (Invitrogen Life Technologies, Carlsbad, CA)), and passaged at 80% confluence until P4. All cells from different femurs were pooled together, frozen at P2 and later expanded to P4, and used for the study.

Cellular aggregate preparation

Aggregates for the current study were generated by the hanging drop technique.^{243, 267} Cellular suspensions (rBMSC) were prepared at two concentrations, either 10.0×10^6 or 20.0×10^6 cells/mL, in rBMSC media. The cellular concentration was confirmed using a Cellometer automatic T4 cell viability counter (Nexcelcom Bioscience, Lawrence, MA). Droplets of cell suspensions at a controlled volume of 10 μ L that had 10,000 or 20,000 cells were pipetted in an array onto the inside surface of a sterile petri dish lid using a 10 μ L pipette (Eppendorf, Hauppauge, NY), making sure that the droplets had a safe distance between each other to prevent mixing. The cells were allowed to aggregate overnight, aided by gravity when the petri dish was reversed. The sterile petri dish bottom was then filled with sterile PBS to prevent drying of these droplets. After 24 hours, the cell aggregates were carefully collected from the dish with a 1 mL pipette and collected in Eppendorf tubes for the study. Aggregates were placed in defects within 3 hours of harvest, as noted below.

Description of Experimental Groups

Four different treatment groups were investigated: (i) Group A, where the defect was created and filled with 75 rBMSC aggregates, each with a cell density of 10 million/mL (note: density based on volume of initial 10 μ L suspension), (ii) Group B, where the defect was created and filled with 75 rBMSC aggregates each with cell density of 20 million/mL, (iii) Sham surgeries, in which a defect was created, but no implant was placed and, (iv) Fibrin groups where the defect was created and only fibrin was used to fill the defects (Fig. 6.1). For group (i) and (ii), each

petri-dish used to make the hanging drop aggregates had exactly 75 drops and care was taken to harvest all of the aggregates, thus making sure we had 75 aggregates for each knee.

Surgical Procedure

Surgical procedures were conducted under an approved IACUC protocol at the University of Kansas (Animal Use Statement #175-20), utilizing a total of 10 male Sprague Dawley rats (200-250 g, Charles River). The IACUC approved the protocol to be used for this particular study. Following stable general anesthesia, hair was shaved from the area around each rat knee. The knee was then disinfected with three alternate scrubs of Betadine and 70% ethanol, and then draped so as to expose only the knee area. Care was taken to use only strict aseptic techniques and sterile instruments, and the surgeon wore sterile gowns, masks, and head covers. All surgical tools, including drill and stoppers, were sterilized prior to surgery. A midline knee incision was made for an intra-articular lateral parapatellar arthrotomy sufficient enough to allow exposure of the trochlear groove. The defect was drilled to a depth of 2.0 mm depth and 2.0 mm diameter using a drill with a stopper attached to the bit. Defects were then filled with either the aggregate groups (Group A or B), or fibrin (Tisseel ®, Baxter, Deerfield, IL) (Fig. 6.1). The aggregates were harvested 3 hours before the surgery, as noted in the 'Cellular aggregate preparation' subsection above, and immersed in rBMSC media until implantation. At the time of implantation, aggregates were carefully pipetted into the defect area. Sham defects were created, in which a hole was drilled, but no implant was placed. Following implantation of the aggregate groups, 50 μ L of fibrin was added on top of the aggregates to seal the clot with the surrounding tissue. Although 6 μ L was enough to cover the defect, a little extra fibrin was added to secure the clot with the surrounding tissue as it hardened over time. The sealing time was approximately 2

minutes. The joint was then washed with sterile pharmaceutical grade saline water and the bursae was closed with absorbable suture. The skin was then closed with polysorb 3.0, a non-absorbable suture. The procedure was followed on the contralateral knee with a different group to ensure independence of knees within groups (Fig. 6.2). After the surgery was completed, the rats were administered carprofen subcutaneously, and returned to be caged individually. The knee joints were allowed unconstrained movement postoperatively.

Post-surgical Care

The rats were continuously monitored for the first three days and any signs of limping or unease was treated with carprofen injection administered subcutaneously only once a day. Three rats (R03, R05, and R07) had signs of limping/uneasiness in walking gait during the first week only. Three times a week, the rats were monitored for general mobility, specific mobility of hind legs, response to touch and signs of inflammation at the surgical area. No adverse events were observed and all the rats progressed at a healthy rate during the entire period of 8 weeks.

Morphological analysis of the retrieved implants

At 8 weeks, the rats were euthanized by controlled exposure to CO₂ that was approved by the IACUC protocol. After the joint retrieval, the knees were scored blindly by three independent co-authors. The scoring was carried out for macroscopic observations based on the presence of repair tissue, presence, edge integration at the boundaries of newly regenerated tissue and the native cartilage, smoothness of the repair surface, degree of filling at the cartilage surface, color of the regenerated cartilage, and the percent of repair tissue relative to the total area. The scoring

criteria were developed as a modification from the ICRS scoring chart, represented in Table 6.2.

²⁴⁹ The joints were photographed and processed for histology.

Histological preparation and staining

At 8 weeks, rat knees were retrieved and immediately placed in 10% neutral buffered formalin (Fisher Scientific, Rockville, NJ) for 72 hours, changed every 24 hours. After fixation, the joints were rinsed in distilled water and decalcified (Cal Rite, Richard-Allan Scientific, Kalamazoo, MI) for 2 weeks and the solution was changed every 3 days. After decalcification, the knees were rinsed briefly and dehydrated in graded ethanol. For paraffin embedding, the samples were cleared with xylene and then infiltrated with paraffin and the infiltrate was changed every 3 hours. After three infiltrations, the trochlear grooves were embedded in paraffin tissue cassettes and allowed to cool down before sectioning. Sagittal sections were taken on a microtome (Thermo Scientific; Microm HM 355S) using a tungsten carbide blade with a sample thickness of 7 μm , and placed on coated glass slides (Superfrost coated slides, Thermo Scientific, NJ) and dried for 24 hours at 44°C. The glass slides were cleared in xylene and slowly hydrated in series of ethanol according to a procedure previously reported ⁷³. After incubating the slides in ddH₂O for 5 minutes, the slides were stained with either Safranin-O/Fast green stain for glycosaminoglycans (GAGs) or hematoxylin and eosin to look at overall structure. Slides were briefly dehydrated and cleared in xylene for mounting. Furthermore, additional slides were processed for immunohistochemistry (collagen I, II, and aggrecan) discussed in the next section. All staining reagents were purchased from Sigma Aldrich (St Louis, MO).

Immunohistochemistry

The slides were processed similar to basic histology as described above up through hydration in distilled water. The sections were then exposed to 3% hydrogen peroxide in methanol for 10 minutes to suppress endogenous peroxidase activity, and the slides were immediately incubated in proteinase K (IHCWORLD IW-1101, Woodstock, MD) at 37°C for 10 minutes. Sections were blocked with 3% blocking horse serum (Vector Laboratories S-2012, Burlingame, CA) for 30 minutes preceding primary antibody incubation. The list of primary antibodies, corresponding dilution and vendor information can be found in Table 6.1. Following primary antibody incubation, slides were exposed to biotinylated secondary antibody (horse anti-rabbit IgG) and ABC reagent (Vectastain ABC kit PK-6200, Burlingame, CA) for 30 minutes each. Visualization was accomplished with ImmPact DAB peroxidase substrate (Vector laboratories SK-4105, Burlingame, CA) before rinsing with distilled water and counter stained with VECTOR hematoxylin QS stain. Following staining, slides were rinsed in tap water; dehydrated in ethanol, cleared in xylene for mounting (Permount SP15-500 Fair Lawn, NJ), and viewed under an upright microscope (Zeiss, Axiomanager 2.0, Thornswood, NY). Negative controls for IHC consisted of isotype IgG controls (Life Technologies) being added instead of the primary antibody.

Histology scoring

A simple scoring system (Table 6.3) was modified from the previously reported system of O'Driscoll *et al.*¹⁹⁷ to evaluate the cartilage and bone regeneration of this pilot study. 3-blinded

observers performed all scoring and the assignment of the scores was aided by evaluating structure using histological and immunohistological images.

Statistical analyses

Wherever applicable, all data are expressed as mean \pm standard deviation. Statistical analyses were performed using one-way ANOVA (Minitab 15, Minitab Incorporated, State College, PA), followed by a Tukey's post hoc comparison test for repeated measurements. The statistical significance threshold was set at 0.05 for all tests (with $p < 0.05$).

RESULTS

Gross morphological observations

All of the rats continued to exhibit normal movement and gait in their hind legs during the 8 week period (other than noted exception in the Methods of three rats during the first week). Gross signs of inflammation (swelling or reddening of the joint) or infection were not evident upon visual inspection of the joint surface at the time of tissue retrieval. Figure 6.3 shows representative gross morphology images of the rat trochlear grooves at 8 weeks. The highest, intermediate and lowest scoring samples are shown for each group. For Group B, the repair tissue was completely flush to the surface and had a smooth texture surrounding the defect area with color similar to the native cartilage, whereas all of the other groups had an opaque, slightly depressed or overgrown surface with either rough or intermediate texture at 8 weeks. Figure 4a represents the mean morphological score and Figure 4b represents the percent area occupied by the regenerated cartilage with respect to the total defect area was determined macroscopically for

each sample at 8 weeks. The percent area values were between 80%-95% for Group A and the sham and fibrin groups. Group B values were between 95%-100%. Group B received a 1.35-fold higher morphological score (Figure 4b) than Group A alone ($p < 0.05$). Group B did not have a statistically significantly higher score compared to sham and fibrin groups. The difference in mean morphological score between Group A and fibrin group and sham group was not statistically significant.

Histomorphometric observations

Figure 6.5 shows representative sections stained with H&E, Safranin O for GAGs, Collagen I, II, and aggrecan immunostaining, for Group A. Rat #2 (i.e., R02) (Fig. 6.2) had intense Saf-O staining, whereas R04 and R09 did not stain very intensely. Figure 6.6b represents the morphometric score distribution of Saf-O stained sections of the defect area, and we observed that 40% of the knees were slightly stained, 20% were moderately stained and the remaining 40% was normally stained. Collagen II staining was prominent in the defect region for R03 and R04, and aggrecan immunostaining was intense for R04 and R09 cartilage region. There was no intense staining of collagen I around the defect area, but overall there was a mild staining throughout the subchondral bone region. 60% of Group A knees received a score of 2 (75%-100% of adjacent cartilage) and the remaining 40% received a score of 3 (100% thickness of the adjacent cartilage) (Figure 6.6a). Additionally, 60% of the Group A knees showed normal subchondral bone regeneration with smooth and intact edge integration of the defect with the surrounding native cartilage. Upon closer observation at the defect region, Group A aggregates (R01 and R04) showed columnar arrangement and are surrounded by tiny lacunae spaces. The lacunae spaces increased in size at the osteochondral junction. R03 and R04 showed intense

collagen II and aggrecan pericellular staining. Apart from R02, there was no presence of cellular clusters in any of the Group A defects. There were small aggregates at the defect site, but it was not possible to say whether they were the implanted rBMSC aggregates or host-cell aggregates.

Figure 6.7 displays representative sections stained with H&E, Saf-O for GAGs, Collagen I, II, and aggrecan immunostaining for Group B. R06 and R08 sections did not display any Saf-O staining, but intense staining for R07 and staining around the defect area for R05. 60% of the samples had a Saf-O score of 1 (slight staining) and the remaining 40% a score of 3 (nearly normal staining) (Figure 6.6a). Collagen II staining was intense in the defect area for R06 and R08, and aggrecan staining was evident in the defect region for R05, R07, and especially R06. Collagen I staining on the other hand was intense only for R06 in the defect area. As indicated by Fig. 6, 80% of the knees exhibited 75%-100% cartilage thickness and reduced subchondral bone reduction. 60% of the knees had a smooth and intact edge integration of the regenerated cartilage with the surrounding tissue. Looking at the cellular appearance in Group B defects, we observed that none of the regenerated tissue showed a columnar arrangement. There were no distinct lacunae observed except for R05 and R08, where the lacunae spaces increased at the osteochondral junction. R06 showed intense collagen II and aggrecan pericellular staining. For R06, the cells in the defect region had a more intense pericellular collagen I and II staining compared to the surrounding tissue. H&E and Saf-O staining of R07 revealed aggregates at the osteochondral interface. In general, the cell aggregates appeared to be dispersed throughout the entire tissue region.

Figure 6.8 shows representative sections stained with H&E, Saf-O for GAGs, Collagen I, II, and aggrecan immunostaining, for the fibrin-only group. Saf-O staining was prevalent in the defect area for R07 and R09. The staining for Saf-O for the native tissue was evident for R02 and R05. 80% of the fibrin group showed moderate staining to Saf-O (Fig. 6.6). Collagen II immunostaining was dense for R09 and R05, whereas aggrecan immunostaining was intense on the surface of the defect area for R03, R05, R07, and R09. Collagen I staining was intense in the defect area for R05 and stained deeper in the bone defect region for R02 and R03. 100% cartilage thickness was observed in 60% of the knees. Just like the sham defect group, 80% of the samples had reduced subchondral bone regeneration and only 60% showed superficial horizontal lamination. The regenerated tissue of the fibrin group did not show any columnar organization of cells. The cells in R05 and R10 sections showed lacunae-like appearance. R10 showed intense collagen II and aggrecan pericellular staining. The cells in the regenerated tissue for R07 showed intense collagen I staining compared to the surrounding cartilage tissue and similarly the defect area tissue had increased aggrecan around the cells compared to the surrounding tissue. In general, there was no appearance of cell clusters in any of the images.

Figure 6.9 displays representative sections stained with H&E, Saf-O for GAGs, Collagen I, II, and aggrecan immunostaining, for the sham knee surgeries. R01 demonstrated distributed Saf-O staining, but the regenerated tissue looked weak with a visible fissure in the bone-cartilage interface. R08 and R10 showed minimal to no Saf-O staining at the defect region. R04 and R06

on the other hand had Saf-O staining at the regenerated cartilage surface. As indicated by the morphometric analysis, 80% of the group had moderate Saf-O staining and the remaining 20% had regular Saf-O staining, comparable to that of native cartilage (Fig. 6.6). Collagen II staining was evident for the regenerated surface for R01, R08 and R10, and aggrecan immunostaining was intense for R08 and R10. Collagen I was not evident for any other group except R08. 40% of the samples showed 100% of normal cartilage thickness and the remaining 60% had 50%-75% of native tissue thickness (Fig. 6.6). 80% of the samples had reduced subchondral bone regeneration and the remaining 20% showed normal bone regeneration without any sclerosis or loss of bone tissue. As far as edge integration with the native tissue was concerned, 60% showed superficial horizontal lamination and 40% showed smooth and intact integration. The regenerated tissue of the sham group did not show any columnar organization. There were no lacunae present in any of the sections. Only R01 and R04 sections displayed intense collagen II pericellular staining. Only R04 showed intense aggrecan staining of cells in the defect area compared to the surrounding tissue. There were no cell clusters in any of the images.

DISCUSSION

In the current pilot study, we have introduced for the first time a new method to incorporate cellular aggregates into an animal model as a proof of concept study. The rat trochlear groove is an established animal model that provided a great insight into both the potential and limitations to the aggregate-based approach.^{45, 46}

As noted at 8 weeks, the fibrin-only control group demonstrated extensive tissue regeneration, marked by full thickness tissue, presence of GAGs, dense collagen II and aggrecan immunostaining. In the experimental groups, Group B had the highest average morphological score and highest percentage filling of the defect area compared to all other groups. From the data presented here, there is evidence that dense rBMSC aggregates (Group B) may be beneficial for osteochondral tissue engineering. Notably, the current immunohistochemistry analyses showed localized pericellular staining of collagen II and aggrecan in the Group B implants that was observed for only one section in the sham surgeries.

A potential limitation with respect to use of rat trochlear grooves for a cartilage regeneration study is that the negative control group may not be ideal. A primary observation was the spontaneous healing of all of the sham groups. Previous studies by other groups that had looked at sham surgeries in the rodent trochlear groove region (rat and rabbit) had also observed that this may be a common trend for a typical small animal model.^{41, 220} Additionally, in the current study made sure the starting weight of the rats were comparable, however the variation in age of the rat might contribute toward a slightly different result owing to different regeneration rates of both the sham and the experimental group.

The trochlear groove in a lower weight bearing region is considered an appropriate model for proof of concept studies.^{124, 194} Upon incumbent success of cartilage regeneration in the groove and observation of regeneration pattern, sufficient information could be collected for the next

iteration of studies on a true load-bearing defect site in a large animal model to show more pronounced differences in regeneration between sham and experimental groups.

Earlier studies that employed biomaterials on rat trochlear groove regeneration for critical sized defects have shown similar rates of regeneration.^{55, 113} Although previous rat studies have not explicitly provided aggrecan immunohistochemistry, based on morphological scoring and basic histology (H&E, Saf-O), similar rates of regeneration may be inferred.^{47, 143} Although there were minor variations in the time period of study and differences in evaluation method, basic histology and morphology scores reveal the parameters associated with determining the technology feasibility. Munirah *et al.*¹⁸⁸ have demonstrated that fibrin mixed with autologous cells resulted in osteochondral regeneration in a sheep model. Similarly, Deponti *et al.*⁶² demonstrated that fibrin mixed with porcine cells possessed enhanced *in vivo* properties compared to *in vitro* conditions, for increased cell viability and activity.

Overall, the current study adequately established proof of concept. The cellular aggregates did not necessarily demonstrate conclusive outperformance of the fibrin group. The results of the current study, with differences between Groups A and B, suggested that there may be more effective ways to combine fibrin with cell aggregates. For example, exploring different cell densities for the aggregates, larger numbers of aggregates, aggregates of other cell types (e.g., Wharton's jelly cells^{63, 256, 259}), pre-treatment of aggregates, or differences in surgical placement procedure may be warranted for future investigation in an attempt to more conclusively prove the hypothesis that aggregates provide superior and more consistent cartilage regeneration compared to the controls.

Now that the feasibility and the potential of the aggregate technology has been demonstrated, experimental designs will be expanded in future studies to include larger defect sizes, bigger animal models, larger aggregate sizes, higher aggregate numbers and cell density of the aggregates and more sophisticated techniques to differentiate between the implanted and host cells even after several months of implantation. From a clinical standpoint, comparison of cell suspensions with fibrin versus cell aggregates with fibrin would yield meaningful and a more direct implication of the efficacy of aggregate technology over conventional cell suspension techniques. Furthermore, aggregate technology may augment current existing methods such as autologous chondrocyte implantation (ACI) to produce a new class of products for treating focal cartilage lesions. The current study has clearly established a proof of concept for a novel approach of incorporating aggregates of rBMSCs with two different cell densities for osteochondral defect repair.

CONCLUSIONS

The current study demonstrated a cell-based approach where stem cell aggregates employed with fibrin were used for regenerating the osteochondral interface tissue in a rat knee defect model. This is the first *in vivo* study that employed dense cellular aggregates in a trochlear knee defect model. Stem cells presented in a 3D aggregate form along with fibrin seemed to enhance regeneration.

In conclusion, the inclusion of fibrin showed some degree of regeneration that may have been enhanced with the higher aggregate density group. Between the two experimental groups, the higher cell density aggregate group (Group B) demonstrated superior cartilage regeneration compared to all other groups and arguably had the most complete defect filling. The complete filling was believed to be the result of denser cellular aggregates in Group B that enabled better cell-to-cell interaction and filled the defect and remained intact due to its relative density. The merit of the study design shows potential in that the cellular density of the aggregates is an important parameter in osteochondral tissue regeneration, which may further be facilitated by the priming of rBMSC aggregates and exploration of even higher cell densities or larger numbers of aggregates, which is certainly worthy of long-term systematic evaluation in the future.

CHAPTER 7: Conclusion

Microsphere-based scaffolds for osteochondral tissue engineering represent a well-established research direction in my advisor's laboratory. The encapsulation of raw materials in scaffolds has several pressing benefits when cells were seeded on these polymeric scaffolds. The individual properties of the acellular scaffolds, however, were not clearly established. I started my thesis by fabricating and characterizing CS and TCP encapsulated microsphere-based scaffolds, by evaluating the dry weight, molecular weight, mechanical properties, and bioactive factor (CS and TCP) retention in these scaffolds over a period of four weeks. Next, the focus shifted entirely to testing the feasibility of stem cell aggregates encapsulated in a hydrogel system and to further refining the aggregates by priming them under different medium compositions and substrate stiffness. Lastly, the *in vivo* potential of the aggregates was tested in a rat knee cartilage defect model. All of these projects have assimilated substantial knowledge in the field of stem cell aggregates for osteochondral applications.

Bone marrow mesenchymal stromal cells (BMSC) are the most investigated MSC for tissue engineering applications and are considered the "gold standard" cell source in musculoskeletal tissue engineering. BMSCs provide an autologous cell source for tissue engineers to avoid potential immune rejection. However, there are some limitations to the applications of BMSCs, including the low number of BMSCs in marrow, their proliferation ability and the fact that their differentiation potential decreases significantly with age. Moreover, the invasive harvesting procedure may lead to complications and morbidity. Financially, the biopsy of the marrow fluid only adds extra cost to the overall healthcare, thus rendering it less feasible in developing countries. The Wharton's jelly cells (hWJC) on the other hand are

obtained from stroma of the discarded human umbilical cord. Human umbilical cord mesenchymal stromal cells are a multipotent stromal cell population that are plastic adherent, share MSC surface markers such as CD73, CD90 and CD105, and are non-hematopoietic cells. The cells represent a steady and sustainable source of cells and do not have any donor site morbidity issues.

Different sources of stem cells have varied potential in generating neo-cartilage tissue under a given set of conditions. Two of the main challenges of using BMSCs are the number of cells that can be isolated from a single biopsy, and donor site morbidity. However, hWJC isolation does not suffer any morbidity issues and can be obtained without an extra surgery, thereby saving healthcare cost. Due to variations between donors, it is eminent to establish quality control and prescreen cells and look for presence of certain surface markers that can then be “approved” as viable hWJC for transplantation. The next important consideration is the delivery of spheroids in a user-friendly manner, so that the end-user, in this case surgeons, can incorporate the spheroids into the defect area without a significant hassle. There are many ways to go about this idea. Currently, the spheroids are only considered for focal defects that are defined as cartilage defects less 2 cm² in area. For such defects, a pre-made solution of fibrinogen with encapsulated spheroids can be delivered in a tight and sterile syringe on the day of the surgery through local-delivery centers. The spheroids would be suspended in a paste-like solution until further use. Upon injection into the defect site, the fibrinogen would clot in the presence of blood to ensure tight adherence of spheroids within the defect region. However, for such controlled procedures, logistics would play a key role in both the starting stages (collection of cells from donor) and the end stages (delivery of spheroids and the hospital).

In an attempt to explore the advantages of stem cell aggregates, rBMSC and hWJC aggregates were fabricated under two different cell densities. When encapsulated in an agarose hydrogel model and testing against cellular suspensions, results indicated that on a per cell basis, the high cell density aggregates outperformed cell suspensions in terms of biochemical analysis and gene expression data. Furthermore, the number of cells per aggregate played an important role in determining the initial performance of the aggregates, with high cell density aggregates (20,000 cells per aggregate) outperforming the low cell density aggregates at initial time points. However, since it was a proof of concept study, the experiment was only conducted for 3 weeks. The limitation of this study design was employing a relatively inert polymer such as agarose. Agarose was selected as a proof of concept model, and upcoming studies would benefit from employing a bioactive material; like hyaluronic acid and poly ethylene glycol. Although the Picogreen assay measures the DNA content, it provides no information on the actual number of live cells.

Similarly, the live-dead assay overall demonstrated that in some cases the aggregate stained only around the edges and staining at the center was not visible. This “Rim Effect” was observed in denser aggregates possibly due to diffusion limitations of the dye. The phase contrast image below showed that there were cells in the center of the aggregate but did not stain mainly due to the diffusion limitation imposed by the dense cellular structure.

To verify better viability, metabolic indicator assays that can be employed for future studies fall under indicator dyes (MTT/MTS/Resazurin), protease marker and ATP. The most commonly employed Resazurin dye based assay works under the principle of NADH (present in metabolically viable cells) reduction of tetrazolium compounds into brightly colored formazon

products. Another assay works by measuring the aminopeptidase activity that is present only in viable cells, using a permeable fluorogenic substrate. Finally, ATP present in viable cells can also be measured using a beetle luciferase reaction to generate light.

Detailed protocols on immunocytochemistry on hydrogels might also shed light on basic differentiation pathways. Evaluation over a period of 6 weeks or longer would yield valuable information on long-term evaluation of aggregates and the influence of cell density and aggregate number.

Next, the roles of surface stiffness and media composition of the rBMSC aggregates were tested. Results suggested that while growth factor primed media (IGF) may have outperformed other groups in terms of SOX-9 gene expression, raw material (CS and aggrecan) primed media demonstrated higher GAG and collagen content per DNA, compared to all of the other groups. The results suggested that raw materials incorporated in the medium might be a new way to look at medium formulations and might have comparable therapeutic properties to those offered by growth factors. In the future, methods to quantify surface stiffness and cellular interaction on the surface may add more insight into understanding the role of surfaces. As enlisted above, cell aggregates are neither considered cells nor a developed tissue and hence falls midway for histology processing. Dedicated aggregate immunohistochemistry protocol development would yield useful information on the aggregate architecture and morphology. Future studies may consider coating well plates with different materials and optimize the coating efficiency of surfaces to ensure sustenance. The other useful information to gather would be the analysis of medium (when medium is changed every day) to check for ECM components and observe other interesting patterns.

In vivo, higher cell density aggregates outperformed the low cell density aggregates and the control groups in terms of morphological scoring and defect filling. Thickness was measured by averaging values from three different points, two on the periphery of the defect and one from the center. This measurement was repeated for all of the samples for all of the groups (n = 5). Similarly, the ratio of defect thickness by healthy cartilage was calculated by measuring of the deepest point in the defect divided by the value of adjacent healthy cartilage thickness. The thickness ratio calculation was again repeated for all of the groups (n = 5).

Additionally, the aggrecan and collagen II staining was intense in higher cell density aggregates and fibrin groups, compared to the low cell density and sham surgeries. What the study sorely missed was assessing the mechanical properties of the rat knees. With the help of proper equipment and expertise, the addition of mechanical testing analysis would help provide a more complete picture. The future experiments can take into consideration a greater weight-bearing region and a larger animal such as rabbit or sheep. Additionally, cell-based *in vivo* studies would benefit from efficient fluorescent labeling of the implanted cells, to accurately determine the contributions of individual groups in the regenerated cartilage.

Overall, the results of the *in vivo* study were instrumental in establishing the feasibility of using stem cell aggregates and helped in setting the stage for future animal experiments, and the next set of *in vitro* studies to refine and enhance the chondrogenic performance of the aggregates. As a future recommendation, using genetically modified stem cells expressing stable GFP/LacZ reporter gene that are developed using recombinant viral vectors to get stable expression could be employed, to better track the cells *in vivo*.

Cell aggregates have been utilized for a myriad of applications such as pancreatic islet cell clusters, spheroids for cancer drug testing, and embryonic aggregates for organ regeneration. The versatile nature of the 3D stem cell aggregates lends itself to be applicable to almost any kind of organ engineering, when presented with the right orchestration of micro-environmental cues. With so many promising applications outside of the osteochondral field, this thesis presents as a first serious attempt at turning the direction toward the articular cartilage phenotype. With the evidence presented within this thesis, it is apparent that the approach of using stem cell aggregates for cartilage regeneration is entirely feasible, and in many instances, efficacious.

Within four years, stem cell aggregates have been taken from conception to practice, and has also produced encouraging *in vivo* data for osteochondral regeneration. Throughout the process of iterations and refining, aggregates have produced several exciting ideas to consider and even more challenges to overcome.

REFERENCES

- ¹Abrams G. D., N. A. Mall, L. A. Fortier, B. L. Roller, and B. J. Cole. BioCartilage: Background and operative technique. *Operative Techniques in Sports Medicine*. 21:116-124, 2013.
- ²Ahern B., J. Parvizi, R. Boston, and T. Schaer. Preclinical animal models in single site cartilage defect testing: a systematic review. *Osteoarthritis and cartilage*. 17:705-713, 2009.
- ³Alexis F. Factors affecting the degradation and drug- release mechanism of poly (lactic acid) and poly [(lactic acid)- co- (glycolic acid)]. *Polymer International*. 54:36-46, 2005.
- ⁴Amini A. A. and L. S. Nair. Injectable hydrogels for bone and cartilage repair. *Biomedical Materials*. 7:024105, 2012.
- ⁵Angele P., J. Yoo, C. Smith, J. Mansour, K. Jepsen, M. Nerlich, and B. Johnstone. Cyclic hydrostatic pressure enhances the chondrogenic phenotype of human mesenchymal progenitor cells differentiated in vitro. *Journal of Orthopaedic Research*. 21:451-457, 2003.
- ⁶Arufe M., A. De la Fuente, I. Fuentes- Boquete, F. J. De Toro, and F. J. Blanco. Differentiation of synovial CD- 105+ human mesenchymal stem cells into chondrocyte- like cells through spheroid formation. *Journal of cellular biochemistry*. 108:145-155, 2009.
- ⁷Assor M. Noncemented total knee arthroplasty with a local prophylactic anti-infection agent: a prospective series of 135 cases. *Canadian Journal of Surgery*. 53:47, 2010.
- ⁸Bae D. K., S. J. Song, K. H. Yoon, D. B. Heo, and T. J. Kim. Survival analysis of microfracture in the osteoarthritic knee—Minimum 10-year follow-up. *Arthroscopy: The Journal of Arthroscopic & Related Surgery*. 29:244-250, 2013.
- ⁹Bailey M. M., L. Wang, C. J. Bode, K. E. Mitchell, and M. S. Detamore. A comparison of human umbilical cord matrix stem cells and temporomandibular joint condylar chondrocytes for tissue engineering temporomandibular joint condylar cartilage. *Tissue Eng*. 13:2003-10, 2007.
- ¹⁰Bailey M. M., L. Wang, C. J. Bode, K. E. Mitchell, and M. S. Detamore. A comparison of human umbilical cord matrix stem cells and

temporomandibular joint condylar chondrocytes for tissue engineering temporomandibular joint condylar cartilage. *Tissue engineering*. 13:2003-2010, 2007.

- ¹¹Baksh D., R. Yao, and R. S. Tuan. Comparison of proliferative and multilineage differentiation potential of human mesenchymal stem cells derived from umbilical cord and bone marrow. *Stem cells*. 25:1384-1392, 2007.
- ¹²Baraniak P. R., M. T. Cooke, R. Saeed, M. A. Kinney, K. M. Fridley, and T. C. McDevitt. Stiffening of human mesenchymal stem cell spheroid microenvironments induced by incorporation of gelatin microparticles. *Journal of the mechanical behavior of biomedical materials*. 11:63-71, 2012.
- ¹³Barry F. P. and J. M. Murphy. Mesenchymal stem cells: clinical applications and biological characterization. *The international journal of biochemistry & cell biology*. 36:568-584, 2004.
- ¹⁴Bartosh T. J. and J. H. Ylostalo. Preparation of Anti- Inflammatory Mesenchymal Stem/Precursor Cells (MSCs) Through Sphere Formation Using Hanging-Drop Culture Technique. *Current protocols in stem cell biology*. 2B. 6.1-2B. 6.23, 2014.
- ¹⁵Bartosh T. J., J. H. Ylostalo, A. Mohammadipoor, N. Bazhanov, K. Coble, K. Claypool, R. H. Lee, H. Choi, and D. J. Prockop. Aggregation of human mesenchymal stromal cells (MSCs) into 3D spheroids enhances their antiinflammatory properties. *Proceedings of the National Academy of Sciences*. 107:13724-13729, 2010.
- ¹⁶Behery O. A., J. D. Harris, J. M. Karnes, R. A. Siston, and D. C. Flanigan. Factors influencing the outcome of autologous chondrocyte implantation: a systematic review. *Journal of Knee Surgery*. 26:203-212, 2013.
- ¹⁷Benders K. E., P. R. van Weeren, S. F. Badylak, D. B. Saris, W. J. Dhert, and J. Malda. Extracellular matrix scaffolds for cartilage and bone regeneration. *Trends in biotechnology*. 31:169-176, 2013.
- ¹⁸Bentley G., L. Biant, R. Carrington, M. Akmal, A. Goldberg, A. Williams, J. Skinner, and J. Pringle. A prospective, randomised comparison of autologous chondrocyte implantation versus mosaicplasty for osteochondral defects in the knee. *Journal of Bone & Joint Surgery, British Volume*. 85:223-230, 2003.
- ¹⁹Bertram T. A., E. Tentoff, P. C. Johnson, B. Tawil, M. Van Dyke, and K. B. Hellman. Hurdles in tissue engineering/regenerative medicine product

commercialization: a pilot survey of governmental funding agencies and the financial industry. *Tissue Engineering Part A*. 18:2187-2194, 2012.

- ²⁰Bhakta G., B. Rai, Z. X. Lim, J. H. Hui, G. S. Stein, A. J. van Wijnen, V. Nurcombe, G. D. Prestwich, and S. M. Cool. Hyaluronic acid-based hydrogels functionalized with heparin that support controlled release of bioactive BMP-2. *Biomaterials*. 33:6113-6122, 2012.
- ²¹Bhumiratana S., R. E. Eton, S. R. Oungoulian, L. Q. Wan, G. A. Ateshian, and G. Vunjak-Novakovic. Large, stratified, and mechanically functional human cartilage grown in vitro by mesenchymal condensation. *Proceedings of the National Academy of Sciences*. 111:6940-6945, 2014.
- ²²Bijlsma J. W., F. Berenbaum, and F. P. Lafeber. Osteoarthritis: an update with relevance for clinical practice. *The Lancet*. 377:2115-2126, 2011.
- ²³Blackman A. J., M. V. Smith, D. C. Flanigan, M. J. Matava, R. W. Wright, and R. H. Brophy. Correlation Between Magnetic Resonance Imaging and Clinical Outcomes After Cartilage Repair Surgery in the Knee A Systematic Review and Meta-analysis. *The American journal of sports medicine*. 41:1426-1434, 2013.
- ²⁴Bosetti M., F. Boccafoschi, M. Leigheb, A. E. Bianchi, and M. Cannas. Chondrogenic induction of human mesenchymal stem cells using combined growth factors for cartilage tissue engineering. *Journal of tissue engineering and regenerative medicine*. 6:205-213, 2012.
- ²⁵Boyan B. D., C. H. Lohmann, J. Romero, and Z. Schwartz. Bone and cartilage tissue engineering. *Clinics in plastic surgery*. 26:629-45, ix, 1999.
- ²⁶Brittberg M. Cell carriers as the next generation of cell therapy for cartilage repair a review of the matrix-induced autologous chondrocyte implantation procedure. *The American journal of sports medicine*. 38:1259-1271, 2010.
- ²⁷Brophy R. H. "Articular Cartilage Repair of the Knee in Athletes," in *Developing Insights in Cartilage Repair*. 2014, Springer. 241-252.
- ²⁸Brown W. E., H. G. Potter, R. G. Marx, T. L. Wickiewicz, and R. F. Warren. Magnetic resonance imaging appearance of cartilage repair in the knee. *Clinical orthopaedics and related research*. 422:214-223, 2004.
- ²⁹Browne J. E., A. F. Anderson, R. Arciero, B. Mandelbaum, J. B. Moseley Jr, L. J. Micheli, F. Fu, and C. Erggelet. Clinical outcome of autologous chondrocyte

- implantation at 5 years in US subjects. *Clinical orthopaedics and related research*. 436:237-245, 2005.
- ³⁰Buckwalter J. Articular cartilage injuries. *Clinical orthopaedics and related research*. 402:21-37, 2002.
- ³¹Bulpitt P. and D. Aeschlimann. New strategy for chemical modification of hyaluronic acid: preparation of functionalized derivatives and their use in the formation of novel biocompatible hydrogels. *Journal of biomedical materials research*. 47:152-169, 1999.
- ³²Burdick J. A. and G. D. Prestwich. Hyaluronic acid hydrogels for biomedical applications. *Advanced materials*. 23:H41-H56, 2011.
- ³⁴Cals F. L. J., C. A. Hellingman, W. Koevoet, R. J. B. de Jong, and G. J. V. M. van Osch. Effects of transforming growth factor- β subtypes on in vitro cartilage production and mineralization of human bone marrow stromal-derived mesenchymal stem cells. *Journal of Tissue Engineering and Regenerative Medicine*. 6:68-76, 2012.
- ³⁵Caminal M., C. Fonseca, D. Peris, X. Moll, R. M. Rabanal, J. Barrachina, D. Codina, F. García, J. J. Cairo, and F. Gòdia. Use of a chronic model of articular cartilage and meniscal injury for the assessment of long-term effects after autologous mesenchymal stromal cell treatment in sheep. *New biotechnology*. 31:492-498, 2014.
- ³⁶Cao Z., C. Dou, and S. Dong. Scaffolding Biomaterials for Cartilage Regeneration. *Journal of Nanomaterials*. 2014, 2014.
- ³⁷Cavallo C., G. Desando, L. Cattini, M. Cavallo, R. Buda, S. Giannini, A. Facchini, and B. Grigolo. Bone marrow concentrated cell transplantation: rationale for its use in the treatment of human osteochondral lesions. *Journal of biological regulators and homeostatic agents*. 27:165-175, 2012.
- ³⁸Centola M., B. Tonnarelli, S. Schären, N. Glaser, A. Barbero, and I. Martin. Priming 3D cultures of human mesenchymal stromal cells toward cartilage formation via developmental pathways. *Stem cells and development*. 22:2849-2858, 2013.
- ³⁹Cevc G. 'Project Launch': From research finding to therapeutic product. *European Journal of Pharmaceutical Sciences*. 51:123-136, 2014.
- ⁴⁰Chang C. H., T. F. Kuo, F. H. Lin, J. H. Wang, Y. M. Hsu, H. T. Huang, S. T. Loo, H. W. Fang, H. C. Liu, and W. C. Wang. Tissue engineering- based cartilage

repair with mesenchymal stem cells in a porcine model. *Journal of Orthopaedic Research*. 29:1874-1880, 2011.

- ⁴¹Chang N.-J., C.-C. Lin, C.-F. Li, K. Su, and M.-L. Yeh. The effect of osteochondral regeneration using polymer constructs and continuous passive motion therapy in the lower weight-bearing zone of femoral trochlear groove in rabbits. *Annals of biomedical engineering*. 41:385-397, 2013.
- ⁴²Cheng N. C., B. T. Estes, H. A. Awad, and F. Guilak. Chondrogenic differentiation of adipose-derived adult stem cells by a porous scaffold derived from native articular cartilage extracellular matrix. *Tissue Eng Part A*. 15:231-41, 2009.
- ⁴³Cheung H. K., T. T. Y. Han, D. M. Marecak, J. F. Watkins, B. G. Amsden, and L. E. Flynn. Composite hydrogel scaffolds incorporating decellularized adipose tissue for soft tissue engineering with adipose-derived stem cells. *Biomaterials*. 35:1914-1923, 2014.
- ⁴⁴Chirba M. A. and S. M. Garfield. FDA oversight of autologous stem cell therapies: legitimate regulation of drugs and devices or groundless interference with the practice of medicine. *J. Health & Biomedical L*. 7:233, 2011.
- ⁴⁵Chu C. R., M. Szczodry, and S. Bruno. Animal models for cartilage regeneration and repair. *Tissue Engineering Part B: Reviews*. 16:105-115, 2010.
- ⁴⁶Chung J. Y., M. Song, C.-W. Ha, J.-A. Kim, C.-H. Lee, and Y.-B. Park. Comparison of articular cartilage repair with different hydrogel-human umbilical cord blood-derived mesenchymal stem cell composites in a rat model. *Stem Cell Res Ther*. 5:39, 2014.
- ⁴⁷Coburn J. M., M. Gibson, S. Monagle, Z. Patterson, and J. H. Elisseeff. Bioinspired nanofibers support chondrogenesis for articular cartilage repair. *Proceedings of the National Academy of Sciences*. 109:10012-10017, 2012.
- ⁴⁸Collins N. J., D. Misra, D. T. Felson, K. M. Crossley, and E. M. Roos. Measures of knee function: International Knee Documentation Committee (IKDC) Subjective Knee Evaluation Form, Knee Injury and Osteoarthritis Outcome Score (KOOS), Knee Injury and Osteoarthritis Outcome Score Physical Function Short Form (KOOS- PS), Knee Outcome Survey Activities of Daily Living Scale (KOS- ADL), Lysholm Knee Scoring Scale, Oxford Knee Score (OKS), Western Ontario and McMaster Universities Osteoarthritis Index (WOMAC), Activity Rating Scale (ARS), and Tegner Activity Score (TAS). *Arthritis care & research*. 63:S208-S228, 2011.

- ⁴⁹Cook J., C. Hung, K. Kuroki, A. Stoker, C. Cook, F. Pfeiffer, S. Sherman, and J. Stannard. Animal models of cartilage repair. *Bone and Joint Research*. 3:89-94, 2014.
- ⁵⁰Cooper C., E. Dennison, M. Edwards, and A. Litwic. Epidemiology of osteoarthritis. *Medicographia*. 35:145-151, 2013.
- ⁵¹Craft A. M., N. Ahmed, J. S. Rockel, G. S. Baht, B. A. Alman, R. A. Kandel, A. E. Grigoriadis, and G. M. Keller. Specification of chondrocytes and cartilage tissues from embryonic stem cells. *Development*. 140:2597-2610, 2013.
- ⁵²Cucchiariini M. and H. Madry. Overexpression of human IGF-I via direct rAAV-mediated gene transfer improves the early repair of articular cartilage defects in vivo. *Gene therapy*. 21:811-819, 2014.
- ⁵³Cucchiariini M., H. Madry, F. Guilak, D. B. Saris, M. J. Stoddart, M. Koon Wong, and P. Roughley. A vision on the future of articular cartilage repair. *Eur Cell Mater*. 27:12-6, 2014.
- ⁵⁴Cushnie E. K., Y. M. Khan, and C. T. Laurencin. Amorphous hydroxyapatite-sintered polymeric scaffolds for bone tissue regeneration: Physical characterization studies. *Journal of Biomedical Materials Research Part A*. 84:54-62, 2008.
- ⁵⁵Dahlin R. L., L. A. Kinard, J. Lam, C. J. Needham, S. Lu, F. K. Kasper, and A. G. Mikos. Articular chondrocytes and mesenchymal stem cells seeded on biodegradable scaffolds for the repair of cartilage in a rat osteochondral defect model. *Biomaterials*. 35:7460-7469, 2014.
- ⁵⁶Dai L.-Y. and L.-S. Jiang. Single-level instrumented posterolateral fusion of lumbar spine with β -tricalcium phosphate versus autograft: a prospective, randomized study with 3-year follow-up. *Spine*. 33:1299-1304, 2008.
- ⁵⁷Dang P. N., L. D. Solorio, and E. Alsberg. Driving cartilage formation in high-density human adipose-derived stem cell aggregate and sheet constructs without exogenous growth factor delivery. *Tissue Engineering Part A*. 20:3163-3175, 2014.
- ⁵⁸Davies B. M., S. Rikabi, A. French, R. Pinedo-Villanueva, M. E. Morrey, K. Wartolowska, A. Judge, R. E. MacLaren, A. Mathur, and D. J. Williams. Quantitative assessment of barriers to the clinical development and adoption of cellular therapies: A pilot study. *Journal of tissue engineering*. 5:2041731414551764, 2014.

- ⁵⁹Davies J. E., D. Baksh, R. Sarugaser, M. Hosseini, and A. D. Lickorish. Progenitor cells from wharton's jelly of human umbilical cord. 2013, Google Patents.
- ⁶⁰Declercq H. A., T. De Caluwé, O. Krysko, C. Bachert, and M. J. Cornelissen. Bone grafts engineered from human adipose-derived stem cells in dynamic 3D-environments. *Biomaterials*. 34:1004-1017, 2013.
- ⁶¹DeKosky B. J., N. H. Dormer, G. C. Ingavle, C. H. Roatch, J. Lomakin, M. S. Detamore, and S. H. Gehrke. Hierarchically designed agarose and poly(ethylene glycol) interpenetrating network hydrogels for cartilage tissue engineering. *Tissue Eng Part C Methods*. 16:1533-42, 2010.
- ⁶²Deponti D., A. Di Giancamillo, L. Mangiavini, A. Pozzi, G. Fraschini, C. Sosio, C. Domeneghini, and G. M. Peretti. Fibrin-based model for cartilage regeneration: tissue maturation from in vitro to in vivo. *Tissue Engineering Part A*. 18:1109-1122, 2012.
- ⁶³Detamore M. S. Human umbilical cord mesenchymal stromal cells in regenerative medicine. *Stem Cell Res Ther*. 4:142, 2013.
- ⁶⁴Devarajan K., M. L. Forrest, M. S. Detamore, and H. Staecker. Adenovector-Mediated Gene Delivery to Human Umbilical Cord Mesenchymal Stromal Cells Induces Inner Ear Cell Phenotype. *Cellular Reprogramming*. 15:43-54, 2013.
- ⁶⁵Dewan A. K., M. A. Gibson, J. H. Elisseff, and M. E. Trice. Evolution of Autologous Chondrocyte Repair and Comparison to Other Cartilage Repair Techniques. *BioMed research international*. 2014, 2014.
- ⁶⁶Dhandayuthapani B., Y. Yoshida, T. Maekawa, and D. S. Kumar. Polymeric scaffolds in tissue engineering application: a review. *International Journal of Polymer Science*. 2011, 2011.
- ⁶⁷Diekman B. O. and F. Guilak. Stem cell-based therapies for osteoarthritis: challenges and opportunities. *Current Opinion in Rheumatology*. 25:119-126, 2013.
- ⁶⁸Dikina A. D., H. A. Strobel, B. P. Lai, M. W. Rolle, and E. Alsberg. Engineered cartilaginous tubes for tracheal tissue replacement via self-assembly and fusion of human mesenchymal stem cell constructs. *Biomaterials*. 52:452-462, 2015.

- ⁶⁹Dormer N. H., C. J. Berkland, and M. S. Detamore. Emerging techniques in stratified designs and continuous gradients for tissue engineering of interfaces. *Ann Biomed Eng.* 38:2121-41, 2010.
- ⁷⁰Dormer N. H., V. Gupta, A. M. Scurto, C. J. Berkland, and M. S. Detamore. Effect of different sintering methods on bioactivity and release of proteins from PLGA microspheres. *Mater Sci Eng C Mater Biol Appl.* 33:4343-51, 2013.
- ⁷¹Dormer N. H., M. Singh, L. Wang, C. J. Berkland, and M. S. Detamore. Osteochondral interface tissue engineering using macroscopic gradients of bioactive signals. *Ann Biomed Eng.* 38:2167-82, 2010.
- ⁷²Dormer N. H., M. Singh, L. Zhao, N. Mohan, C. J. Berkland, and M. S. Detamore. Osteochondral interface regeneration of the rabbit knee with macroscopic gradients of bioactive signals. *Journal of Biomedical Materials Research Part A.* 100:162-170, 2012.
- ⁷⁴DuRaine G. D., W. E. Brown, J. C. Hu, and K. A. Athanasiou. Emergence of Scaffold-Free Approaches for Tissue Engineering Musculoskeletal Cartilages. *Annals of biomedical engineering.* 43:543-554, 2015.
- ⁷⁵Ebihara G., M. Sato, M. Yamato, G. Mitani, T. Kutsuna, T. Nagai, S. Ito, T. Ukai, M. Kobayashi, and M. Kokubo. Cartilage repair in transplanted scaffold-free chondrocyte sheets using a minipig model. *Biomaterials.* 33:3846-3851, 2012.
- ⁷⁶Fan H., Y. Hu, L. Qin, X. Li, H. Wu, and R. Lv. Porous gelatin–chondroitin–hyaluronate tri- copolymer scaffold containing microspheres loaded with TGF- β 1 induces differentiation of mesenchymal stem cells in vivo for enhancing cartilage repair. *Journal of Biomedical Materials Research Part A.* 77:785-794, 2006.
- ⁷⁷Farr J., B. J. Cole, S. Sherman, and V. Karas. Particulated articular cartilage: CAIS and DeNovo NT. *Journal of Knee Surgery.* 25:023-030, 2012.
- ⁷⁸Farr J. and A. Gomoll. "Particulated/Minced Cartilage," in *Cartilage Restoration.* 2014, Springer. 161-168.
- ⁷⁹Farr J. and J. Q. Yao. Chondral defect repair with particulated juvenile cartilage allograft. *Cartilage.* 2:346-353, 2011.
- ⁸⁰Fennema E., N. Rivron, J. Rouwkema, C. van Blitterswijk, and J. de Boer. Spheroid culture as a tool for creating 3D complex tissues. *Trends in biotechnology.* 31:108-115, 2013.

- ⁸¹Ferreira L. S., S. Gerecht, J. Fuller, H. F. Shieh, G. Vunjak-Novakovic, and R. Langer. Bioactive hydrogel scaffolds for controllable vascular differentiation of human embryonic stem cells. *Biomaterials*. 28:2706-2717, 2007.
- ⁸²Filardo G., E. Kon, F. Perdisa, F. Balboni, and M. Marcacci. Autologous osteochondral transplantation for the treatment of knee lesions: results and limitations at two years' follow-up. *International orthopaedics*.1-8, 2014.
- ⁸³Florine E. M., R. E. Miller, R. M. Porter, C. H. Evans, B. Kurz, and A. J. Grodzinsky. Effects of Dexamethasone on Mesenchymal Stromal Cell Chondrogenesis and Aggrecanase Activity Comparison of Agarose and Self-Assembling Peptide Scaffolds. *Cartilage*. 4:63-74, 2013.
- ⁸⁴French A., R. L. Buckler, and D. A. Brindley. Commercialization of regenerative medicine: learning from spin-outs. *Rejuvenation research*. 16:164-170, 2013.
- ⁸⁵Freyria A.-M. and F. Mallein-Gerin. Chondrocytes or adult stem cells for cartilage repair: the indisputable role of growth factors. *Injury*. 43:259-265, 2012.
- ⁸⁶Friedrich J., C. Seidel, R. Ebner, and L. A. Kunz-Schughart. Spheroid-based drug screen: considerations and practical approach. *Nature protocols*. 4:309-324, 2009.
- ⁸⁷Fulco I., R. D. Largo, S. Miot, A. Wixmerten, I. Martin, D. J. Schaefer, and M. D. Haug. Toward Clinical Application of Tissue-Engineered Cartilage. *Facial Plastic Surgery*. 29:099-105, 2013.
- ⁸⁸Garrigues N. W., D. Little, J. Sanchez-Adams, D. S. Ruch, and F. Guilak. Electrospun cartilage-derived matrix scaffolds for cartilage tissue engineering. *J Biomed Mater Res A*. 102:3998-4008, 2014.
- ⁸⁹Georgi N., C. van Blitterswijk, and M. Karperien. Mesenchymal Stromal/Stem Cell-or Chondrocyte-Seeded Microcarriers as Building Blocks for Cartilage Tissue Engineering. *Tissue Engineering Part A*. 2014.
- ⁹⁰Geyer M. R., W. G. Rodkey, and J. R. Steadman. "Clinical Relevance of Chondral Lesions in the Treatment of the ACL-Deficient Knee: Microfracture Technique," in *The ACL-Deficient Knee*. 2013, Springer. 271-279.
- ⁹¹Gille J., P. Behrens, P. Volpi, L. De Girolamo, E. Reiss, W. Zoch, and S. Anders. Outcome of Autologous Matrix Induced Chondrogenesis (AMIC) in cartilage knee surgery: data of the AMIC Registry. *Archives of orthopaedic and trauma surgery*. 133:87-93, 2013.

- ⁹²Gimble J. M., B. A. Bunnell, and F. Guilak. Human adipose-derived cells: an update on the transition to clinical translation. *Regenerative medicine*. 7:225-235, 2012.
- ⁹³Goebel L., P. Orth, A. Müller, D. Zurakowski, A. Bückler, M. Cucchiarini, D. Pape, and H. Madry. Experimental scoring systems for macroscopic articular cartilage repair correlate with the MOCART score assessed by a high-field MRI at 9.4 T—comparative evaluation of five macroscopic scoring systems in a large animal cartilage defect model. *Osteoarthritis and Cartilage*. 20:1046-1055, 2012.
- ⁹⁴Goude M. C., T. C. McDevitt, and J. S. Temenoff. Chondroitin Sulfate Microparticles Modulate Transforming Growth Factor- β 1-Induced Chondrogenesis of Human Mesenchymal Stem Cell Spheroids. *Cells Tissues Organs*. 199:117-130, 2014.
- ⁹⁵Grimaud E., D. Heymann, and F. R dini. Recent advances in TGF- β effects on chondrocyte metabolism: potential therapeutic roles of TGF- β in cartilage disorders. *Cytokine & growth factor reviews*. 13:241-257, 2002.
- ⁹⁶Gudas R., A. Gudait , T. Mickevi cius, N. Masiulis, R. Simonaityt , E.  ekanauskas, and A. Skurvydas. Comparison of osteochondral autologous transplantation, microfracture, or debridement techniques in articular cartilage lesions associated with anterior cruciate ligament injury: a prospective study with a 3-year follow-up. *Arthroscopy: The Journal of Arthroscopic & Related Surgery*. 29:89-97, 2013.
- ⁹⁷Gudas R., E. Stankevi cius, E. Monastyreckien , D. Pranys, and R. J. Kalesinskas. Osteochondral autologous transplantation versus microfracture for the treatment of articular cartilage defects in the knee joint in athletes. *Knee Surgery, Sports Traumatology, Arthroscopy*. 14:834-842, 2006.
- ⁹⁸Guerit D., F. Djouad, M. Maumus, C. Bony, C. Jorgensen, and D. Noel. Therapeutic Applications of Mesenchymal Stem Cells for Cartilage Repair. *Journal of Biomaterials and Tissue Engineering*. 2:29-39, 2012.
- ⁹⁹Gupta V., N. Mohan, C. J. Berkland, and M. S. Detamore. Microsphere-based scaffolds carrying opposing gradients of chondroitin sulfate and tricalcium phosphate. *Frontiers in Bioengineering and Biotechnology*. 3:1-15, 2015.
- ¹⁰⁰Gupta V., N. Mohan, and M. S. Detamore. Microsphere-Based Scaffolds Carrying Opposing Gradients of Chondroitin Sulfate and Tricalcium Phosphate. *Frontiers in Bioengineering and Biotechnology*. 0.

- ¹⁰¹Ha C., K. Lee, B. Lee, S. Park, J. Cho, T. Kim, M. Noh, and M. Lee. *Efficacy of Tissuegene-C (TG-C), a cell mediated gene therapy, in patients with osteoarthritis: A phase IIa clinical study.* in *JOURNAL OF TISSUE ENGINEERING AND REGENERATIVE MEDICINE*. 2012: WILEY-BLACKWELL 111 RIVER ST, HOBOKEN 07030-5774, NJ USA.
- ¹⁰²Ha C.-W., M. J. Noh, K. B. Choi, and K. H. Lee. Initial phase I safety of retrovirally transduced human chondrocytes expressing transforming growth factor-beta-1 in degenerative arthritis patients. *Cytotherapy*. 14:247-256, 2012.
- ¹⁰³Halvorsen Y.-D. C., W. O. Wilkison, and J. M. Gimble. Use of adipose tissue-derived stromal cells for chondrocyte differentiation and cartilage repair. 2014, Google Patents.
- ¹⁰⁴Hangody L. and Á. Berta. Mosaicplasty for Articular Cartilage Defects. *European Surgical Orthopaedics and Traumatology: The EFORT Textbook*. 2913-2924, 2014.
- ¹⁰⁵Hangody L. and Á. Berta. "Surgical Techniques in Cartilage Repair Surgery: Osteochondral Autograft Transfer (OATS, Mosaicplasty)," in *Techniques in Cartilage Repair Surgery*. 2014, Springer. 131-140.
- ¹⁰⁶Hardikar A. A., B. Marcus-Samuels, E. Geras-Raaka, B. M. Raaka, and M. C. Gershengorn. Human pancreatic precursor cells secrete FGF2 to stimulate clustering into hormone-expressing islet-like cell aggregates. *Proceedings of the National Academy of Sciences*. 100:7117-7122, 2003.
- ¹⁰⁷Hatic S. O. and G. C. Berlet. Particulated juvenile articular cartilage graft (DeNovo NT Graft) for treatment of osteochondral lesions of the talus. *Foot & ankle specialist*. 3:361-364, 2010.
- ¹⁰⁸Hatsushika D., T. Muneta, T. Nakamura, M. Horie, H. Koga, Y. Nakagawa, K. Tsuji, S. Hishikawa, E. Kobayashi, and I. Sekiya. Repetitive allogeneic intraarticular injections of synovial mesenchymal stem cells promote meniscus regeneration in a porcine massive meniscus defect model. *Osteoarthritis and Cartilage*. 22:941-950, 2014.
- ¹⁰⁹Hentze H., R. Graichen, and A. Colman. Cell therapy and the safety of embryonic stem cell-derived grafts. *Trends in biotechnology*. 25:24-32, 2007.
- ¹¹⁰Hines J. Z., P. Lurie, E. Yu, and S. Wolfe. Left to their own devices: breakdowns in United States medical device premarket review. *PLoS medicine*. 7:e1000280, 2010.

- ¹¹¹Hoemann C., R. Kandel, S. Roberts, D. B. Saris, L. Creemers, P. Mainil-Varlet, S. Méthot, A. P. Hollander, and M. D. Buschmann. International Cartilage Repair Society (ICRS) recommended guidelines for histological endpoints for cartilage repair studies in animal models and clinical trials. *Cartilage*. 2:153-172, 2011.
- ¹¹²Huang C.-C., D.-Y. Chen, H.-J. Wei, K.-J. Lin, C.-T. Wu, T.-Y. Lee, H.-Y. Hu, S.-M. Hwang, Y. Chang, and H.-W. Sung. Hypoxia-induced therapeutic neovascularization in a mouse model of an ischemic limb using cell aggregates composed of HUVECs and cbMSCs. *Biomaterials*. 34:9441-9450, 2013.
- ¹¹³Huang H., X. Zhang, X. Hu, Z. Shao, J. Zhu, L. Dai, Z. Man, L. Yuan, H. Chen, and C. Zhou. A functional biphasic biomaterial homing mesenchymal stem cells for in vivo cartilage regeneration. *Biomaterials*. 35:9608-9619, 2014.
- ¹¹⁴Huey D. J., J. C. Hu, and K. A. Athanasiou. Chondrogenically-tuned expansion enhances the cartilaginous matrix forming capabilities of primary, adult, leporine chondrocytes. *Cell transplantation*. 22:331, 2013.
- ¹¹⁵Hurtig M. B., M. D. Buschmann, L. A. Fortier, C. D. Hoemann, E. B. Hunziker, J. S. Jurvelin, P. Mainil-Varlet, C. W. Mellwraith, R. L. Sah, and R. A. Whiteside. Preclinical Studies for Cartilage Repair Recommendations from the International Cartilage Repair Society. *Cartilage*. 2:137-152, 2011.
- ¹¹⁶Ilic N., S. Savic, E. Siegel, K. Atkinson, and L. Tasic. Examination of the regulatory frameworks applicable to biologic drugs (including stem cells and their progeny) in Europe, the US, and Australia: Part II—A method of software documentary analysis. *Stem cells translational medicine*. 1:909-920, 2012.
- ¹¹⁷Ingavle G. C., A. W. Frei, S. H. Gehrke, and M. S. Detamore. Incorporation of aggrecan in interpenetrating network hydrogels to improve cellular performance for cartilage tissue engineering. *Tissue Engineering Part A*. 19:1349-1359, 2013.
- ¹¹⁸Insall J. Intra-articular surgery for degenerative arthritis of the knee. *J Bone Joint Surg [Br]*. 49:211-228, 1967.
- ¹¹⁹Jaklenec A., A. Hinckfuss, B. Bilgen, D. M. Ciombor, R. Aaron, and E. Mathiowitz. Sequential release of bioactive IGF-I and TGF- β 1 from PLGA microsphere-based scaffolds. *Biomaterials*. 29:1518-1525, 2008.

- ¹²⁰Jo C. H., Y. G. Lee, W. H. Shin, H. Kim, J. W. Chai, E. C. Jeong, J. E. Kim, H. Shim, J. S. Shin, and I. S. Shin. Intra- Articular Injection of Mesenchymal Stem Cells for the Treatment of Osteoarthritis of the Knee: A Proof- of- Concept Clinical Trial. *Stem Cells*. 32:1254-1266, 2014.
- ¹²¹Johnson K., S. Zhu, M. S. Tremblay, J. N. Payette, J. Wang, L. C. Bouchez, S. Meeusen, A. Althage, C. Y. Cho, and X. Wu. A stem cell–based approach to cartilage repair. *Science*. 336:717-721, 2012.
- ¹²²Johnstone B., M. Alini, M. Cucchiaroni, G. R. Dodge, D. Eglin, F. Guilak, H. Madry, A. Mata, R. L. Mauck, C. E. Semino, and M. J. Stoddart. TISSUE ENGINEERING FOR ARTICULAR CARTILAGE REPAIR - THE STATE OF THE ART. *European Cells & Materials*. 25:248-267, 2013.
- ¹²³Jones B. A. and M. Pei. Synovium-derived stem cells: a tissue-specific stem cell for cartilage engineering and regeneration. *Tissue Engineering Part B: Reviews*. 18:301-311, 2012.
- ¹²⁴Jurgens W. J., R. J. Kroeze, B. Zandieh-Doulabi, A. van Dijk, G. A. Renders, T. H. Smit, F. J. van Milligen, M. J. Ritt, and M. N. Helder. One-step surgical procedure for the treatment of osteochondral defects with adipose-derived stem cells in a caprine knee defect: a pilot study. *BioResearch open access*. 2:315-325, 2013.
- ¹²⁵K Batsali A., M.-C. Kastrinaki, H. A Papadaki, and C. Pontikoglou. Mesenchymal stem cells derived from Wharton's Jelly of the umbilical cord: biological properties and emerging clinical applications. *Current stem cell research & therapy*. 8:144-155, 2013.
- ¹²⁶Keaveny T. M. and W. C. Hayes. A 20-year perspective on the mechanical properties of trabecular bone. *Journal of biomechanical engineering*. 115:534-542, 1993.
- ¹²⁷Kelm J. M., N. E. Timmins, C. J. Brown, M. Fussenegger, and L. K. Nielsen. Method for generation of homogeneous multicellular tumor spheroids applicable to a wide variety of cell types. *Biotechnology and bioengineering*. 83:173-180, 2003.
- ¹²⁸Kim H. Influence of Mesenchymal Stem Cells on Cryopreserved Tracheal Allografts in Rabbits. *The Korean journal of thoracic and cardiovascular surgery*. 46:328-339, 2013.

- ¹²⁹Kim I. L., R. L. Mauck, and J. A. Burdick. Hydrogel design for cartilage tissue engineering: a case study with hyaluronic acid. *Biomaterials*. 32:8771-8782, 2011.
- ¹³⁰Knutsen G., L. Engebretsen, T. C. Ludvigsen, J. O. Drogset, T. Grøntvedt, E. Solheim, T. Strand, S. Roberts, V. Isaksen, and O. Johansen. Autologous chondrocyte implantation compared with microfracture in the knee. *The Journal of Bone & Joint Surgery*. 86:455-464, 2004.
- ¹³¹Kock L. M., R. M. Schulz, C. C. van Donkelaar, C. B. Thümmler, A. Bader, and K. Ito. RGD-dependent integrins are mechanotransducers in dynamically compressed tissue-engineered cartilage constructs. *Journal of biomechanics*. 42:2177-2182, 2009.
- ¹³²Koh Y.-G., S.-B. Jo, O.-R. Kwon, D.-S. Suh, S.-W. Lee, S.-H. Park, and Y.-J. Choi. Mesenchymal stem cell injections improve symptoms of knee osteoarthritis. *Arthroscopy: The Journal of Arthroscopic & Related Surgery*. 29:748-755, 2013.
- ¹³³Kon E., G. Filardo, A. Di Martino, and M. Marcacci. ACI and MACI. *Journal of Knee Surgery*. 25:017-022, 2012.
- ¹³⁴Kon E., G. Filardo, F. Perdisa, G. Venieri, and M. Marcacci. Clinical results of multilayered biomaterials for osteochondral regeneration. *Journal of Experimental Orthopaedics*. 1:1-8, 2014.
- ¹³⁵Kon E., G. Filardo, D. Robinson, J. Eisman, A. Levy, K. Zaslav, J. Shani, and N. Altschuler. Osteochondral regeneration using a novel aragonite-hyaluronate bi-phasic scaffold in a goat model. *Knee Surgery, Sports Traumatology, Arthroscopy*. 22:1452-1464, 2014.
- ¹³⁶Kramer J., F. Böhrnsen, U. Lindner, P. Behrens, P. Schlenke, and J. Rohwedel. In vivo matrix-guided human mesenchymal stem cells. *Cellular and molecular life sciences*. 63:616-626, 2006.
- ¹³⁷Krampera M., G. Pizzolo, G. Aprili, and M. Franchini. Mesenchymal stem cells for bone, cartilage, tendon and skeletal muscle repair. *Bone*. 39:678-683, 2006.
- ¹³⁸Kuroda T., T. Matsumoto, Y. Mifune, T. Fukui, S. Kubo, T. Matsushita, T. Asahara, M. Kurosaka, and R. Kuroda. Therapeutic strategy of third-generation autologous chondrocyte implantation for osteoarthritis. *Upsala journal of medical sciences*. 116:107-114, 2011.

- ¹³⁹Lai J.-Y. and I.-H. Tu. Adhesion, phenotypic expression, and biosynthetic capacity of corneal keratocytes on surfaces coated with hyaluronic acid of different molecular weights. *Acta biomaterialia*. 8:1068-1079, 2012.
- ¹⁴⁰Lai J.-Y., I.-H. Tu, and T.-C. Yu. Method of Forming Cell Spheroids Cultured in Serum-Free Manner on Nanoscale Coatings of Hyaluronic Acid with High Molecular Weight. 2012, Google Patents.
- ¹⁴¹Lane N., K. Brandt, G. Hawker, E. Peeva, E. Schreyer, W. Tsuji, and M. Hochberg. OARSI-FDA initiative: defining the disease state of osteoarthritis. *Osteoarthritis and Cartilage*. 19:478-482, 2011.
- ¹⁴²Lee J., M. Sato, H. Kim, and J. Mochida. Transplantation of scaffold-free spheroids composed of synovium-derived cells and chondrocytes for the treatment of cartilage defects of the knee. *Eur Cell Mater*. 22:275-90, 2011.
- ¹⁴³Lee J.-M. and G.-I. Im. SOX trio-co-transduced adipose stem cells in fibrin gel to enhance cartilage repair and delay the progression of osteoarthritis in the rat. *Biomaterials*. 33:2016-2024, 2012.
- ¹⁴⁴Lee J. K., D. J. Responde, D. D. Cissell, J. C. Hu, J. A. Nolta, and K. A. Athanasiou. Clinical translation of stem cells: insight for cartilage therapies. *Critical reviews in biotechnology*. 34:89-100, 2013.
- ¹⁴⁵Lei J., L. T. McLane, J. E. Curtis, and J. S. Temenoff. Characterization of a multilayer heparin coating for biomolecule presentation to human mesenchymal stem cell spheroids. *Biomaterials Science*. 2:666-673, 2014.
- ¹⁴⁶Levato R., J. Visser, J. A. Planell, E. Engel, J. Malda, and M. A. Mateos-Timoneda. Biofabrication of tissue constructs by 3D bioprinting of cell-laden microcarriers. *Biofabrication*. 6, 2014.
- ¹⁴⁷Levett P. A., F. P. Melchels, K. Schrobback, D. W. Hutmacher, J. Malda, and T. J. Klein. A biomimetic extracellular matrix for cartilage tissue engineering centered on photocurable gelatin, hyaluronic acid and chondroitin sulfate. *Acta biomaterialia*. 10:214-223, 2014.
- ¹⁴⁸Liao J., K. Shi, Q. Ding, Y. Qu, F. Luo, and Z. Qian. Recent developments in scaffold-guided cartilage tissue regeneration. *Journal of Biomedical Nanotechnology*. 10:3085-3104, 2014.
- ¹⁴⁹Lim C. T., X. Ren, M. H. Afizah, S. Tarigan-Panjaitan, Z. Yang, Y. Wu, K. S. Chian, A. G. Mikos, and J. H. P. Hui. Repair of osteochondral defects with rehydrated freeze-dried oligo [poly (ethylene glycol) fumarate] hydrogels

- seeded with bone marrow mesenchymal stem cells in a porcine model. *Tissue Engineering Part A*. 19:1852-1861, 2013.
- ¹⁵⁰Lima A. C., P. Batista, T. A. Valente, A. S. Silva, I. J. Correia, and J. F. Mano. Novel methodology based on biomimetic superhydrophobic substrates to immobilize cells and proteins in hydrogel spheres for applications in bone regeneration. *Tissue Engineering Part A*. 19:1175-1187, 2013.
- ¹⁵¹Little C. B. and D. J. Hunter. Post-traumatic osteoarthritis: from mouse models to clinical trials. *Nature Reviews Rheumatology*. 9:485-497, 2013.
- ¹⁵²Liu S., K. D. Hou, M. Yuan, J. Peng, L. Zhang, X. Sui, B. Zhao, W. Xu, A. Wang, and S. Lu. Characteristics of mesenchymal stem cells derived from Wharton's jelly of human umbilical cord and for fabrication of non-scaffold tissue-engineered cartilage. *Journal of bioscience and bioengineering*. 117:229-235, 2014.
- ¹⁵³Loessner D., K. S. Stok, M. P. Lutolf, D. W. Hutmacher, J. A. Clements, and S. C. Rizzi. Bioengineered 3D platform to explore cell-ECM interactions and drug resistance of epithelial ovarian cancer cells. *Biomaterials*. 31:8494-8506, 2010.
- ¹⁵⁴Long T., Z. Zhu, H. A. Awad, E. M. Schwarz, M. J. Hilton, and Y. Dong. The effect of mesenchymal stem cell sheets on structural allograft healing of critical sized femoral defects in mice. *Biomaterials*. 35:2752-2759, 2014.
- ¹⁵⁵Lopa S. and H. Madry. Bioinspired scaffolds for osteochondral regeneration. *Tissue Engineering Part A*. 2014.
- ¹⁵⁶Lu H. H., S. D. Subramony, M. K. Boushell, and X. Zhang. Tissue engineering strategies for the regeneration of orthopedic interfaces. *Annals of biomedical engineering*. 38:2142-2154, 2010.
- ¹⁵⁷Lv Q., L. Nair, and C. T. Laurencin. Fabrication, characterization, and in vitro evaluation of poly (lactic acid glycolic acid)/nano- hydroxyapatite composite microsphere- based scaffolds for bone tissue engineering in rotating bioreactors. *Journal of Biomedical Materials Research Part A*. 91:679-691, 2009.
- ¹⁵⁸Ma A., L. Jiang, L. Song, Y. Hu, H. Dun, P. Daloz, Y. Yu, J. Jiang, M. Zafarullah, and H. Chen. Reconstruction of cartilage with clonal mesenchymal stem cell-acellular dermal matrix in cartilage defect model in nonhuman primates. *International immunopharmacology*. 16:399-408, 2013.

- ¹⁵⁹Madry H., U. W. Grün, and G. Knutsen. Medikamentöse und operative Möglichkeiten.
- ¹⁶⁰Madry H., G. Kaul, D. Zurakowski, G. Vunjak-Novakovic, and M. Cucchiari. Cartilage constructs engineered from chondrocytes overexpressing IGF-I improve the repair of osteochondral defects in a rabbit model. *Eur Cell Mater.* 25:229-247, 2013.
- ¹⁶¹Mainil-Varlet P., B. Van Damme, D. Nestic, G. Knutsen, R. Kandel, and S. Roberts. A new histology scoring system for the assessment of the quality of human cartilage repair: ICRS II. *The American journal of sports medicine.* 38:880-890, 2010.
- ¹⁶²Marcacci M., G. Filardo, and E. Kon. Treatment of cartilage lesions: What works and why? *Injury.* 44, Supplement 1:S11-S15, 2013.
- ¹⁶³Martinez I., J. Elvenes, R. Olsen, K. Bertheussen, and O. Johansen. Redifferentiation of in vitro expanded adult articular chondrocytes by combining the hanging-drop cultivation method with hypoxic environment. *Cell transplantation.* 17:987-996, 2008.
- ¹⁶⁴Matsuura K., Y. Haraguchi, T. Shimizu, and T. Okano. Cell sheet transplantation for heart tissue repair. *Journal of Controlled Release.* 169:336-340, 2013.
- ¹⁶⁵McCormick F., B. J. Cole, B. Nwachukwu, J. D. Harris, H. D. Adkisson IV, and J. Farr. Treatment of Focal Cartilage Defects With a Juvenile Allogeneic 3-Dimensional Articular Cartilage Graft. *Operative Techniques in Sports Medicine.* 21:95-99, 2013.
- ¹⁶⁶McGowan K. B. and G. Stiegman. Regulatory challenges for cartilage repair technologies. *Cartilage.* 4:4-11, 2013.
- ¹⁶⁷Mellott A. J., K. Devarajan, H. E. Shinogle, D. S. Moore, Z. Talata, J. S. Laurence, M. L. Forrest, S. Noji, E. Tanaka, and H. Staecker. Nonviral Reprogramming of Human Wharton's Jelly Cells Reveals Differences Between ATOH1 Homologues. *Tissue Engineering Part A.* 21:1795-1809, 2015.
- ¹⁶⁸Mellott A. J., M. E. Godsey, H. E. Shinogle, D. S. Moore, M. L. Forrest, and M. S. Detamore. Improving viability and transfection efficiency with human umbilical cord wharton's jelly cells through use of a ROCK inhibitor. *Cell Reprogram.* 16:91-7, 2014.
- ¹⁶⁹Meyerkort D., D. Wood, and M.-H. Zheng. One-stage vs two-stage cartilage repair: a current review. *Orthopedic Research and Reviews.* 2:95-1, 2011.

- ¹⁷⁰Middleton-Hardie C., M. Lazarov, and D. Rosen. Peptide composition and a method of promoting cartilage formation. 2013, Google Patents.
- ¹⁷¹Mikael P. E., A. R. Amini, J. Basu, M. J. Arellano-Jimenez, C. T. Laurencin, M. M. Sanders, C. B. Carter, and S. P. Nukavarapu. Functionalized carbon nanotube reinforced scaffolds for bone regenerative engineering: fabrication, in vitro and in vivo evaluation. *Biomedical Materials*. 9:035001, 2014.
- ¹⁷²Milano G., L. Deriu, E. S. Passino, G. Masala, A. Manunta, R. Postacchini, M. F. Saccomanno, and C. Fabbriani. Repeated platelet concentrate injections enhance reparative response of microfractures in the treatment of chondral defects of the knee: an experimental study in an animal model. *Arthroscopy: The Journal of Arthroscopic & Related Surgery*. 28:688-701, 2012.
- ¹⁷³Miller M. J., S. Ahmed, P. Bobrowski, and T. M. Haqqi. The chondroprotective actions of a natural product are associated with the activation of IGF-1 production by human chondrocytes despite the presence of IL-1 β . *BMC complementary and alternative medicine*. 6:13, 2006.
- ¹⁷⁴Minas T. Chondrocyte implantation in the repair of chondral lesions of the knee: economics and quality of life. *American journal of orthopedics (Belle Mead, NJ)*. 27:739-744, 1998.
- ¹⁷⁵Mithoefer K., T. McAdams, R. J. Williams, P. C. Kreuz, and B. R. Mandelbaum. Clinical efficacy of the microfracture technique for articular cartilage repair in the knee an evidence-based systematic analysis. *The American journal of sports medicine*. 37:2053-2063, 2009.
- ¹⁷⁶Mithoefer K., D. B. Saris, J. Farr, E. Kon, K. Zaslav, B. J. Cole, J. Ranstam, J. Yao, M. Shive, and D. Levine. Guidelines for the Design and Conduct of Clinical Studies in Knee Articular Cartilage Repair International Cartilage Repair Society Recommendations Based on Current Scientific Evidence and Standards of Clinical Care. *Cartilage*. 2:100-121, 2011.
- ¹⁷⁷Mithoefer K., R. J. Williams, R. F. Warren, H. G. Potter, C. R. Spock, E. C. Jones, T. L. Wickiewicz, and R. G. Marx. The microfracture technique for the treatment of articular cartilage lesions in the knee. *The Journal of Bone & Joint Surgery*. 87:1911-1920, 2005.
- ¹⁷⁸Mobasheri A., G. Kalamegam, G. Musumeci, and M. E. Batt. Chondrocyte and mesenchymal stem cell-based therapies for cartilage repair in osteoarthritis and related orthopaedic conditions. *Maturitas*. 78:188-198, 2014.

- ¹⁷⁹Mohan N., N. H. Dormer, K. L. Caldwell, V. H. Key, C. J. Berkland, and M. S. Detamore. Continuous gradients of material composition and growth factors for effective regeneration of the osteochondral interface. *Tissue Engineering Part A*. 17:2845-2855, 2011.
- ¹⁸⁰Mohan N., V. Gupta, B. Sridharan, A. J. Mellott, J. T. Easley, R. H. Palmer, R. A. Galbraith, V. H. Key, C. J. Berkland, and M. S. Detamore. Microsphere-based gradient implants for osteochondral regeneration: a long term study in sheep. *Regen Med*. Accepted, 2015.
- ¹⁸¹Mohan N., V. Gupta, B. Sridharan, A. Sutherland, and M. S. Detamore. The potential of encapsulating "raw materials" in 3D osteochondral gradient scaffolds. *Biotechnol Bioeng*. 111:829-41, 2014.
- ¹⁸²Mohan N., V. Gupta, B. Sridharan, A. Sutherland, and M. S. Detamore. The potential of encapsulating "raw materials" in 3D osteochondral gradient scaffolds. *Biotechnology and bioengineering*. 111:829-841, 2014.
- ¹⁸³Montgomery S. R., B. D. Foster, S. S. Ngo, R. D. Terrell, J. C. Wang, F. A. Petrigliano, and D. R. McAllister. Trends in the surgical treatment of articular cartilage defects of the knee in the United States. *Knee Surgery, Sports Traumatology, Arthroscopy*. 22:2070-2075, 2014.
- ¹⁸⁴Moreira Teixeira L., J. Leijten, J. Sobral, R. Jin, v. A. Apeldoorn, J. Feijen, v. C. Blitterswijk, P. Dijkstra, and H. Karperien. High throughput generated micro-aggregates of chondrocytes stimulate cartilage formation in vitro and in vivo. *European cells & materials*. 23:387-399, 2012.
- ¹⁸⁶Moriguchi Y., K. Tateishi, W. Ando, K. Shimomura, Y. Yonetani, Y. Tanaka, K. Kita, D. A. Hart, A. Gobbi, and K. Shino. Repair of meniscal lesions using a scaffold-free tissue-engineered construct derived from allogenic synovial MSCs in a miniature swine model. *Biomaterials*. 34:2185-2193, 2013.
- ¹⁸⁷Moseley J. B., K. O'Malley, N. J. Petersen, T. J. Menke, B. A. Brody, D. H. Kuykendall, J. C. Hollingsworth, C. M. Ashton, and N. P. Wray. A controlled trial of arthroscopic surgery for osteoarthritis of the knee. *New England Journal of Medicine*. 347:81-88, 2002.
- ¹⁸⁸Munirah S., O. Samsudin, H. Chen, S. S. Salmah, B. Aminuddin, and B. Ruszymah. Articular cartilage restoration in load-bearing osteochondral defects by implantation of autologous chondrocyte-fibrin constructs AN EXPERIMENTAL STUDY IN SHEEP. *Journal of Bone & Joint Surgery, British Volume*. 89:1099-1109, 2007.

- ¹⁸⁹Murphy K. C., S. Y. Fang, and J. K. Leach. Human mesenchymal stem cell spheroids in fibrin hydrogels exhibit improved cell survival and potential for bone healing. *Cell and tissue research*. 357:91-99, 2014.
- ¹⁹⁰Musumeci G., P. Castrogiovanni, R. Leonardi, F. M. Trovato, M. A. Szychlinska, A. Di Giunta, C. Loreto, and S. Castorina. New perspectives for articular cartilage repair treatment through tissue engineering: A contemporary review. *World journal of orthopedics*. 5:80, 2014.
- ¹⁹¹Nerem R. M. Regenerative medicine: the emergence of an industry. *Journal of The Royal Society Interface*. 7:S771-S775, 2010.
- ¹⁹²NEW ORLEANS L., M. E. TRICE, W. D. BUGBEE, A. S. GREENWALD, and C. S. HEIM. ARTICULAR CARTILAGE RESTORATION: A REVIEW OF CURRENTLY AVAILABLE METHODS. 2010.
- ¹⁹³Ng K., J. DeFrancis, L. Kugler, T.-A. Kelly, M. Ho, C. O'Connor, G. Ateshian, and C. Hung. Amino acids supply in culture media is not a limiting factor in the matrix synthesis of engineered cartilage tissue. *Amino acids*. 35:433-438, 2008.
- ¹⁹⁴Ng V. Y., S. S. Jump, K. S. Santangelo, D. S. Russell, and A. L. Bertone. Genetic engineering of juvenile human chondrocytes improves scaffold-free mosaic neocartilage grafts. *Clinical Orthopaedics and Related Research*[®]. 471:26-38, 2013.
- ¹⁹⁵Niemeyer P., S. Andereya, P. Angele, A. Ateschrang, M. Aurich, M. Baumann, P. Behrens, U. Bosch, C. Erggelet, and S. Fickert. [Autologous chondrocyte implantation (ACI) for cartilage defects of the knee: a guideline by the working group "Tissue Regeneration" of the German Society of Orthopaedic Surgery and Traumatology (DGOU)]. *Zeitschrift fur Orthopadie und Unfallchirurgie*. 151:38-47, 2013.
- ¹⁹⁶Nooeaid P., V. Salih, J. P. Beier, and A. R. Boccaccini. Osteochondral tissue engineering: scaffolds, stem cells and applications. *Journal of cellular and molecular medicine*. 16:2247-2270, 2012.
- ¹⁹⁷O'Driscoll S. W., F. W. Keeley, and R. Salter. The chondrogenic potential of free autogenous periosteal grafts for biological resurfacing of major full-thickness defects in joint surfaces under the influence of continuous passive motion. An experimental investigation in the rabbit. *The Journal of Bone & Joint Surgery*. 68:1017-1035, 1986.

- ¹⁹⁸Orozco L., A. Munar, R. Soler, M. Alberca, F. Soler, M. Huguet, J. Sentís, A. Sánchez, and J. García-Sancho. Treatment of knee osteoarthritis with autologous mesenchymal stem cells: a pilot study. *Transplantation*. 95:1535-1541, 2013.
- ¹⁹⁹Orth P., A. Rey-Rico, J. K. Venkatesan, H. Madry, and M. Cucchiariini. Current perspectives in stem cell research for knee cartilage repair. *Stem cells and cloning: advances and applications*. 7:1, 2014.
- ²⁰⁰Ossendorf C., M. R. Steinwachs, P. C. Kreuz, G. Osterhoff, A. Lahm, P. P. Ducommun, and C. Erggelet. Autologous chondrocyte implantation (ACI) for the treatment of large and complex cartilage lesions of the knee. *BMC Sports Science, Medicine and Rehabilitation*. 3:11, 2011.
- ²⁰¹Panseri S., A. Russo, C. Cunha, A. Bondi, A. Di Martino, S. Patella, and E. Kon. Osteochondral tissue engineering approaches for articular cartilage and subchondral bone regeneration. *Knee Surgery, Sports Traumatology, Arthroscopy*. 20:1182-1191, 2012.
- ²⁰²Pelletier J.-P., L. Wildi, J.-P. Raynald, A. Beaulieu, L. Bessette, F. Morin, F. Abram, M. Dorais, and J. Martel-Pelletier. 323 TREATMENT WITH CHONDROITIN SULFATE REDUCES CARTILAGE VOLUME LOSS IN KNEE OA PATIENTS ASSESSED BY MRI: A RANDOMIZED, DOUBLE-BLIND, PLACEBO CONTROLLED PILOT STUDY. *Osteoarthritis and Cartilage*. 18:S143, 2010.
- ²⁰³Pelttari K., B. Pippenger, M. Mumme, S. Feliciano, C. Scotti, P. Mainil-Varlet, A. Procino, B. von Rechenberg, T. Schwamborn, and M. Jakob. Adult human neural crest-derived cells for articular cartilage repair. *Science translational medicine*. 6:251ra119-251ra119, 2014.
- ²⁰⁴Petri M., M. Broese, A. Simon, E. Liodakis, M. Ettinger, D. Guenther, J. Zeichen, C. Krettek, M. Jagodzinski, and C. Haasper. CaReS®(MACT) versus microfracture in treating symptomatic patellofemoral cartilage defects: a retrospective matched-pair analysis. *Journal of Orthopaedic Science*. 18:38-44, 2013.
- ²⁰⁵Pirnay J.-P., A. Vanderkelen, D. De Vos, J.-P. Draye, T. Rose, C. Ceulemans, N. Ectors, I. Huys, S. Jennes, and G. Verbeken. Business oriented EU human cell and tissue product legislation will adversely impact Member States' health care systems. *Cell and tissue banking*. 14:525-560, 2013.
- ²⁰⁶Pleumeekers M., L. Nimeskern, W. Koevoet, N. Kops, R. Poublon, K. Stok, and G. van Osch. The in vitro and in vivo capacity of culture-expanded human cells

- from several sources encapsulated in alginate to form cartilage. *European cells & materials*. 27:264-280, 2014.
- ²⁰⁷Qi Y., Y. Du, W. Li, X. Dai, T. Zhao, and W. Yan. Cartilage repair using mesenchymal stem cell (MSC) sheet and MSCs-loaded bilayer PLGA scaffold in a rabbit model. *Knee Surgery, Sports Traumatology, Arthroscopy*. 22:1424-1433, 2014.
- ²⁰⁸Raghothaman D., M. F. Leong, T. C. Lim, J. K. Toh, A. C. Wan, Z. Yang, and E. H. Lee. Engineering cell matrix interactions in assembled polyelectrolyte fiber hydrogels for mesenchymal stem cell chondrogenesis. *Biomaterials*. 35:2607-2616, 2014.
- ²⁰⁹Renth A. N. and M. S. Detamore. Leveraging "raw materials" as building blocks and bioactive signals in regenerative medicine. *Tissue Eng Part B Rev*. 18:341-62, 2012.
- ²¹⁰Restrepo A., S. Méthot, W. D. Stanish, and M. S. Shive. "BST-CarGel®: An Enhanced Bone Marrow Stimulation Treatment," in *Techniques in Cartilage Repair Surgery*. 2014, Springer. 97-110.
- ²¹¹Rettinger C. L., A. B. Fourcaudot, S. J. Hong, T. A. Mustoe, R. G. Hale, and K. P. Leung. In vitro characterization of scaffold-free three-dimensional mesenchymal stem cell aggregates. *Cell and tissue research*. 358:395-405, 2014.
- ²¹²Rodríguez-Merchán E. C. The treatment of cartilage defects in the knee joint: microfracture, mosaicplasty, and autologous chondrocyte implantation. *Am J Orthop (Belle Mead NJ)*. 41:236-9, 2012.
- ²¹³Roos E. M., L. Engelhart, J. Ranstam, A. F. Anderson, J. J. Irrgang, R. G. Marx, Y. Tegner, and A. M. Davis. ICRS Recommendation Document Patient-Reported Outcome Instruments for Use in Patients with Articular Cartilage Defects. *Cartilage*. 2:122-136, 2011.
- ²¹⁴Ruan D., Y. Zhang, D. Wang, C. Zhang, J. Wu, C. Wang, Z. Shi, H. Xin, C. Xu, and H. Li. Differentiation of human Wharton's jelly cells toward nucleus pulposus-like cells after coculture with nucleus pulposus cells in vitro. *Tissue Engineering Part A*. 18:167-175, 2011.
- ²¹⁵Salzmann G. M., P. Niemeyer, M. Steinwachs, P. Kreuz, N. Südkamp, and H. Mayr. Cartilage repair approach and treatment characteristics across the knee joint: a European survey. *Archives of orthopaedic and trauma surgery*. 131:283-291, 2011.

- ²¹⁶Saris D. B., J. Vanlauwe, J. Victor, K. F. Almqvist, R. Verdonk, J. Bellemans, and F. P. Luyten. Treatment of symptomatic cartilage defects of the knee characterized chondrocyte implantation results in better clinical outcome at 36 months in a randomized trial compared to microfracture. *The American journal of sports medicine*. 37:10S-19S, 2009.
- ²¹⁷Sart S., A.-C. Tsai, Y. Li, and T. Ma. Three-dimensional aggregates of mesenchymal stem cells: cellular mechanisms, biological properties, and applications. *Tissue Engineering Part B: Reviews*. 2013.
- ²¹⁸Sato M., M. Yamato, K. Hamahashi, T. Okano, and J. Mochida. Articular Cartilage Regeneration Using Cell Sheet Technology. *Anatomical Record-Advances in Integrative Anatomy and Evolutionary Biology*. 297:36-43, 2014.
- ²¹⁹Sato M., M. Yamato, K. Hamahashi, T. Okano, and J. Mochida. Articular cartilage regeneration using cell sheet technology. *The Anatomical Record*. 297:36-43, 2014.
- ²²⁰Shimizu R., N. Kamei, N. Adachi, M. Hamanishi, G. Kamei, E. E. Mahmoud, T. Nakano, T. Iwata, M. Yamato, and T. Okano. Repair Mechanism of Osteochondral Defect Promoted by Bioengineered Chondrocyte Sheet. *Tissue Engineering Part A*. 21:1131-1141, 2014.
- ²²¹Shimizu T., M. Yamato, A. Kikuchi, and T. Okano. Cell sheet engineering for myocardial tissue reconstruction. *Biomaterials*. 24:2309-2316, 2003.
- ²²²Shimomura K., Y. Moriguchi, W. Ando, R. Nansai, H. Fujie, D. A. Hart, A. Gobbi, K. Kita, S. Horibe, and K. Shino. Osteochondral Repair Using a Scaffold-Free Tissue-Engineered Construct Derived from Synovial Mesenchymal Stem Cells and a Hydroxyapatite-Based Artificial Bone. *Tissue Engineering Part A*. 2014.
- ²²³Shimomura K., Y. Moriguchi, C. D. Murawski, H. Yoshikawa, and N. Nakamura. Osteochondral tissue engineering with biphasic scaffold: current strategies and techniques. *Tissue Engineering Part B: Reviews*. 20:468-476, 2014.
- ²²⁴Shin Y. S., B. H. Lee, J. W. Choi, B.-H. Min, J. W. Chang, S. S. Yang, and C.-H. Kim. Tissue-engineered tracheal reconstruction using chondrocyte seeded on a porcine cartilage-derived substance scaffold. *International journal of pediatric otorhinolaryngology*. 78:32-38, 2014.
- ²²⁵Shive M. S., W. D. Stanish, R. McCormack, F. Forriol, N. Mohtadi, S. Pelet, J. Desnoyers, S. Méthot, K. Vehik, and A. Restrepo. BST-CarGel® Treatment

- Maintains Cartilage Repair Superiority over Microfracture at 5 Years in a Multicenter Randomized Controlled Trial. *Cartilage*. 6:62-72, 2015.
- ²²⁶Siddappa R., R. Licht, C. van Blitterswijk, and J. de Boer. Donor variation and loss of multipotency during in vitro expansion of human mesenchymal stem cells for bone tissue engineering. *Journal of orthopaedic research*. 25:1029-1041, 2007.
- ²²⁷Singh M., N. Dormer, J. R. Salash, J. M. Christian, D. S. Moore, C. Berklund, and M. S. Detamore. Three-dimensional macroscopic scaffolds with a gradient in stiffness for functional regeneration of interfacial tissues. *J Biomed Mater Res A*. 94:870-6, 2010.
- ²²⁸Singh M., C. P. Morris, R. J. Ellis, M. S. Detamore, and C. Berklund. Microsphere-based seamless scaffolds containing macroscopic gradients of encapsulated factors for tissue engineering. *Tissue Eng Part C Methods*. 14:299-309, 2008.
- ²²⁹Singh M., C. P. Morris, R. J. Ellis, M. S. Detamore, and C. Berklund. Microsphere-based seamless scaffolds containing macroscopic gradients of encapsulated factors for tissue engineering. *Tissue Engineering Part C: Methods*. 14:299-309, 2008.
- ²³⁰Skaalure S. C., S. O. Dimson, A. M. Pennington, and S. J. Bryant. Semi-interpenetrating networks of hyaluronic acid in degradable PEG hydrogels for cartilage tissue engineering. *Acta biomaterialia*. 10:3409-3420, 2014.
- ²³²Smith F. D. Bone Products in Surgery: A Blueprint for Standardization. *AORN journal*. 95:239-254, 2012.
- ²³³Solheim E., J. Hegna, J. Øyen, T. Harlem, and T. Strand. Results at 10 to 14 years after osteochondral autografting (mosaicplasty) in articular cartilage defects in the knee. *The Knee*. 20:287-290, 2013.
- ²³⁴Spiller K. L., Y. Liu, J. L. Holloway, S. A. Maher, Y. Cao, W. Liu, G. Zhou, and A. M. Lowman. A novel method for the direct fabrication of growth factor-loaded microspheres within porous nondegradable hydrogels: Controlled release for cartilage tissue engineering. *Journal of Controlled Release*. 157:39-45, 2012.
- ²³⁵Sridharan B., B. Sharma, and M. S. Detamore. A Roadmap to Commercialization of Cartilage Therapy in the United States of America. *Tissue Engineering Part B*. 2015.

- ²³⁶ Stanish W. D., R. McCormack, F. Forriol, N. Mohtadi, S. Pelet, J. Desnoyers, A. Restrepo, and M. S. Shive. Novel scaffold-based BST-CarGel treatment results in superior cartilage repair compared with microfracture in a randomized controlled trial. *The Journal of Bone & Joint Surgery*. 95:1640-1650, 2013.
- ²³⁷ Steinert A. F., L. Rackwitz, F. Gilbert, U. Noeth, and R. S. Tuan. Concise Review: The Clinical Application of Mesenchymal Stem Cells for Musculoskeletal Regeneration: Current Status and Perspectives. *Stem Cells Translational Medicine*. 1:237-247, 2012.
- ²³⁸ Sutherland A. J., E. C. Beck, S. C. Dennis, G. L. Converse, R. A. Hopkins, C. J. Berkland, and M. S. Detamore. Decellularized cartilage may be a chondroinductive material for osteochondral tissue engineering. *PLoS One*. 10:e0121966, 2015.
- ²³⁹ Sutherland A. J., G. L. Converse, R. A. Hopkins, and M. S. Detamore. The bioactivity of cartilage extracellular matrix in articular cartilage regeneration. *Adv Healthc Mater*. 4:29-39, 2015.
- ²⁴⁰ Sutherland A. J. and M. S. Detamore. Bioactive microsphere-based scaffolds containing decellularized cartilage. *Macromol Biosci*. Epub, 2015.
- ²⁴¹ Suzuki S., T. Muneta, K. Tsuji, S. Ichinose, H. Makino, A. Umezawa, and I. Sekiya. Properties and usefulness of aggregates of synovial mesenchymal stem cells as a source for cartilage regeneration. *Arthritis Res Ther*. 14:R136, 2012.
- ²⁴² Tan H., C. R. Chu, K. A. Payne, and K. G. Marra. Injectable in situ forming biodegradable chitosan–hyaluronic acid based hydrogels for cartilage tissue engineering. *Biomaterials*. 30:2499-2506, 2009.
- ²⁴³ Toh W. S., C. B. Foldager, M. Pei, and J. H. P. Hui. Advances in Mesenchymal Stem Cell-based Strategies for Cartilage Repair and Regeneration. *Stem Cell Reviews and Reports*. 1-11, 2014.
- ²⁴⁵ Toh W. S., M. Spector, E. H. Lee, and T. Cao. Biomaterial-mediated delivery of microenvironmental cues for repair and regeneration of articular cartilage. *Molecular pharmaceuticals*. 8:994-1001, 2011.
- ²⁴⁶ Tompkins M., H. D. Adkisson, and K. F. Bonner. DeNovo NT allograft. *Operative Techniques in Sports Medicine*. 21:82-89, 2013.

- ²⁴⁷Ulstein S., A. Årøen, J. H. Røtterud, S. Løken, L. Engebretsen, and S. Heir. Microfracture technique versus osteochondral autologous transplantation mosaicplasty in patients with articular chondral lesions of the knee: a prospective randomized trial with long-term follow-up. *Knee Surgery, Sports Traumatology, Arthroscopy*. 22:1207-1215, 2014.
- ²⁴⁹Van Den Borne M., N. Raijmakers, J. Vanlauwe, J. Victor, S. de Jong, J. Bellemans, and D. Saris. International Cartilage Repair Society (ICRS) and Oswestry macroscopic cartilage evaluation scores validated for use in Autologous Chondrocyte Implantation (ACI) and microfracture. *Osteoarthritis and Cartilage*. 15:1397-1402, 2007.
- ²⁵⁰Van Vlierberghe S., P. Dubrue, and E. Schacht. Biopolymer-based hydrogels as scaffolds for tissue engineering applications: a review. *Biomacromolecules*. 12:1387-1408, 2011.
- ²⁵¹Vanlauwe J., D. B. Saris, J. Victor, K. F. Almqvist, J. Bellemans, F. P. Luyten, M. Bohnsack, T. Claes, Y. Fortems, and F. Handelberg. Five-year outcome of characterized chondrocyte implantation versus microfracture for symptomatic cartilage defects of the knee early treatment matters. *The American journal of sports medicine*. 39:2566-2574, 2011.
- ²⁵²Vasiliadis H. S. and J. Wasiak. Autologous chondrocyte implantation for full thickness articular cartilage defects of the knee. *Cochrane Database Syst Rev*. 10, 2010.
- ²⁵³Vinardell T., E. J. Sheehy, C. T. Buckley, and D. J. Kelly. A comparison of the functionality and in vivo phenotypic stability of cartilaginous tissues engineered from different stem cell sources. *Tissue Engineering Part A*. 18:1161-1170, 2012.
- ²⁵⁴Wang L. and M. S. Detamore. Effects of growth factors and glucosamine on porcine mandibular condylar cartilage cells and hyaline cartilage cells for tissue engineering applications. *archives of oral biology*. 54:1-5, 2009.
- ²⁵⁵Wang L. and M. S. Detamore. Insulin- like growth factor- I improves chondrogenesis of predifferentiated human umbilical cord mesenchymal stromal cells. *Journal of Orthopaedic Research*. 27:1109-1115, 2009.
- ²⁵⁶Wang L., L. Ott, K. Seshareddy, M. L. Weiss, and M. S. Detamore. Musculoskeletal tissue engineering with human umbilical cord mesenchymal stromal cells. *Regen Med*. 6:95-109, 2011.

- ²⁵⁷Wang L., I. Tran, K. Seshareddy, M. L. Weiss, and M. S. Detamore. A comparison of human bone marrow-derived mesenchymal stem cells and human umbilical cord-derived mesenchymal stromal cells for cartilage tissue engineering. *Tissue Eng Part A*. 15:2259-66, 2009.
- ²⁵⁹Wang L., M. L. Weiss, and M. S. Detamore. Recent patents pertaining to immune modulation and musculoskeletal regeneration with Wharton's jelly cells. *Recent Patents on Regenerative Medicine*. 3:182-192, 2013.
- ²⁶⁰Watterson J. R. and J. M. Esdaile. Viscosupplementation: therapeutic mechanisms and clinical potential in osteoarthritis of the knee. *Journal of the American Academy of Orthopaedic Surgeons*. 8:277-284, 2000.
- ²⁶¹Wei C.-C., A. B. Lin, and S.-C. Hung. Mesenchymal Stem Cells in Regenerative Medicine for Musculoskeletal Diseases: Bench, Bedside, and Industry. *Cell transplantation*. 23:505-512, 2014.
- ²⁶²Wildi L. M., J.-P. Raynauld, J. Martel-Pelletier, A. Beaulieu, L. Bessette, F. Morin, F. Abram, M. Dorais, and J.-P. Pelletier. Chondroitin sulphate reduces both cartilage volume loss and bone marrow lesions in knee osteoarthritis patients starting as early as 6 months after initiation of therapy: a randomised, double-blind, placebo-controlled pilot study using MRI. *Annals of the rheumatic diseases*. 70:982-989, 2011.
- ²⁶³Williams D. Business models for biomaterials in regenerative medicine. *Medical device technology*. 16:7-8, 2005.
- ²⁶⁴Wilson R., D. Belluoccio, C. B. Little, A. J. Fosang, and J. F. Bateman. Proteomic characterization of mouse cartilage degradation in vitro. *Arthritis & Rheumatism*. 58:3120-3131, 2008.
- ²⁶⁵Winter A., S. Breit, D. Parsch, K. Benz, E. Steck, H. Hauner, R. M. Weber, V. Ewerbeck, and W. Richter. Cartilage- like gene expression in differentiated human stem cell spheroids: A comparison of bone marrow-derived and adipose tissue-derived stromal cells. *Arthritis & Rheumatism*. 48:418-429, 2003.
- ²⁶⁶Wohn D. Y. Korea okays stem cell therapies despite limited peer-reviewed data. *Nature medicine*. 18:329-329, 2012.
- ²⁶⁷Xu F., B. Sridharan, S. Wang, U. A. Gurkan, B. Syverud, and U. Demirci. Embryonic stem cell bioprinting for uniform and controlled size embryoid body formation. *Biomicrofluidics*. 5:022207, 2011.

- ²⁶⁸Ye K., C. Di Bella, D. E. Myers, and P. F. Choong. The osteochondral dilemma: review of current management and future trends. *ANZ journal of surgery*. 84:211-217, 2014.
- ²⁶⁹Ylöstalo J. H., T. J. Bartosh, K. Coble, and D. J. Prockop. Human Mesenchymal Stem/Stromal Cells Cultured as Spheroids are Self- activated to Produce Prostaglandin E2 that Directs Stimulated Macrophages into an Anti-inflammatory Phenotype. *Stem Cells*. 30:2283-2296, 2012.
- ²⁷⁰Yoon H. H., S. H. Bhang, J.-Y. Shin, J. Shin, and B.-S. Kim. Enhanced cartilage formation via three-dimensional cell engineering of human adipose-derived stem cells. *Tissue Engineering Part A*. 18:1949-1956, 2012.
- ²⁷¹Yoshioka T., H. Mishima, S. Sakai, and T. Uemura. Long-Term Results of Cartilage Repair after Allogeneic Transplantation of Cartilaginous Aggregates Formed from Bone Marrow-Derived Cells for Large Osteochondral Defects in Rabbit Knees. *Cartilage*. 4:339-344, 2013.
- ²⁷²Yu Y., J. E. Fisher, J. B. Lillegard, B. Rodysill, B. Amiot, and S. L. Nyberg. Cell therapies for liver diseases. *Liver transplantation*. 18:9-21, 2012.
- ²⁷³Zaslav K., B. Cole, R. Brewster, T. DeBerardino, J. Farr, P. Fowler, and C. Nissen. A Prospective Study of Autologous Chondrocyte Implantation in Patients With Failed Prior Treatment for Articular Cartilage Defect of the Knee Results of the Study of the Treatment of Articular Repair (STAR) Clinical Trial. *QNRS Repository*. 2011, 2011.
- ²⁷⁴Zhu S. and T. Segura. Hydrogel-based nanocomposites of therapeutic proteins for tissue repair. *Current opinion in chemical engineering*. 4:128-136, 2014.

APPENDIX A: Figures

CHAPTER 1: No figures.
CHAPTER 2: Figure 2.1
CHAPTER 3: Figures 3.1- 3.4
CHAPTER 4: Figures 4.1 - 4.10
CHAPTER 5: Figures 5.1 - 5.7
CHAPTER 6: Figures 6.1 - 6.10
CHAPTER 7: No figures

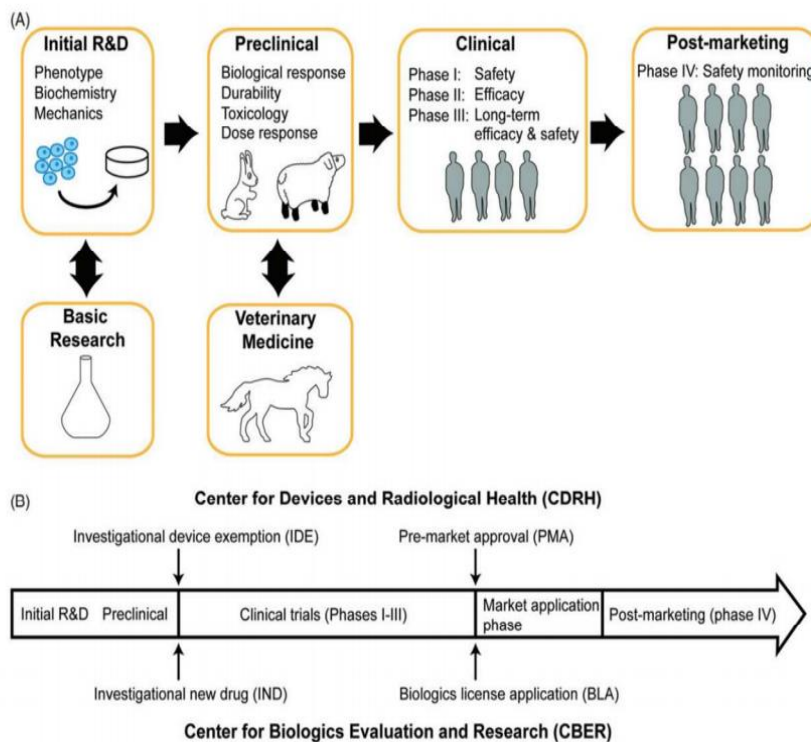


Figure 2.1: Translation of devices and stem cell products for cartilage regeneration

Translation of devices and stem cell products for cartilage regeneration (from Lee et al.¹⁴⁴) (A) FDA regulation of biologics requires stem cell products to exhibit purity, reproducibility, and stability. Neocartilage is evaluated in preclinical trials for biological response, durability, toxicology, and dose response. Multi-phase clinical studies are used to evaluate dosage, efficacy, and safety. (B) Two major regulatory centers exist: CDRH for devices and CBER for drugs and biologics. Prior to initiating clinical trials, a product must receive an IDE or IND. After clinical trials, market approval enables clinical application of the product.

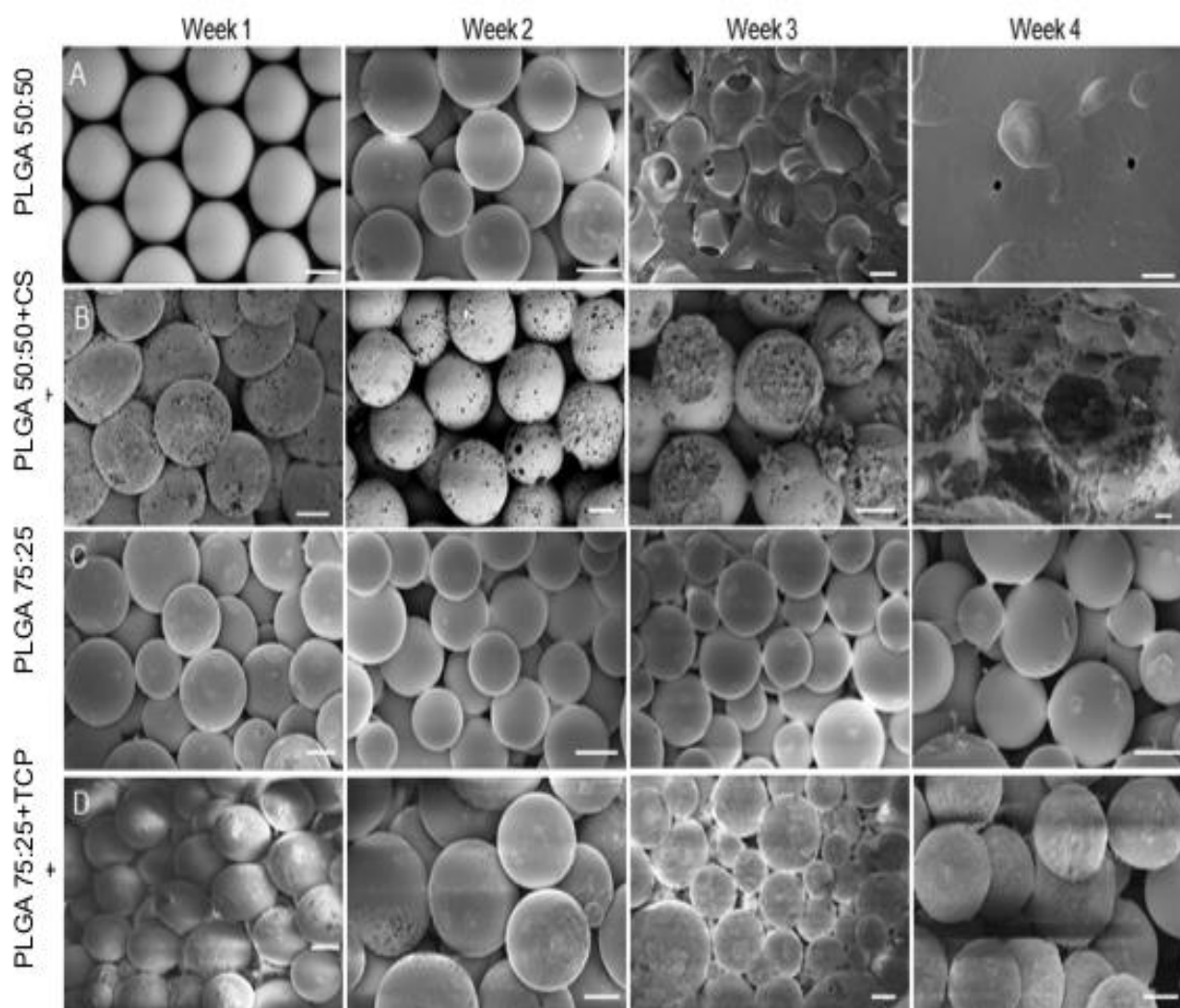


Figure 3.1: SEM micrographs of the different groups

SEM micrographs of scaffold taken at weeks 1, 2, 3 and 4. In general, PLGA 50:50 (CS control) degraded faster than PLGA 75:25 and the CS group microspheres displayed interconnected pores and large cracks right from week 1. TCP group microspheres have a “glazed” surface due to the crystalline TCP. Scale bars = 200 μm .

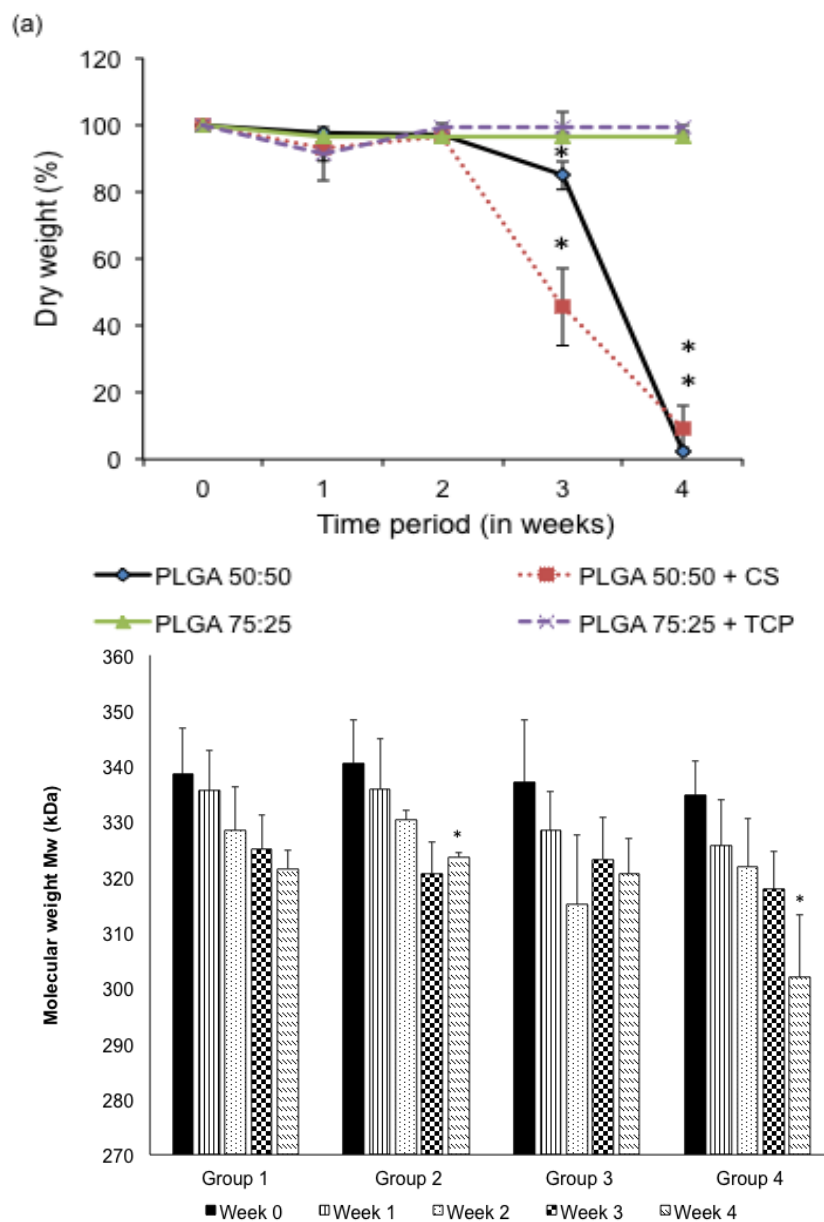


Figure 3.2: Dry weight and molecular weight of the scaffolds

Dry weight and molecular weight analysis of the scaffolds. (a) Relative dry mass ($n=5$), of all the groups over a 4 week period, (b) weight-average molecular weight change M_w ($n=4$), of polymeric scaffolds in the aqueous medium over time. Raw materials (CS & TCP) encapsulation led to faster decrease in M_w than the control groups. All groups exhibited more than 10% decrease in M_w by the end of week 4. (*) denotes statistically significant difference ($p < 0.05$) in value from week 0.

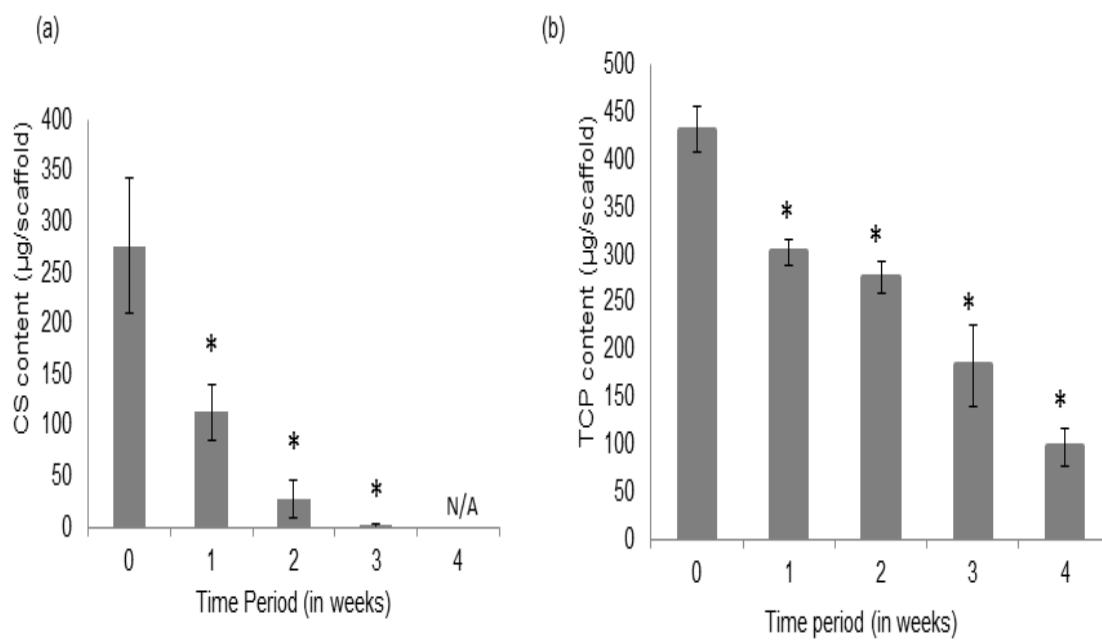


Figure 3.3: CS and TCP retention in scaffolds

Retention of (a) CS and (b) TCP, in the CS group and TCP group scaffolds, respectively ($n = 5$). The CS microsphere-based scaffolds degraded at a much faster than the TCP group microspheres. Error bars represent mean \pm SD. (*) denotes statistically significant difference ($p < 0.05$) from week 0.

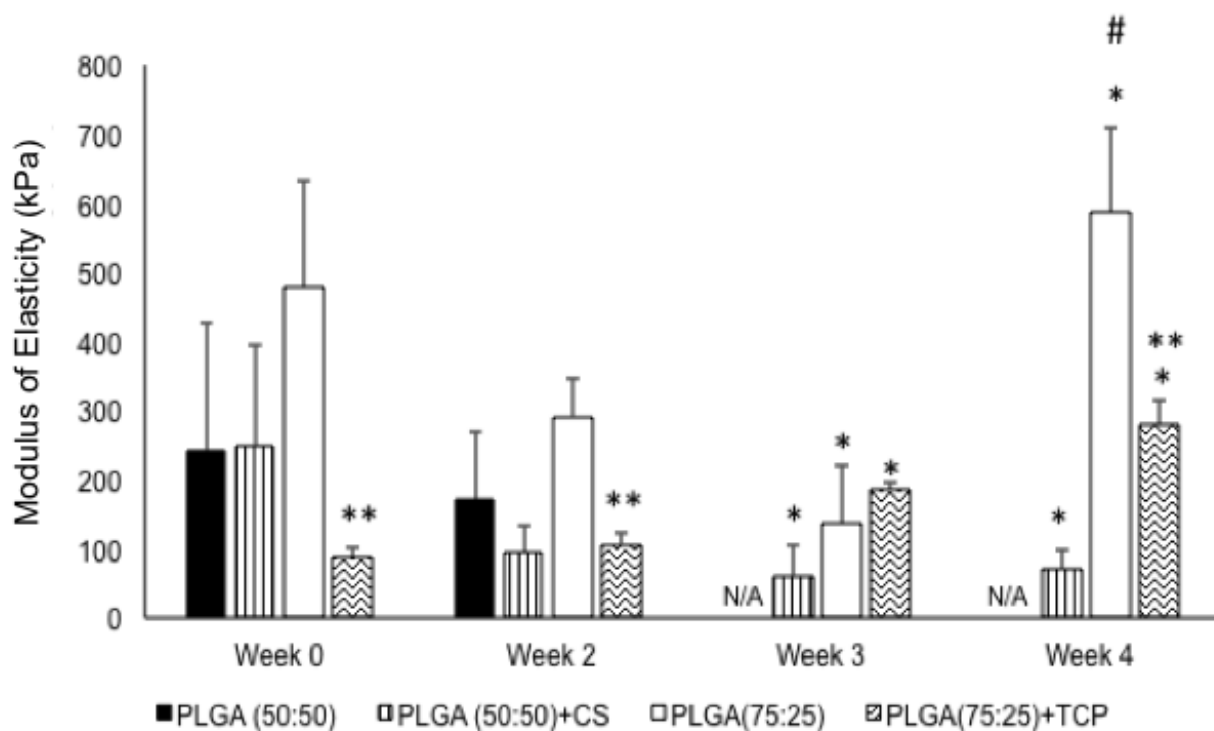


Figure 3.4: Compressive elastic moduli at different time points

Compressive elastic modulus at different time points. CS group scaffolds lost shape by week 3 and hence there was no solid material for measurement at week 3 and week 4. (*) indicates statistically significant difference ($p < 0.05$) from week 0. (**) indicates statistically significant difference ($p < 0.05$) from the corresponding control group. (#) indicates statistically significant highest value of the parameter ($p < 0.05$) along the particular group.

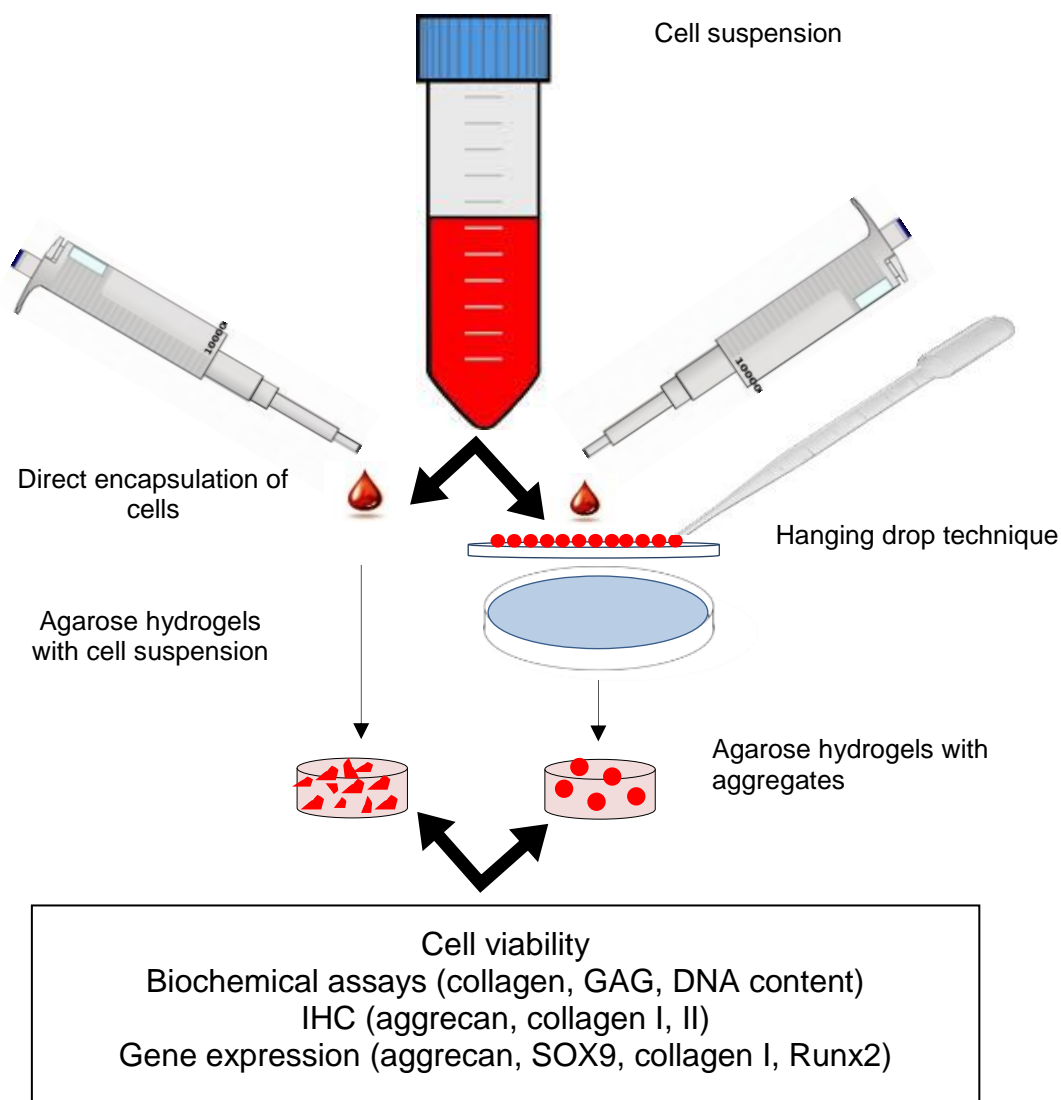


Figure 4.1: Schematic representation of the hanging drop approach

Schematic representation of the hanging down approach and aggregate-encapsulation in agarose hydrogels. The aggregates/CS is encapsulated in pre-polymer solution and undergoes thermal crosslinking to form the hydrogel.

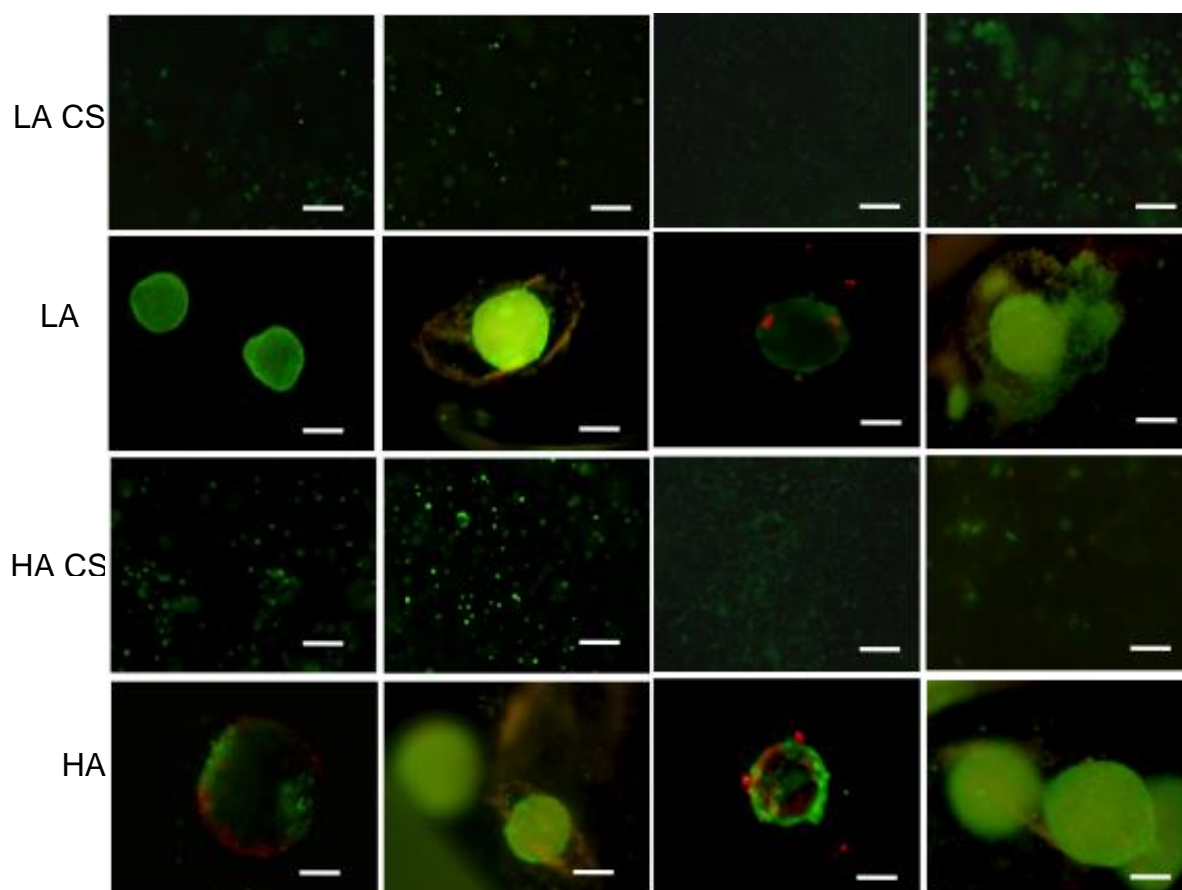


Figure 4.2: Cell viability of the rBMSC aggregates

Cell viability at weeks 0 and 3. (A) Live-dead images of the 10M/mL rBMSC aggregates and controls. (B) Live-dead images of the 20M/mL rBMSC aggregates and controls. Scale bar =100 μ m.

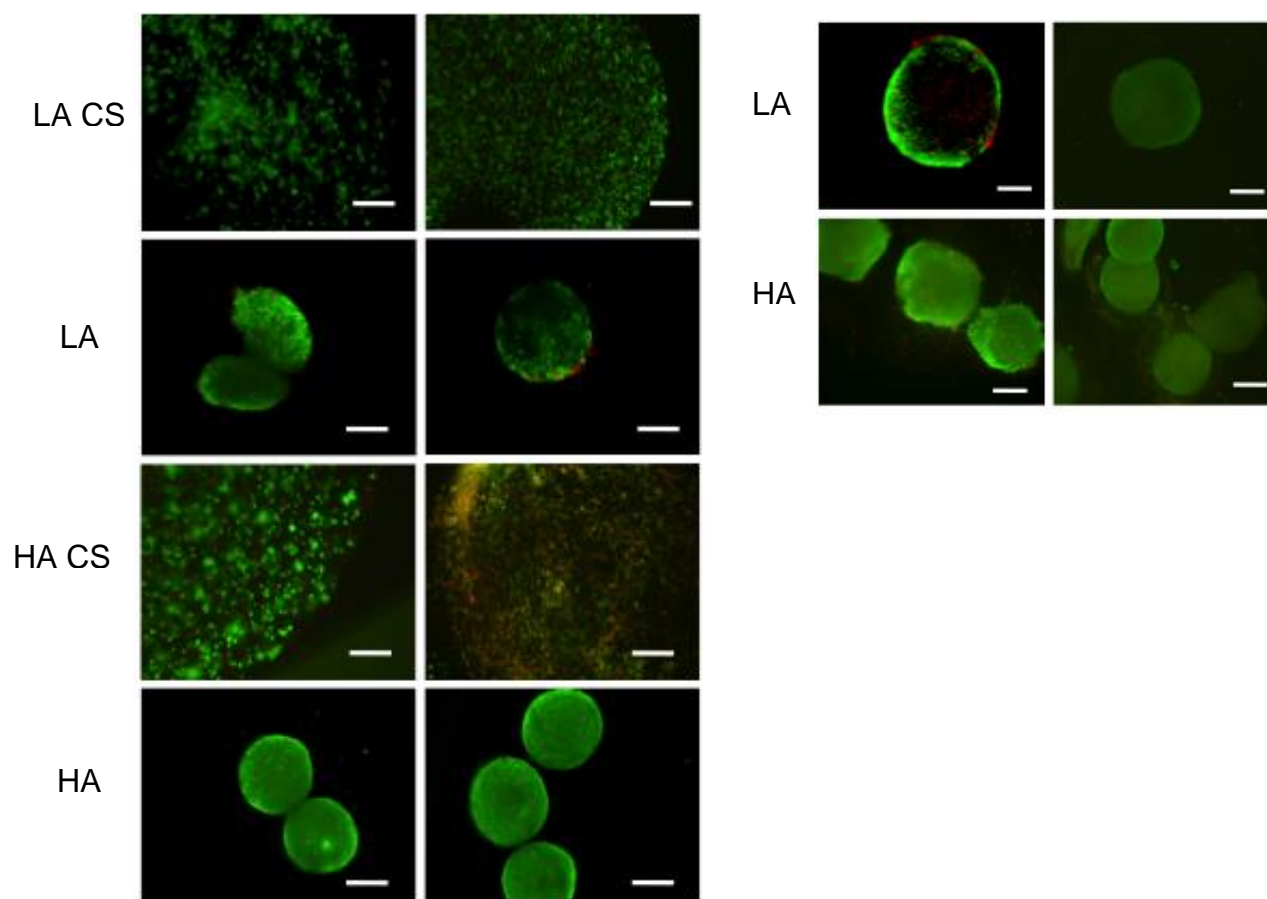


Figure 4.3: Cell viability of the hWJC aggregates

Cell viability at weeks 0 and 3. (A) Live-dead images of the 10M/mL hWJC aggregates and controls. (B) Live dead images of the 20M/mL hWJC aggregates. Scale bar =100 μ m.

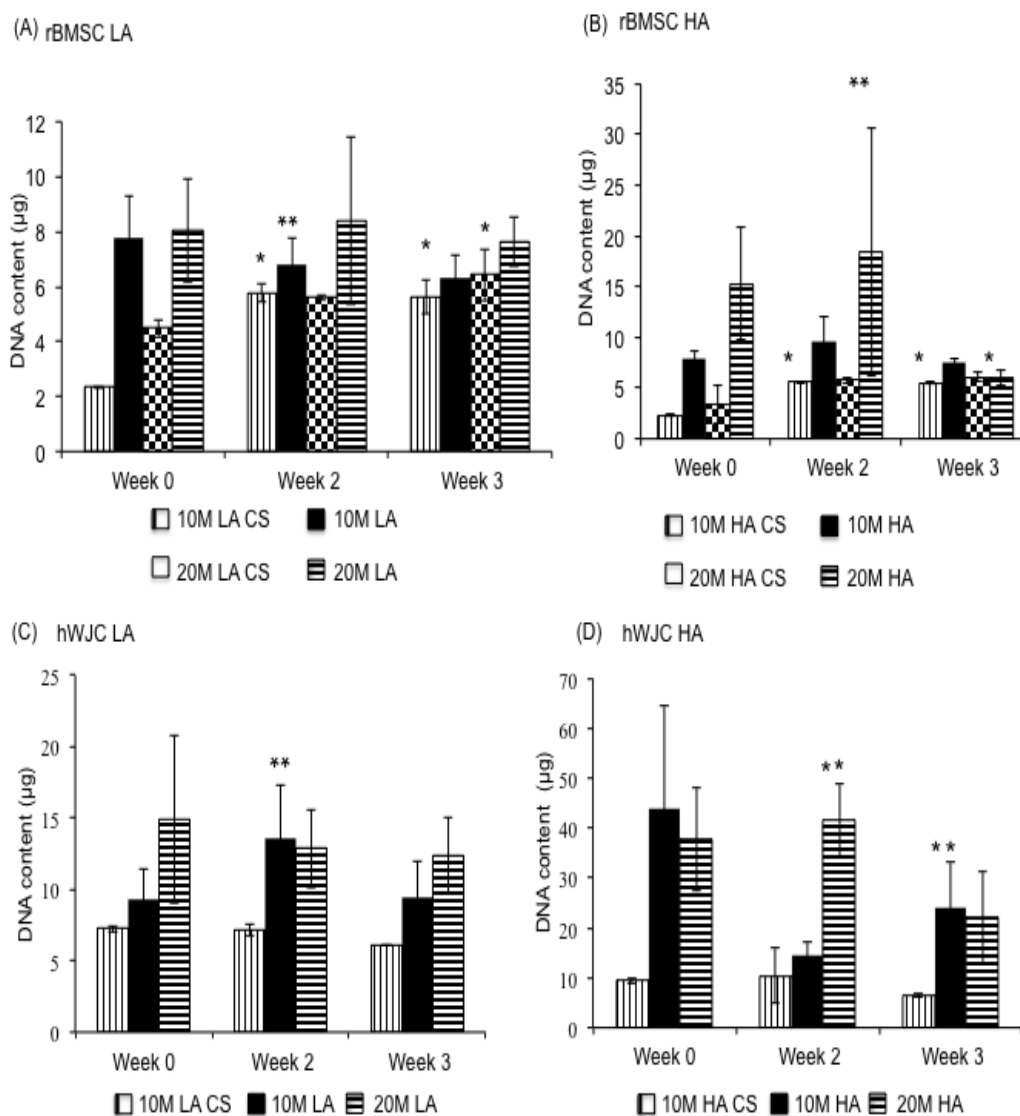


Figure 4.4: DNA content for all of the groups

DNA content for all the rBMSC and hWJC groups at 0, 2, and 3 weeks expressed as DNA (µg/ scaffold). (A) DNA content of all the rBMSC LA and LA CS groups. (B) DNA content of all the rBMSC HA and HA CS groups. (C) DNA content of all the hWJC LA and LA CS groups. (D) DNA content of all the hWJC HA and HA CS groups. All aggregate groups had statistically significant increase in DNA over week 0, HA groups had significantly higher values compared to the CS control groups at week 3. Values are reported as mean \pm standard deviation, $n=4$. (*) represents statistically significant difference from the week 0 value. (#) represents statistically significant difference from the previous time point and (**) represents statistically significant difference from the control at that time point ($p < 0.05$).

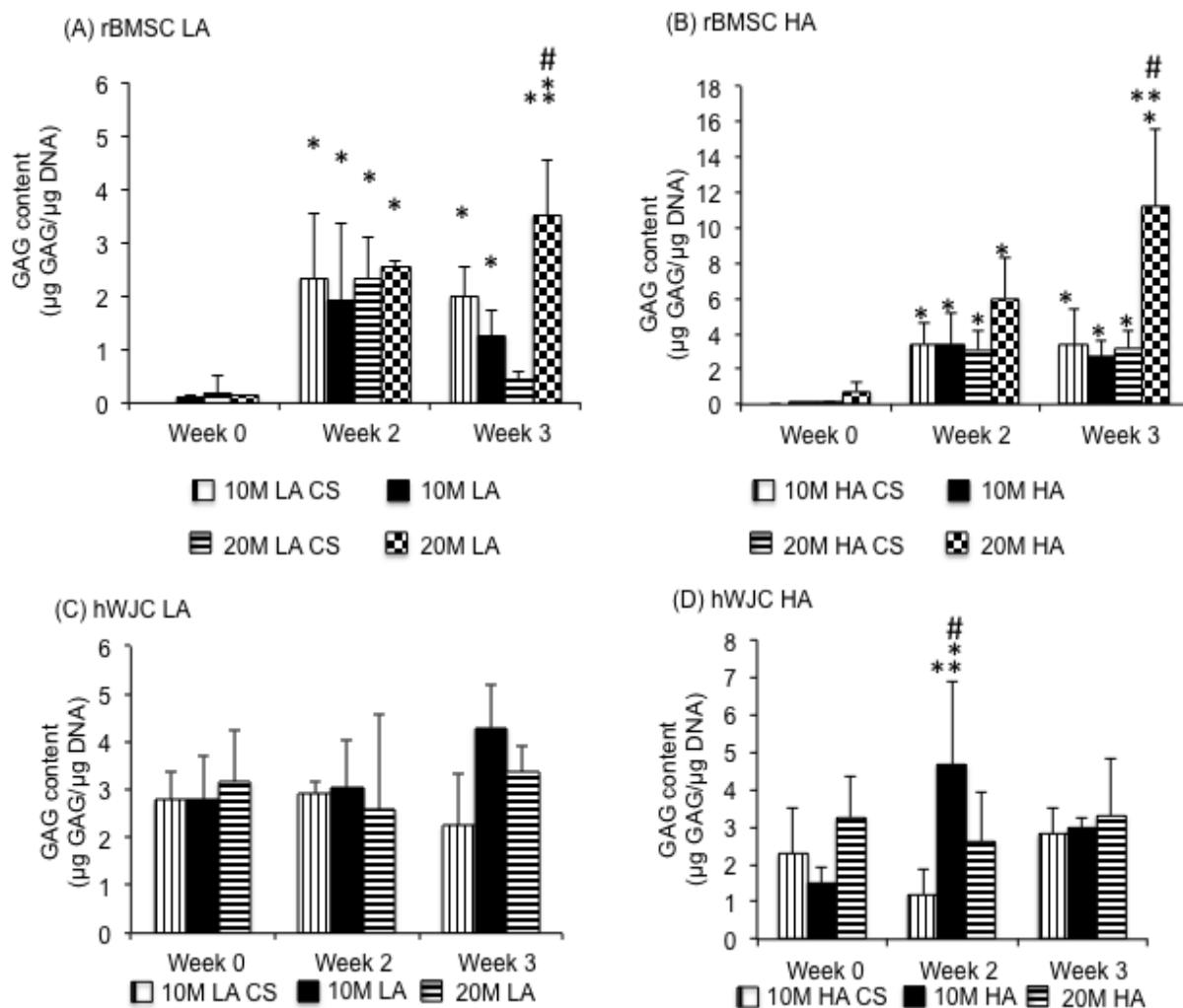


Figure 4.5: GAG content for all of the groups

GAG content for all the rBMSC groups at 0, 2, and 3 weeks expressed as GAG/DNA (A&B). All aggregate groups had statistically significant increase in GAG/DNA over week 0, and select aggregates groups had significantly higher values compared to the control groups at week 3. GAG content for all the hWJC groups at week expressed as GAG/ DNA (C&D) at week 0, 2, and 3. 10 M HA at week 2 exhibited the highest GAG/DNA value and decreased at week 3. Values are reported as mean \pm standard deviation, n=4. (*) represents statistically significant difference from the week 0 value. (#) represents statistically significant difference from the previous time point and (**) represents statistically significant difference from the control at that time point. ($p < 0.05$).

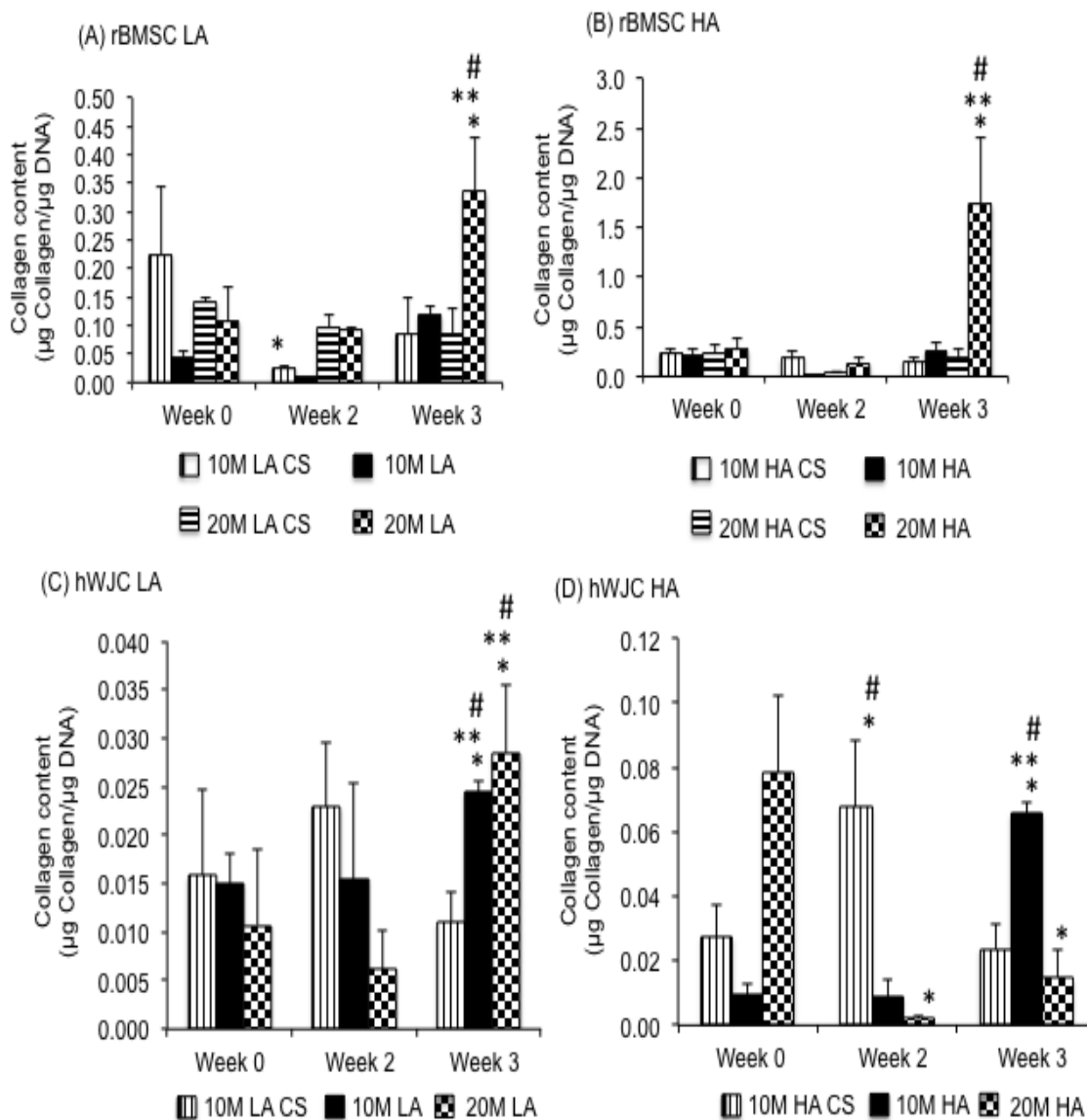
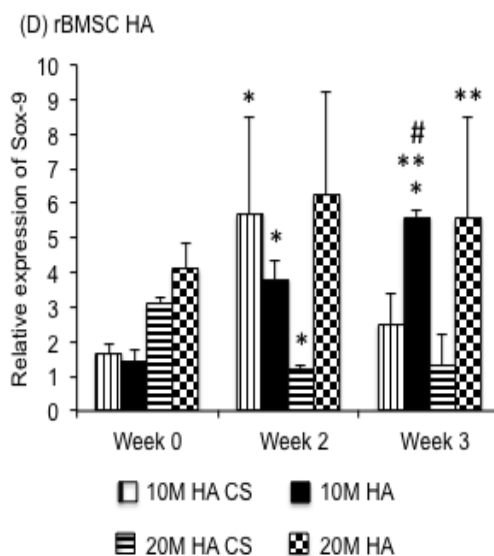
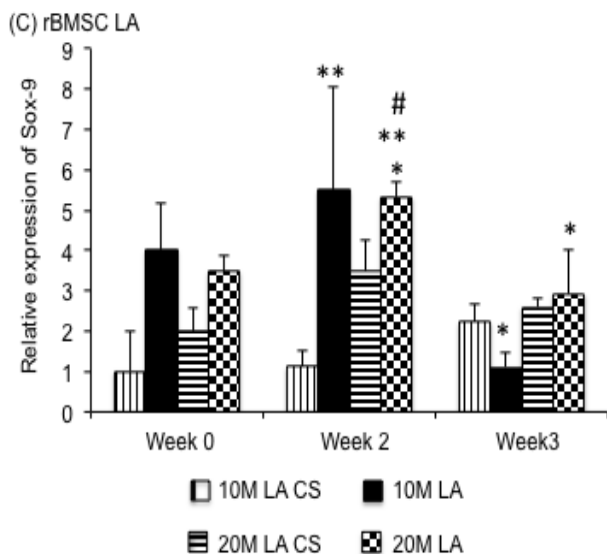
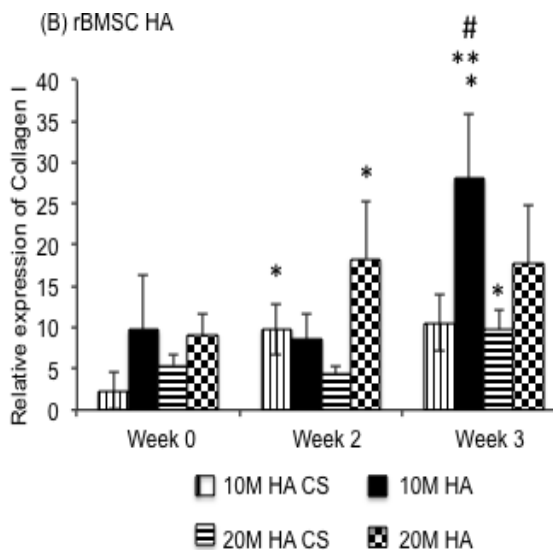
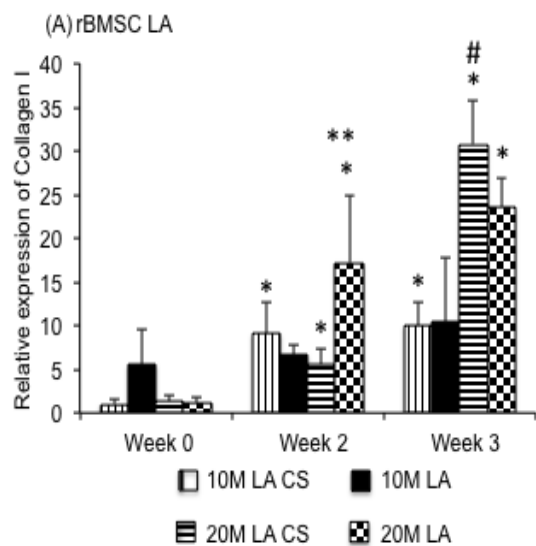


Figure 4.6: Collagen content for all of the groups

Collagen content for all the rBMSC groups expressed as collagen/DNA (A&B) at week 0, 2, and 3. All aggregate groups had statistically significant increase in collagen over week 0. At week 3, 20 M HA also displayed the highest collagen/DNA. Collagen content for all the hWJC groups expressed as collagen/DNA (C&D) at week 0, 2, and 3. We noticed that the 20 M HA at week 0 had the highest collagen/DNA value. Values are reported as mean \pm standard deviation, $n=4$. (*) represents statistically significant difference over the week 0 value. (#) represents statistically significant highest value of the particular group and (**) represents statistically significant difference from the control at that time point. ($p < 0.05$).



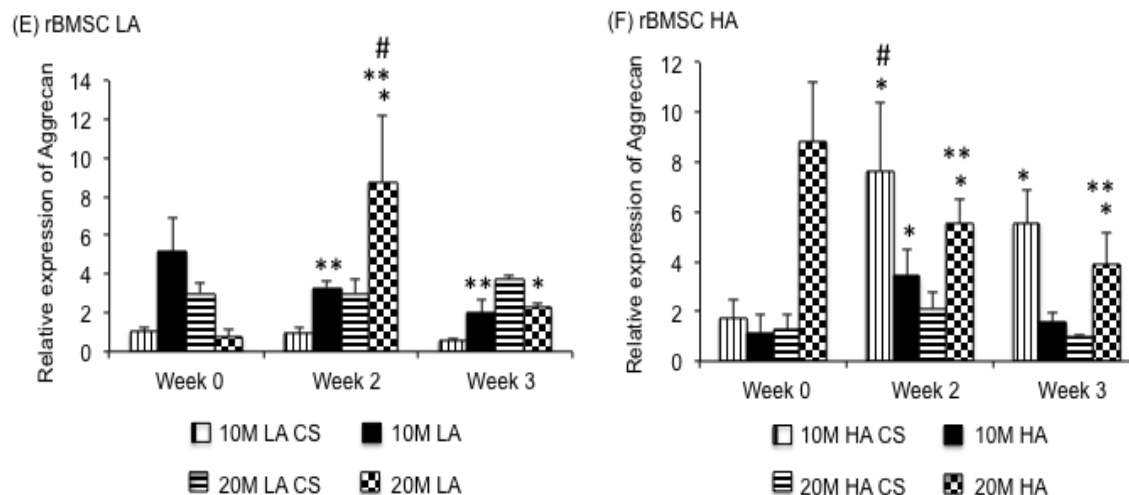
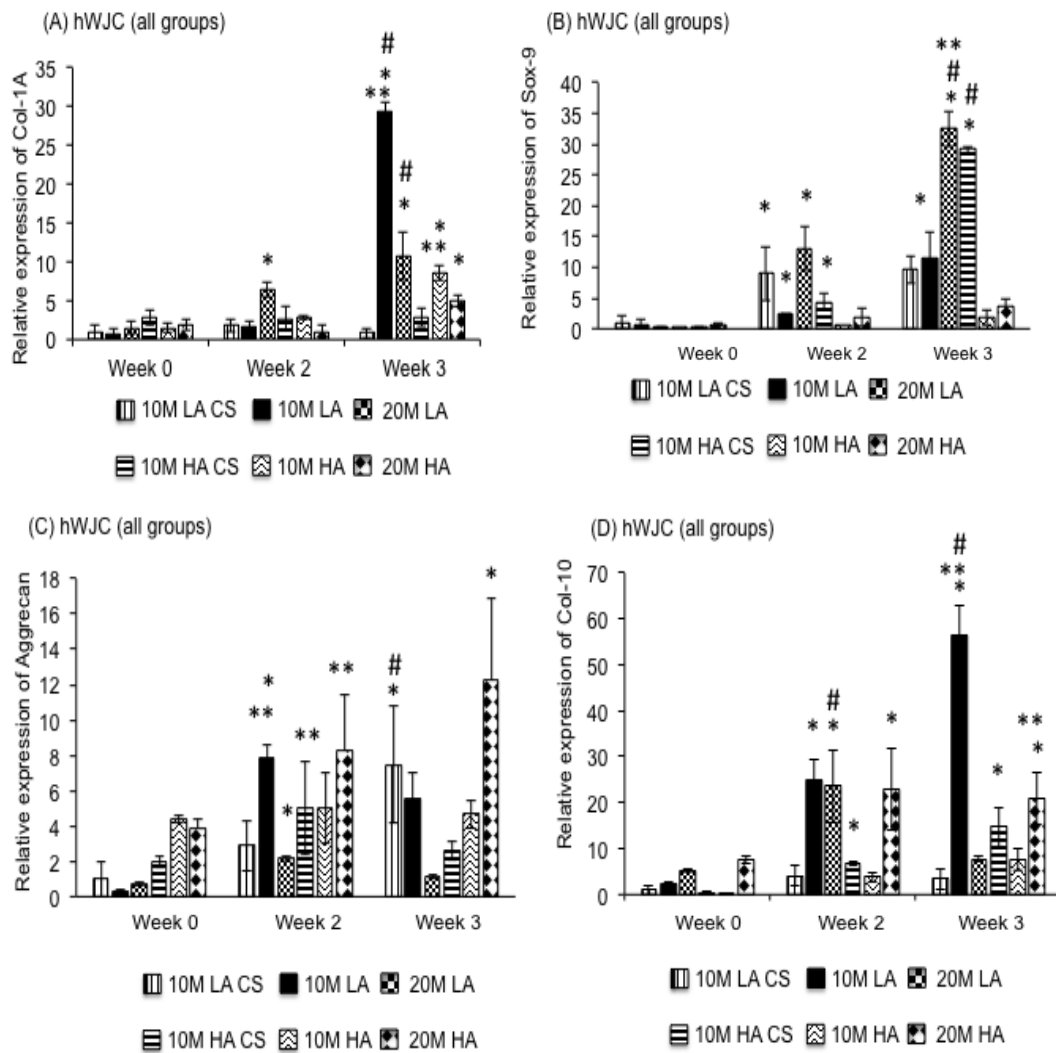
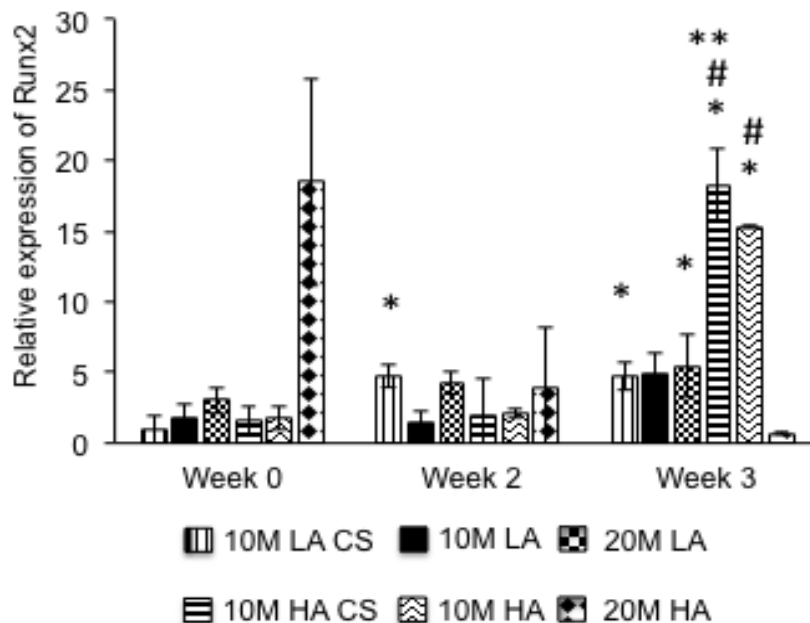


Figure 4.7: Gene expression for all of the rBMSC groups

Gene expression of Collagen I, Aggrecan and SOX9 for rBMSC groups at week 0, 2, and 3. There was significant increase in the SOX9 and Aggrecan value at week 2 and 3 for 20 M HA group, compared to the controls. Values are reported as mean \pm standard deviation, $n=4$. (*) represents statistically significant difference over the week 0 value. (#) represents statistically significant highest value of the group (**) represents statistically significant difference from the control at that time point. ($p < 0.05$).



(E) hWJC (all groups)

**Figure 4.8:** Gene expression for all of the hWJC groups

Gene expression of Collagen I, Aggrecan and SOX9 for hWJC groups at week 0, 2, and 3. There was significant difference in SOX9 and Aggrecan gene expression at week by groups @)M HA and 20 M HA CS groups. Values are reported as mean \pm standard deviation, n=4. (*) represents statistically significant difference over the week 0 value. (#) represents statistically significant highest value of the group (**) represents statistically significant difference from the control at that time point. (p < 0.05).

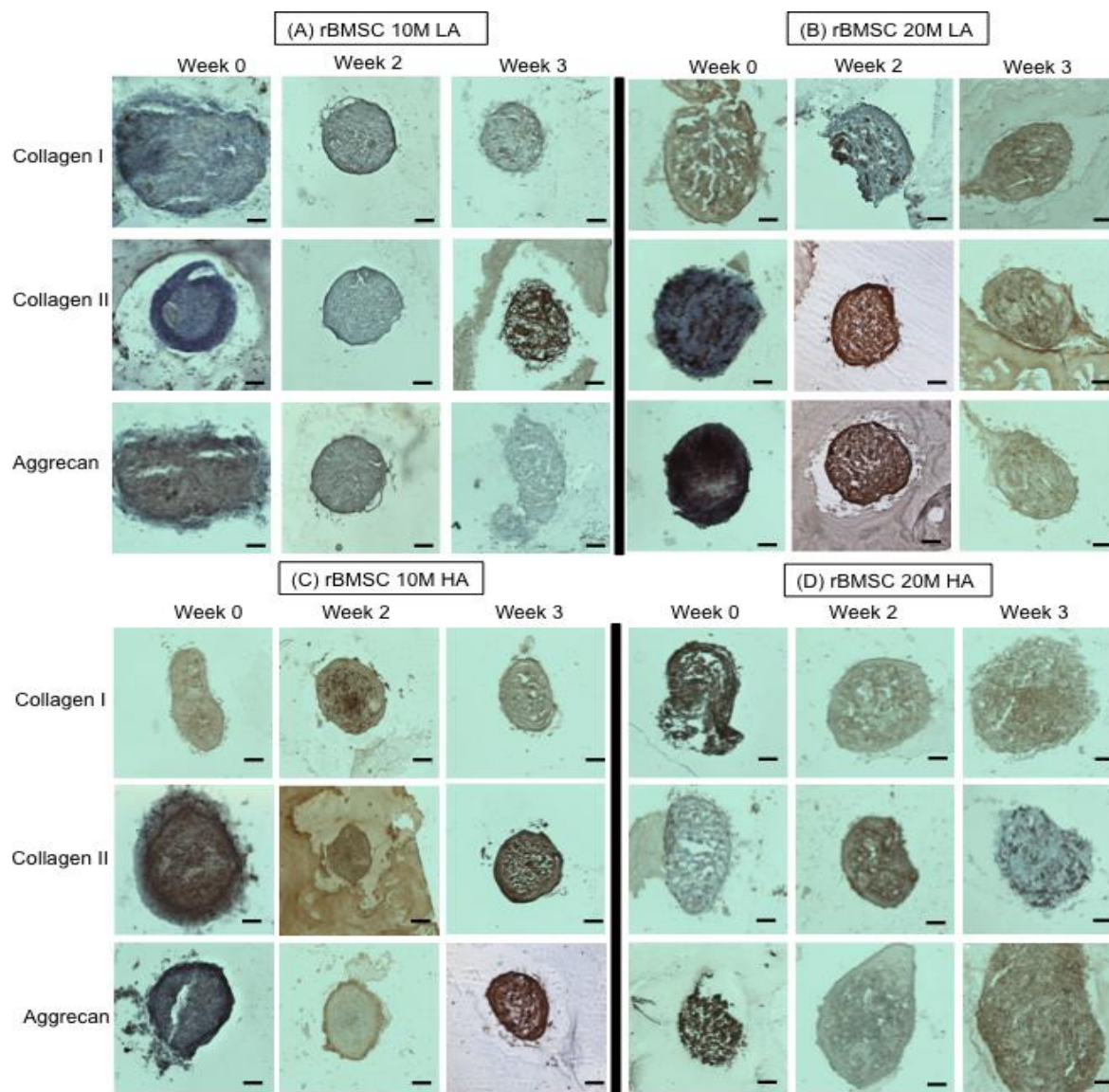


Figure 4.9: Immunohistochemistry for all of the rBMSC groups

Representative images for immunohistochemistry analysis for collagen I, collagen II, and aggrecan staining for rBMSC groups at weeks 0, 2, and 3. At week 2, 20M LA had the most intense staining for collagen II and aggrecan. At week 3, 10M LA had the highest staining intensity at collagen II. Scale bar = 200 μm .

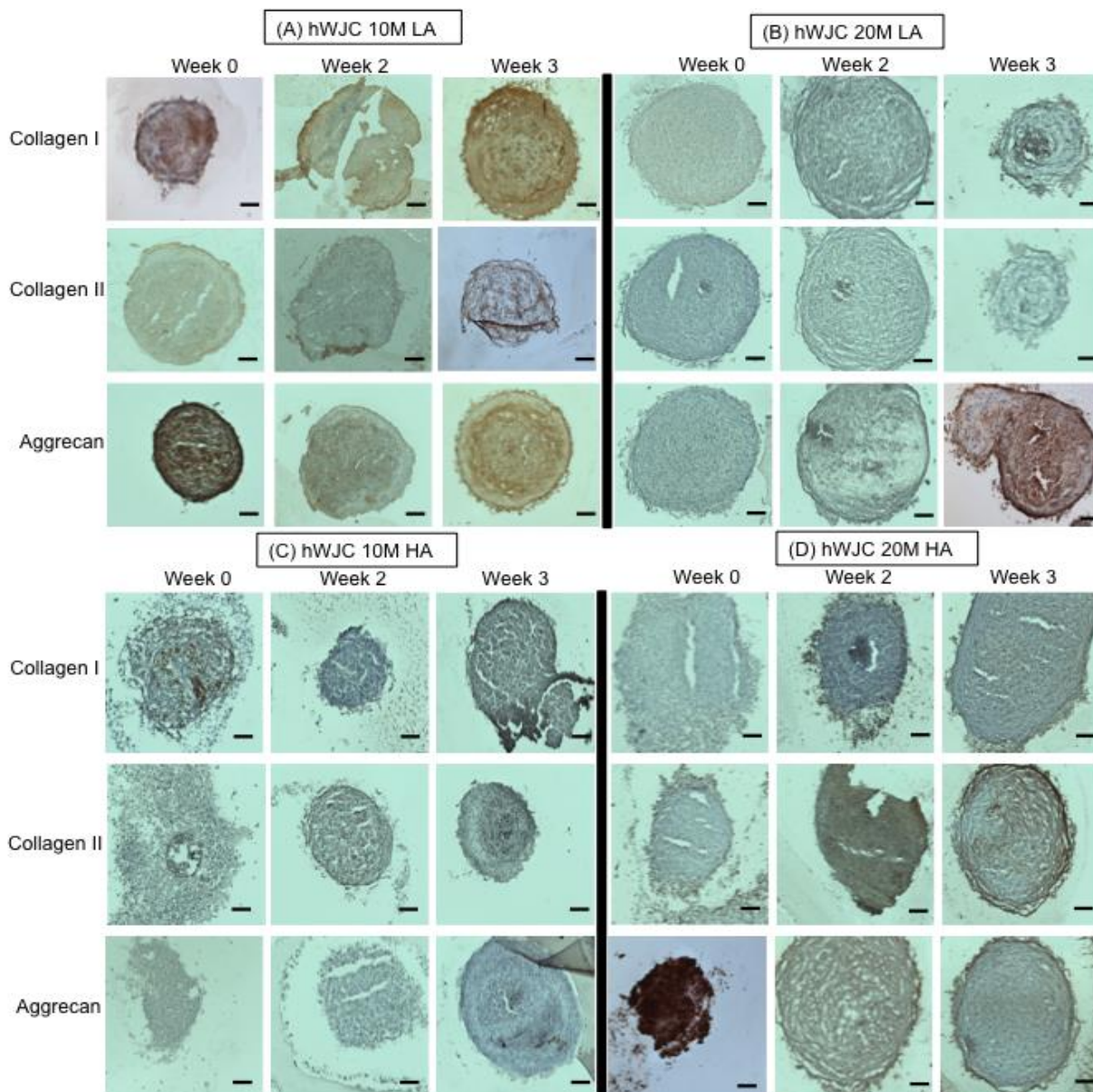


Figure 4.10: Immunohistochemistry for all of the hWJC groups

Representative images for immunohistochemistry analysis for collagen I, collagen II, and aggrecan staining for hWJC groups at weeks 0, 2, and 3. At week 2, 20M LA had the most intense staining for collagen II and aggrecan. At week 3, 10M LA had the highest staining intensity at collagen II. Scale bar = 200 μm .

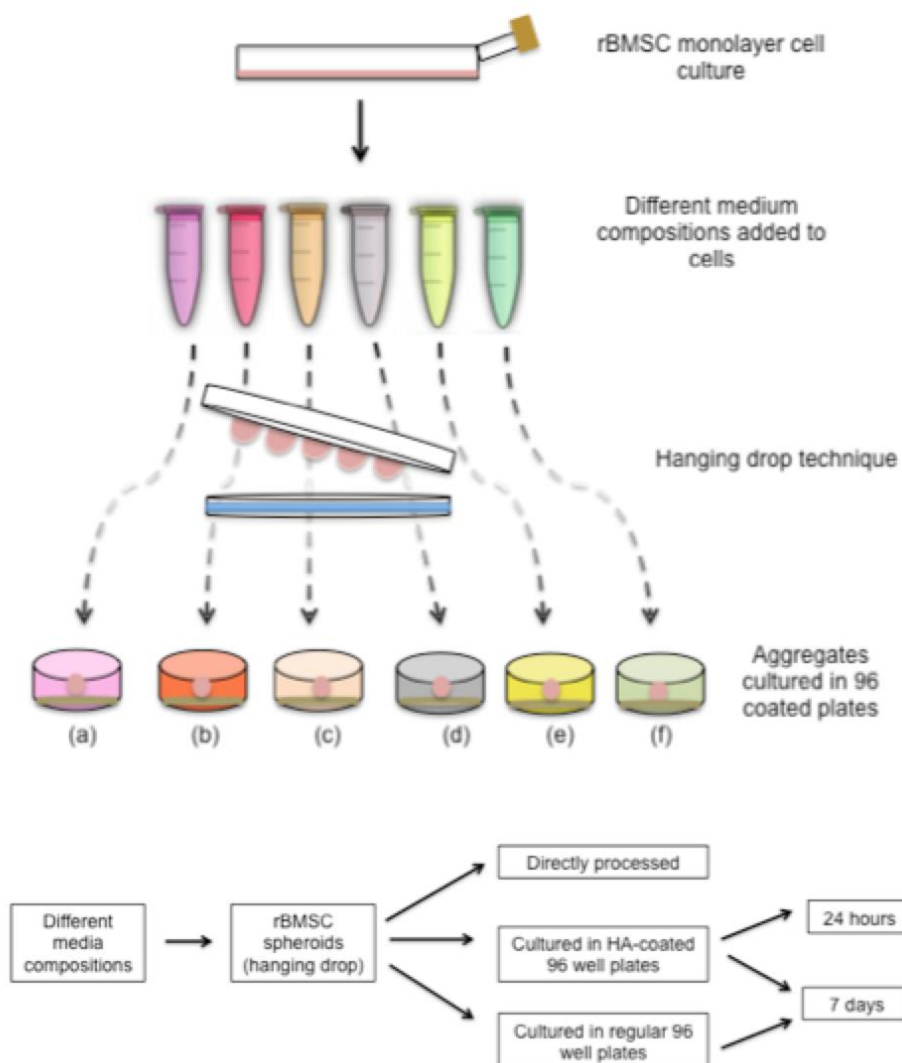


Figure 5.1: Schematic representation of the experimental design

rBMSCs were aggregated via the hanging drop technique and harvested after 24 h. Subsequently, aggregates were plated onto HA-coated 96 well plates and cultured for 0 and 7 days. The individual aggregates were subjected to five different culture medium conditions, namely Dulbecco's modified eagle medium (DMEM) with (a) 5 ng/mL TGF- β_3 , (b) 100 ng/mL IGF, (c) 40 μ g/mL of porcine chondroitin sulfate (d) 40 μ g/mL aggrecan, and (e) control medium (f) TGF/IGF group

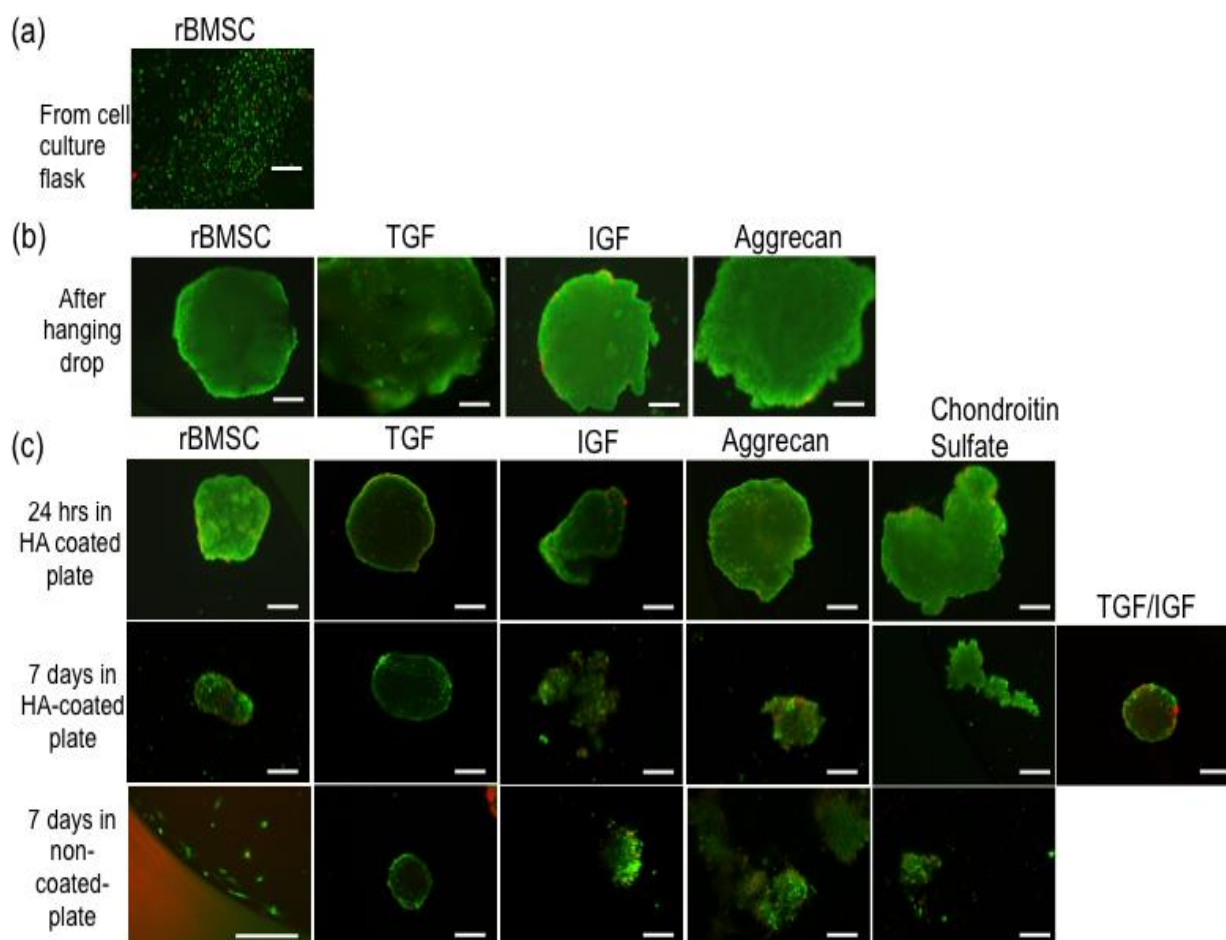


Figure 5.2: Live-dead images for all the different time points

Live/dead images demonstrating cell viability at different time points (a) rBMSC group before aggregate formation, (b) rBMSC aggregates 24 h after hanging drop, (c) 24 h after aggregates were placed in HA coated substrates and 7 days after they are placed in HA-coated or non-coated surface. Scale bar = 100 μ m.

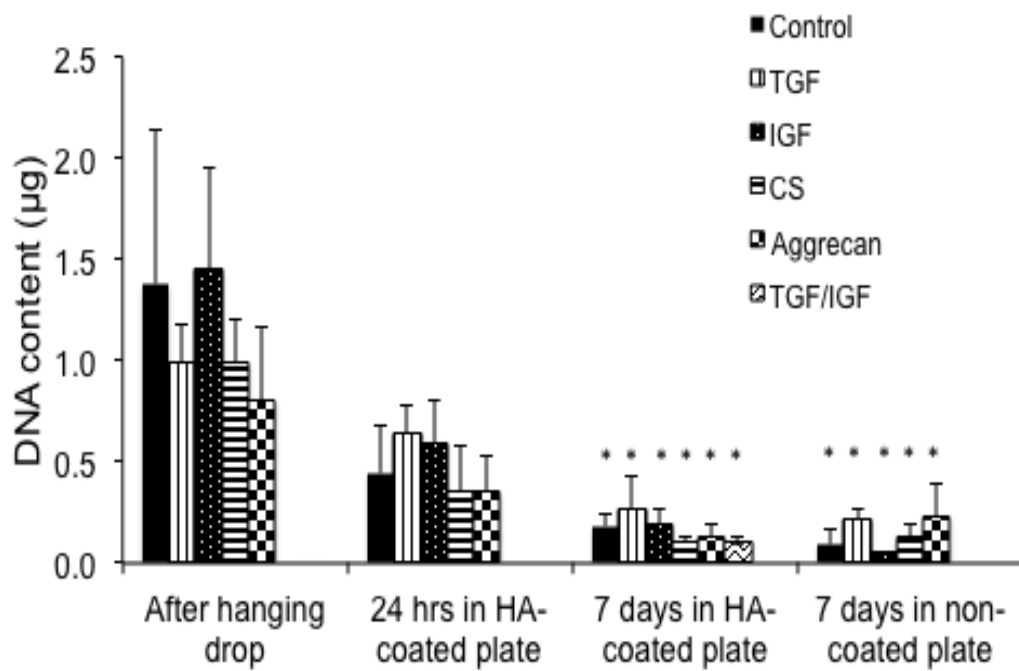


Figure 5.3: DNA content for all of the groups

DNA content analysis of the different groups using the picogreen assay measured at 0 and 7 days. Please note the decrease in DNA content for all of the groups after 7 days of culture. Values are reported as mean \pm standard deviation, $n=4$. (*) represents statistically significant difference from hanging drop time point.

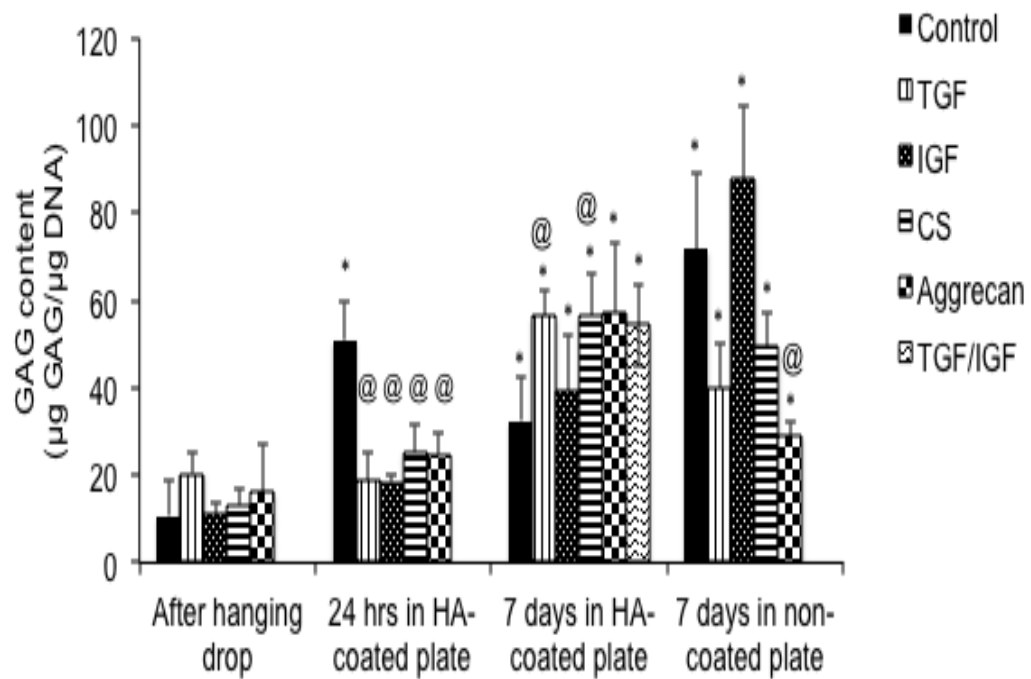


Figure 5.4: Normalized GAG content for all of the groups

Normalized GAG content measured at 0, and 7 days, expressed as GAG/DNA. The IGF group had the highest GAG/DNA content at 7 days non-coated time point. Values are reported as mean \pm standard deviation, $n = 4$. (@) represents statistically significant difference from the control group at that time point and (*) represents statistically significant difference from hanging drop time point.

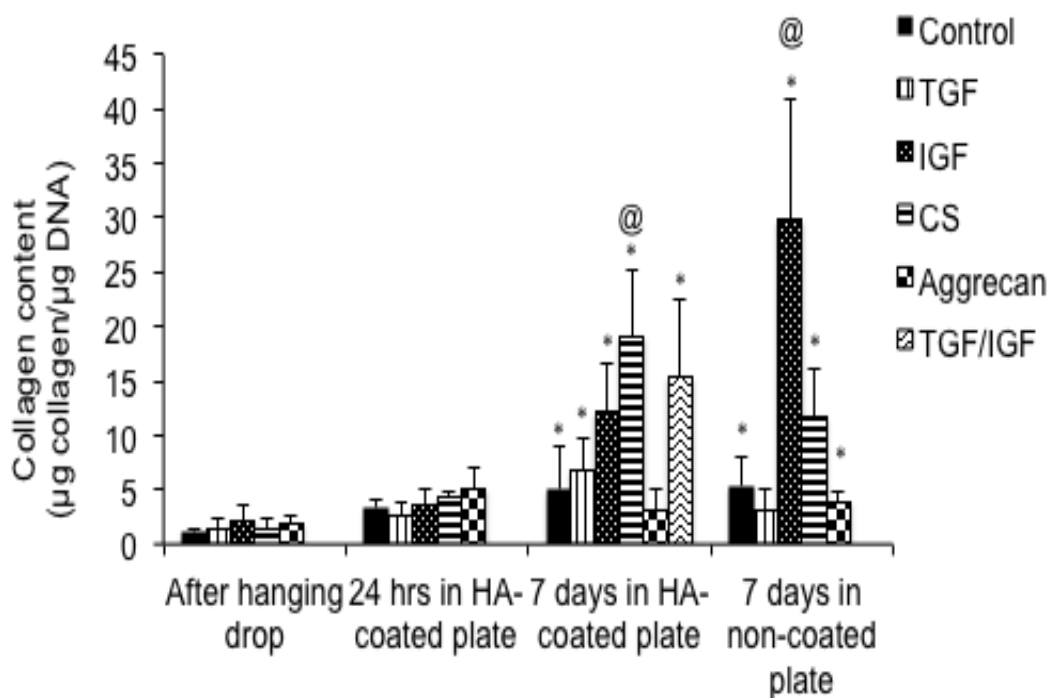


Figure 5.5: Normalized collagen content for all of the groups

Normalized collagen content measured at 0, 7 and 14 days, expressed as collagen/DNA. The IGF group at 7 days non-coated time point, had the highest collagen/DNA content. Values are reported as mean \pm standard deviation, $n = 4$. (@) represents statistically significant difference from the control group at that time point and (*) represents statistically significant difference from hanging drop time point.

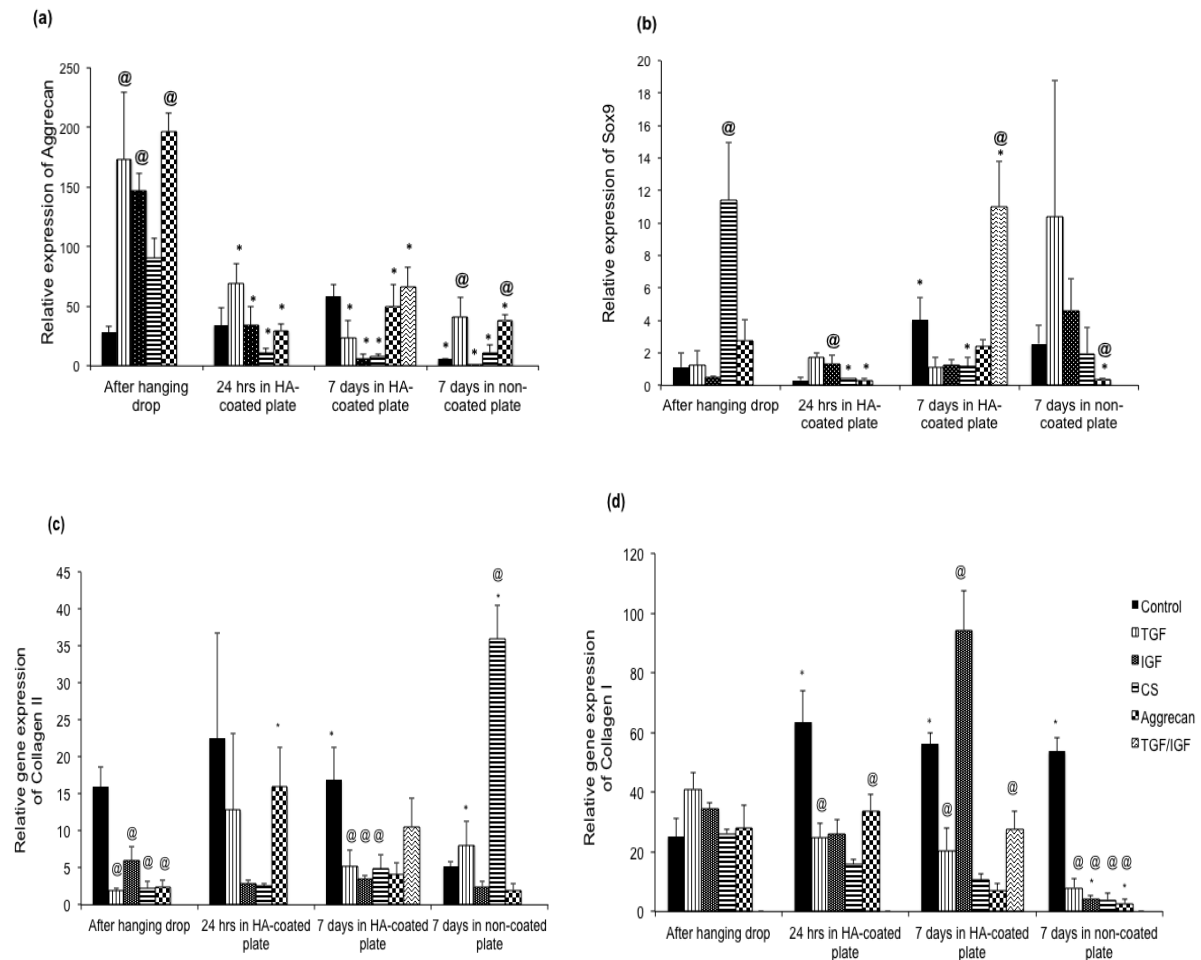


Figure 5.6: Gene expression for all of the groups

Gene expression of Aggrecan, SOX9, collagen I, and collagen II. While aggreacan gene expression was enhanced for hanging drop group, the collagen II and SOX9 gene expression was highest at the 7 day coated/non-coated group. Values are reported as mean \pm standard deviation, $n = 4$. (*) represents statistically significant difference over the week 0 value, (@) represents statistically significant difference from the control group at that time point and (*) represents statistically significant difference from hanging drop time point ($p < 0.05$).

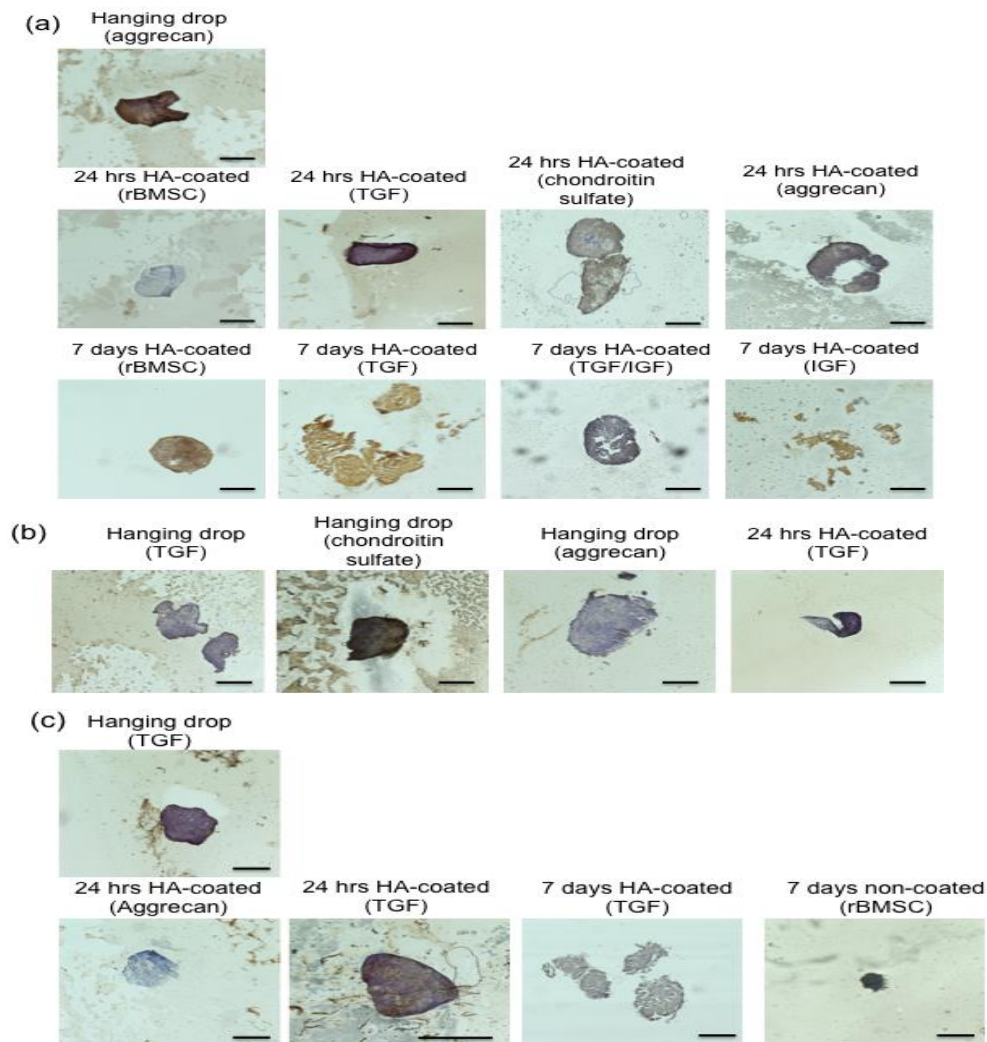


Figure 5.7: Immunohistochemistry for all the rBMSC groups

Representative images for immunohistochemistry analysis for collagen II, collagen I, and aggrecan staining. Scale bars = 150 μm .

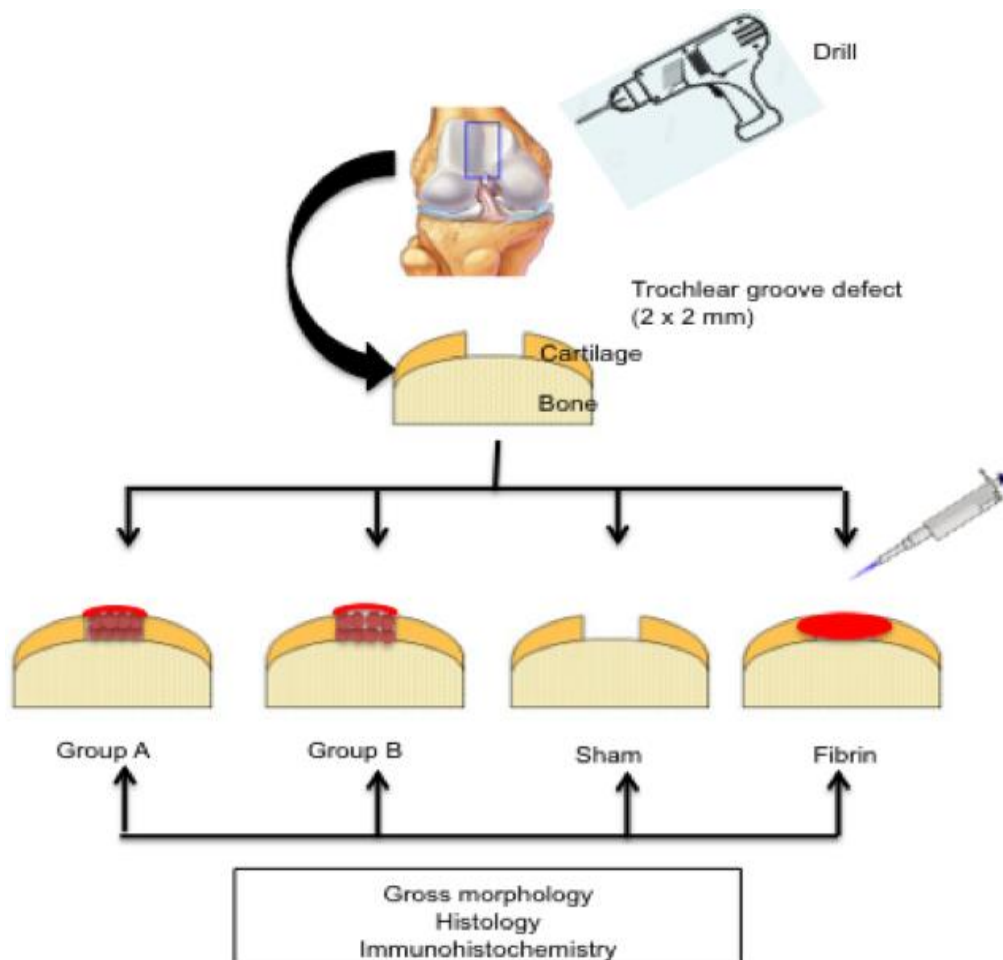


Figure 6.1: Schematic representation of the surgical procedure

After defect creation with a drill bit, the rat knees were subjected to one of four treatments. Group A and Group B refer to the 10 million/mL and 20 million/mL aggregates, respectively. After aggregates were added in the defect area, 50 μ L of fibrin sealant (Tisseel[®]) was additionally added as a topmost layer to form a secured clot. Sham refers to an empty defect without any filling and fibrin Group refers to filling the defect with only Tisseel[®] fibrin sealant.






<u>Rat Number</u>	<u>Left knee</u>	<u>Right knee</u>	
R01	Group A	Sham	<div data-bbox="982 478 1406 569" style="border: 1px solid black; padding: 2px;">Defect at the trochlear groove</div> 
R02	Group A	Fibrin	
R03	Group A	Fibrin	<div data-bbox="982 905 1406 995" style="border: 1px solid black; padding: 2px;">Filled with aggregates and sealed with fibrin</div> 
R04	Group A	Sham	
R05	Group B	Fibrin	<div data-bbox="982 905 1406 995" style="border: 1px solid black; padding: 2px;">Filled with aggregates and sealed with fibrin</div> 
R06	Group B	Sham	
R07	Group B	Fibrin	<div data-bbox="982 905 1406 995" style="border: 1px solid black; padding: 2px;">Filled with aggregates and sealed with fibrin</div> 
R08	Group B	Sham	
R09	Group A	Fibrin	<div data-bbox="982 905 1406 995" style="border: 1px solid black; padding: 2px;">Filled with aggregates and sealed with fibrin</div> 
R10	Group B	Sham	

Figure 6.2: Experimental design and surgery photos

Overall experimental design and photos of the rat trochlear groove, before and after aggregate filling. Note $n = 5$ knees for each Group. To maintain independence of samples within groups, each individual rat received a different group for the left and right knee. Circled region points to surgical area on the trochlear groove.

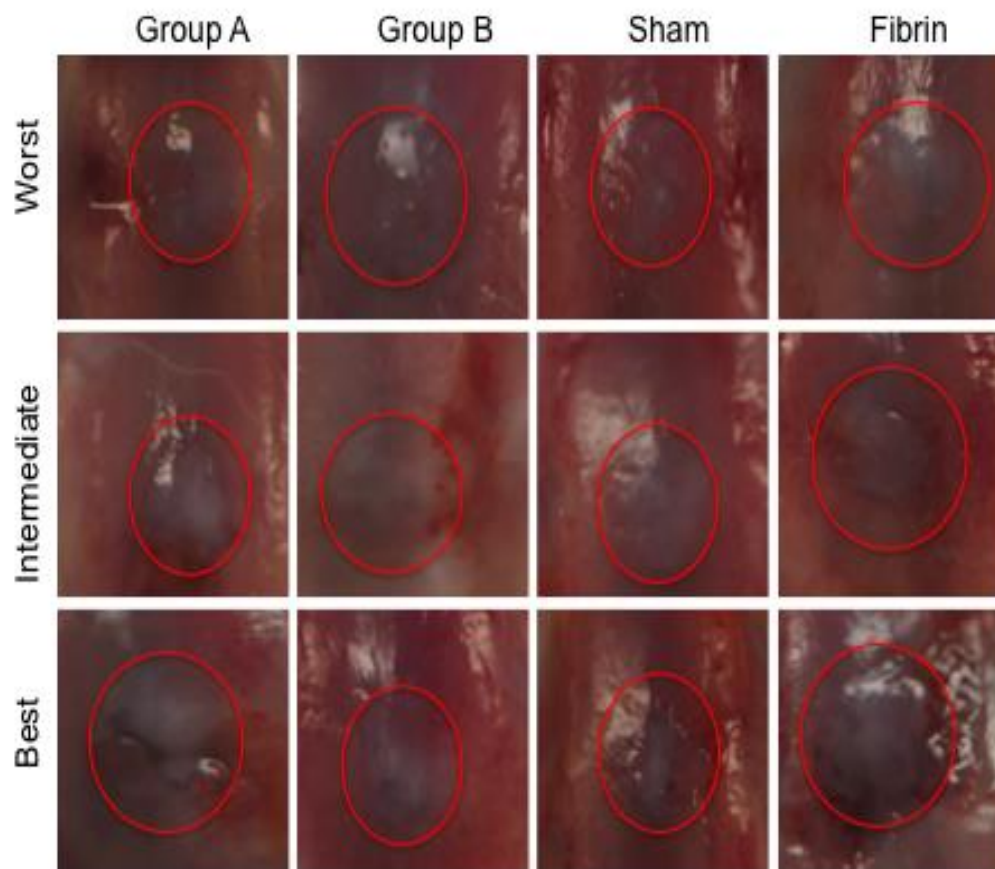


Figure 6.3: Gross morphological images of the different groups

Representative gross morphological images of all the experimental and control Groups. They are divided into three categories based on the relative morphological appearance. The repair tissue was opaque, almost flush to the surface and had smooth or intermediate texture in Group B implants, whereas all of the other groups had opaque, slightly depressed or overgrown surface, with either a rough or intermediate texture at 8 weeks. (Circled region points to the defect area on the trochlear groove on the retrieved knees). Scale bar = 2 mm.

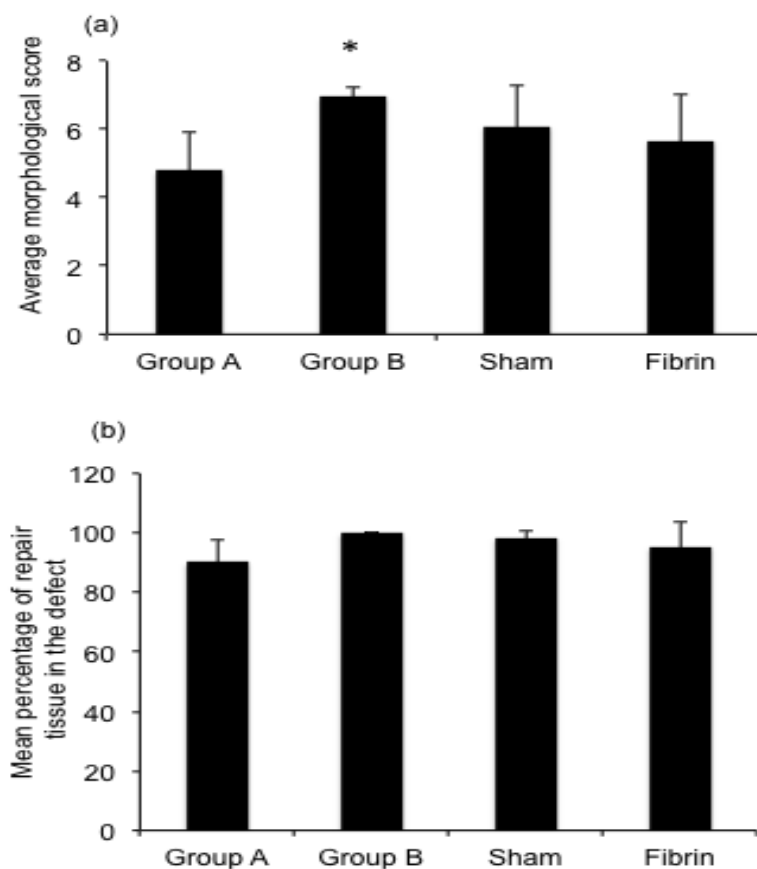


Figure 6.4: Morphological assessment of the rat knees

- (a) Average morphological score of the rat knees. (b) percentage of repair tissue filled at the defect site in for all the groups. Three independent co-authors compiled morphological scores based on parameters in Table 6.2. Average scores are represented as mean \pm standard deviation. The maximum possible score a healthy cartilage can receive is 10. All groups had a sample size of $n=5$. (*) indicates statistically significant difference from Group A.

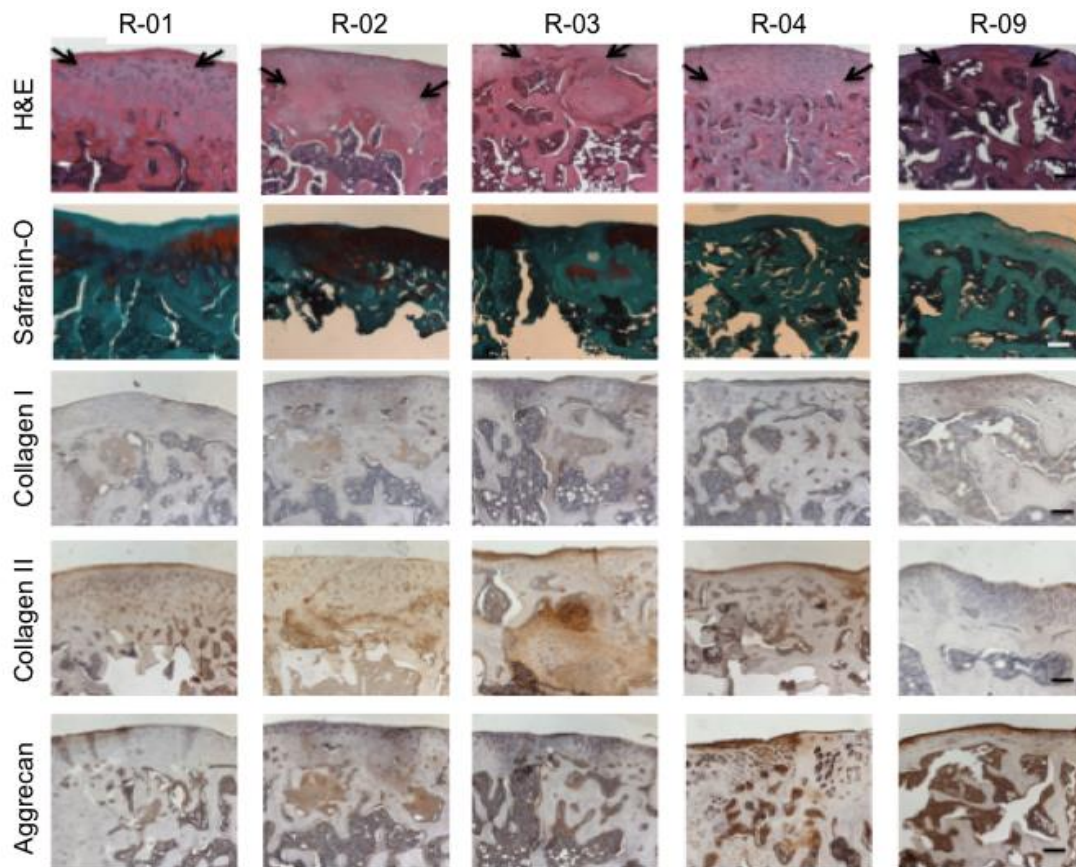


Figure 6.5: Histology and IHC for Group A implants

Histology (H&E, Saf-O) and immunohistochemistry (collagen I, II, and, aggrecan antibody staining) for Group A. Black arrowheads indicate defect region. Numbers on the top refer to the rat number (see Fig. 2). Note that the aggrecan and collagen II staining were most intense for the R04 left knee. Scale bar = 200 μm .

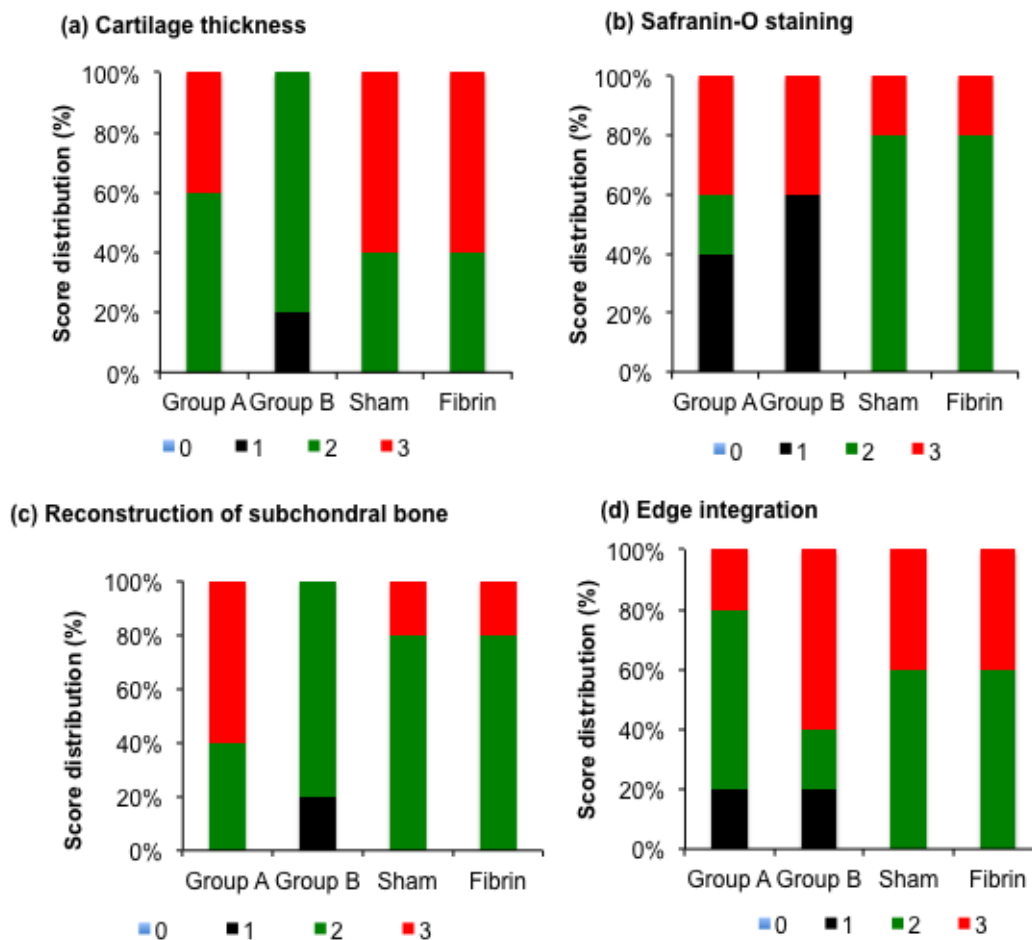


Figure 6.6: Histological score distribution plots

Stacked column plot showing the histological score distribution for (a) cartilage thickness, (b) Safranin O staining, (c) reconstruction of subchondral bone, and (d) edge integration for the newly regenerated tissue at the defect area for 8-week implants. The sections were scored using modified O’Driscoll score as shown in Table 6.3. All groups had a sample size of n=5.

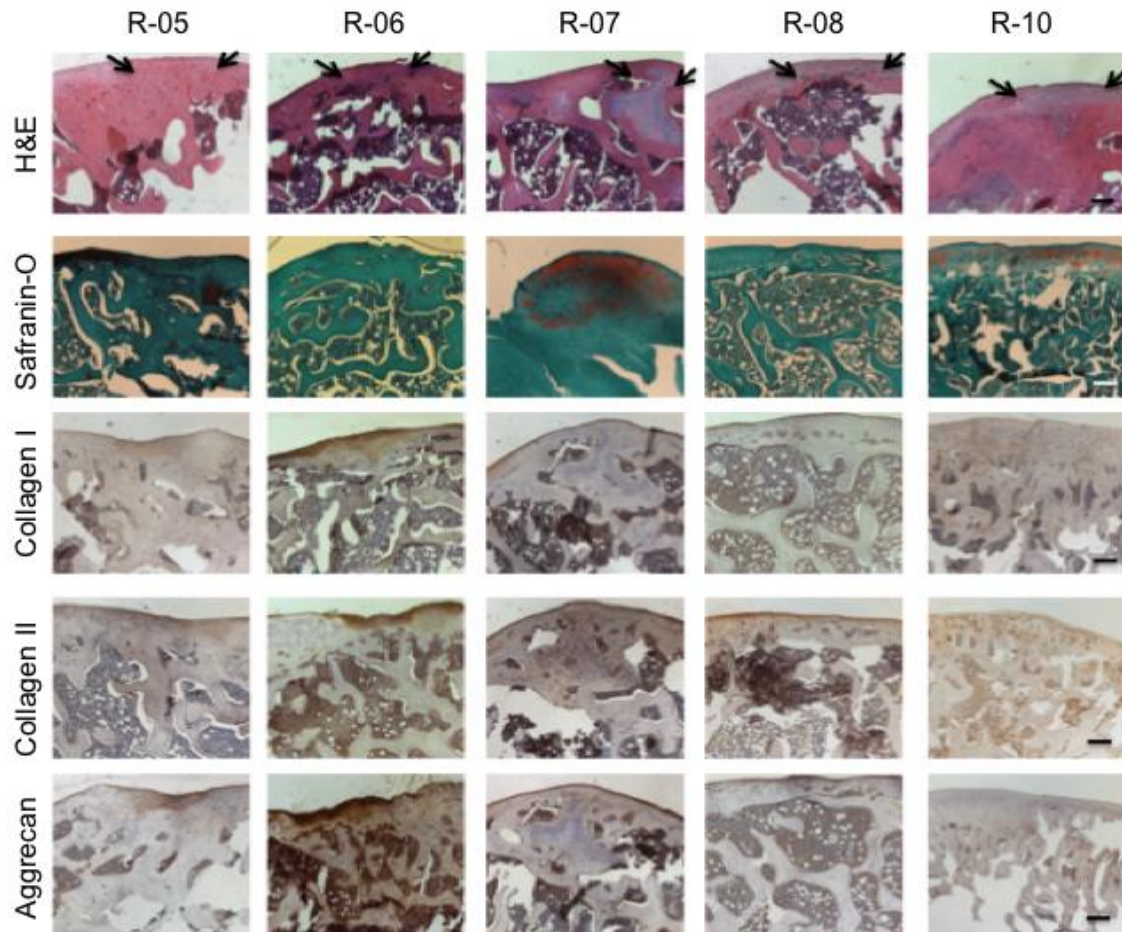


Figure 6.7: Histology and IHC for Group B implants

Histology (H&E, Saf-O) and immunohistochemistry (collagen I, II, and aggrecan antibody staining) for Group B. Black arrowheads indicate defect region. Numbers on the top refer to the rat number (see Fig. 2). Note the more intense stain for collagen II in R06. Scale bar = 200 μ m.

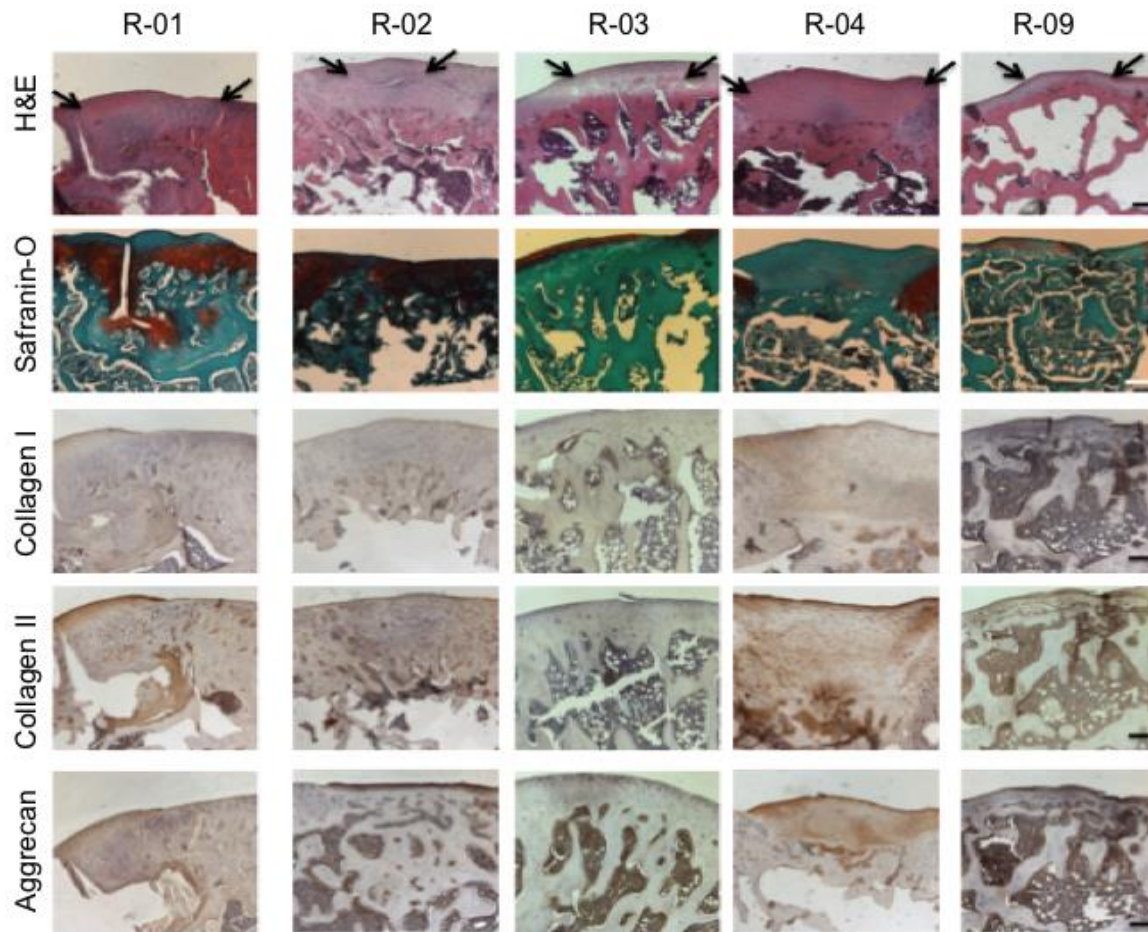


Figure 6.8: Histology and IHC for Fibrin-alone implants

Histology (H&E, Saf-O) and immunohistochemistry (collagen I, II, and aggrecan antibody staining) for the Fibrin group. Black arrowheads indicate defect region. Numbers on the top refer to the rat number (see Fig. 2). Note that the R05 section showed almost zero staining for Saf-O and the bone region for R09 was deeply stained for Saf-O, suggesting neo-cartilage formation. Scale bar = 200 μ m.

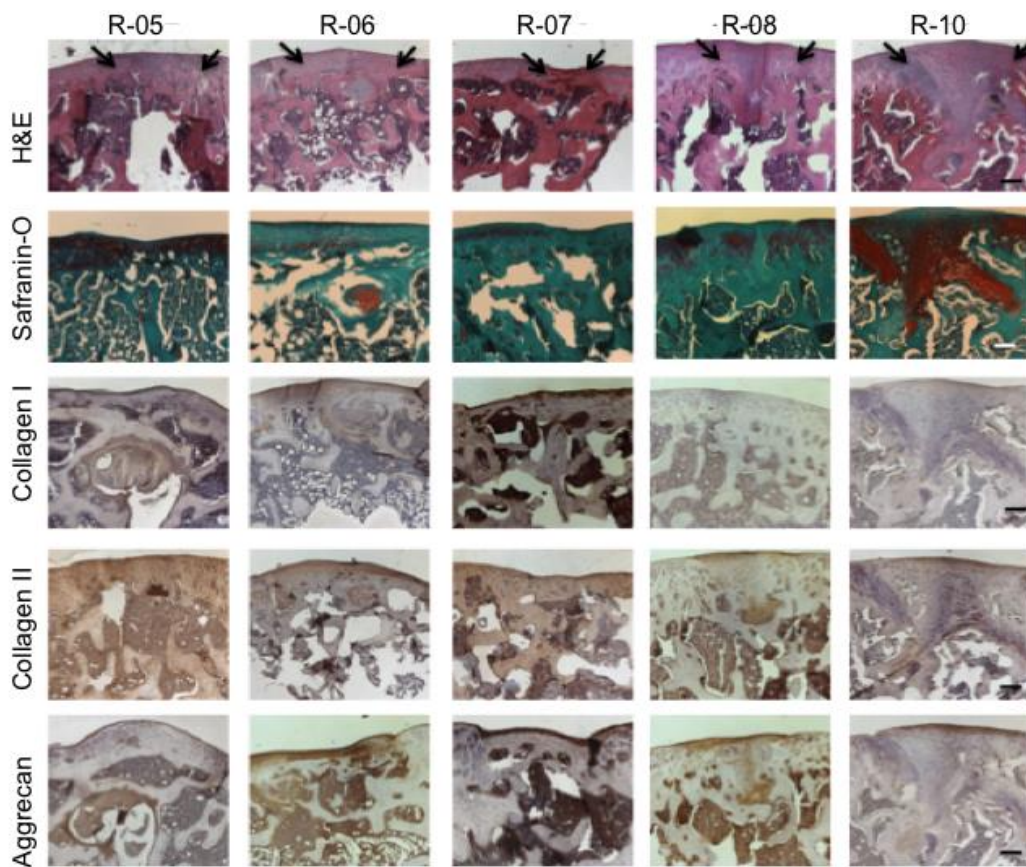


Figure 6.9: Histology and IHC for the sham surgeries

Histology (H&E, Saf-O) and immunohistochemistry (collagen I, II, and, aggrecan antibody staining) for the sham Group. Black arrowheads indicate defect region. Numbers on the top refer to the rat number (see Fig. 2). Note that R01 has a deep crevice on the cartilage surface. Scale bar = 200 μm .

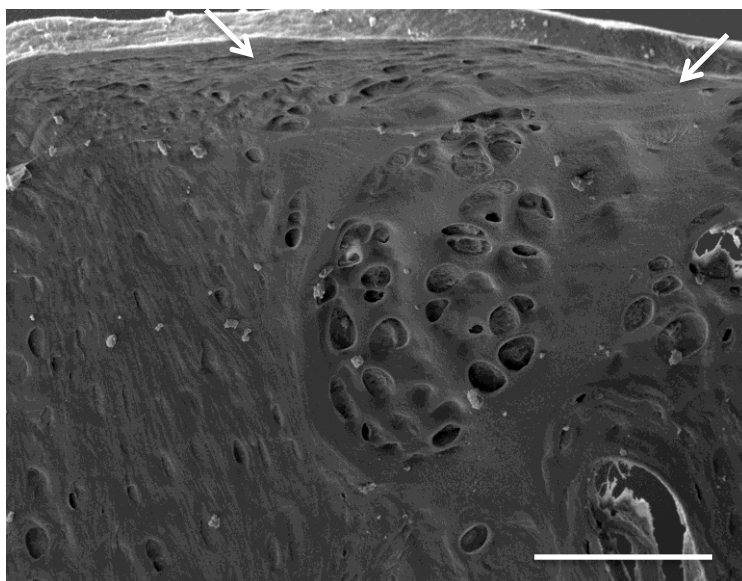


Figure 6.10: Dual-beam microscopic image of the defect area

(FEI Versa, 3D Dual beam, Hillsboro, OR) of rat #4 (R04) left knee (Group A). Scale bar = 200 μm . White arrows mark the two boundaries of the defect area in the osteochondral interface.

APPENDIX B: Tables

CHAPTER 1: No tables.
CHAPTER 2: Tables 2.1 - 2.6
CHAPTER 3: Table 3.1
CHAPTER 4: Tables 4.1 - 4.2
CHAPTER 5: Tables 5.1- 5.3
CHAPTER 6: Table 6.1-6.4
CHAPTER 7: No tables

Table 2.1: List of abbreviations

AC	Articular cartilage
ACI	Autologous chondrocyte implantation
ACL	Anterior cruciate ligament
ASC/ADSC	Adipose derived stem cells
BMI	Body mass index
DMEM	Dulbecco's modified eagle medium
ECM	Extracellular matrix
GMP	Good manufacturing practice
HA	Hyaluronic acid
IGF	Insulin-like growth factor
IKDC	International knee documentation committee
IND	Investigational new drug
KOOS	Knee injury and osteoarthritis information store
MRI	Magnetic resonance imaging
MSC	Mesenchymal stem cells
N/A	Not applicable
NDA	New drug application
OA	Osteoarthritis
OATS	Osteochondral autograft transplantation procedure
OCD	Osteochondritis dissecans
PCL	Polycaprolactone
PDS	Polydioxanone
PEG	Poly(ethylene glycol)
PEO	Polyethyleneoxide
PGA	Polyglycolic acid
PRF	Platelet rich fibrin
PRP	Platelet rich plasma
PLGA	Poly (L-lactic-co-glycolic-acid)
SVF	Stromal vascular fraction
WOMAC	Western Ontario and McMaster universities osteoarthritis index

Table 2.2: List of devices under clinical trials for treating knee focal defects or osteoarthritis (Source: clinicaltrials.gov)

Product	Clinical study center(s)	FDA phase	Technology overview	Material composition	Defect size	Treatment condition	Comparator group
CAIS	Canada	2	Morselized autologous cartilage affixed on resorbable implant using fibrin sealant and implanted back into the knee	Resorbable implant: copolymer of PGA & PCL reinforced with PDS mesh	1-5 cm ²	Osteochondritis dissecans and ICRS grade 3 lesions	MF
Maioregen Surgery	Italy	4	Bioceramic multilayer scaffold composed of deantogenated type 1 equine collagen and magnesium enriched hydroxyapatite	<u>Chondral layer:</u> 100% Type I Collagen, <u>Tide-mark layer:</u> 60% collagen 40% HA, <u>Bone gradient:</u> 30% collagen and 70% HA	2-9 cm ²	Knee osteochondral lesion	MF
HYTOP® graft	Germany	N/A	HYTOP® is typically grafted with debridement or MF	Upper layer of porcine splint skin and lower layer of collagen fleece containing hyaluronan	Width and length: 20x30 mm Thickness: 1.1- 2 mm	Focal chondral defects	None (open-label, single-group safety study)
Matrix encapsulated chondrocytes	Mexico	3	Cells implanted in a collagen scaffold are arthroscopically implanted	6 million cells are implanted in a 10 mm collagen scaffold	1.5-4 cm ²	Focal chondral defects	MF
TruFit CB	EU- mc	4	TruFit CB plugs are implanted into defect regions	TruFit CB: resorbable material composed of PLG copolymer, calcium-sulfate, PGA fibers and surfactant	1 cm ² - 2 cm ²	Single cartilage lesion	MF
Agili C Biphasic implant	EU- mc	4	Graft implanted perpendicular to defect site	<u>Cartilage phase:</u> modified aragonite & HA, <u>bone phase:</u> aragonite	Area < 2 cm ² after debridement, Depth up to 3 mm	Osteochondritis dissecans	Agili C Implant
Denovo ®	USA, Canada	Post-market analysis	A miniarthrotomy is performed and after removal of defective cartilage, the cartilage pieces are implanted and held in place with fibrin sealant	Viable juvenile cartilage pieces held in place with fibrin sealant	Each package fills 2.5 cm ²	Femoral and Patellar Articular Cartilage Lesions	None (open-label, single-group safety study)
Bone Graft	Canada	Pilot; 0	Chondral lesions are filled with Augment Bone Graft	Material: matrix of beta tricalcium phosphate and highly purified recombinant human platelet-derived growth factor	OCD>1 cm ²	Osteochondral defects	None (open-label, single-group safety study)
Chondron™	Republic of Korea	3	Patients implanted with Chondron are analyzed to evaluate device performance	Cell-gel mixture: autologous chondrocytes are mixed with fibrin and cultured for three days	1-15 cm ²	Ankle cartilage defect	None (open-label, single-group safety study)
BST-CarGel	Canada	NA	Chitosan-based matrix which acts like a plug after the ACI procedure	Cytocompatible liquid chitosan solution at physiological pH	No specific size mentioned	Focal articular cartilage defects	MF

Table 2.3: List of biologic products under clinical trials for treating knee focal defects or osteoarthritis (Source: clinicaltrials.gov)

Company/ Institute Name	Product	Clinical Study Center(s)	FDA phase	Technology Overview	Treatment condition	Comparator group
Medipost Co Ltd	CARTISTE M®	USA	1,2	Human umbilical cord mesenchymal stem cells are mixed with biopolymer solution	Full-thickness Grade 3-4 Articular Cartilage Defects of the Knee	MF
Royan Institute	N/A	Islamic Republic of Iran	1	Single intra- articular injection of MSC	Osteoarthritis	Placebo injection
TissueGen e Inc.	TG-C	USA	2	MSC injections of different cell concentration	Osteoarthritis	Placebo injection
Taipei medical university and Wanfang hospital	PRF	Taipei, Taiwan	N/A	PRP injection, following success in pig model	Knee meniscal repair	None (open-label, single- group safety study)
The Catholic University of Korea	N/A	Korea	1,2	PRP injection, second injection after 4 weeks	Degenerative Chondropathy, early osteoarthritis	None (open-label, single- group safety study)
Stanford University	ASC	USA	1	Fibrin glue, dermal matrix and ADSC cells	Degenerative Lesion of Articular Cartilage	MF
University of Marsielle	Arthroscopi c Marrow cells with protein injection	France	0	Autologous cells are isolated and mixed with patient's protein and injected	Defect of Articular Cartilage	None (open-label, single- group safety study)
Red de terapia celular	MSV	Spain	1,2	ACI followed by MSC injections	Osteoarthritis of grade II-IV	Intra-articular injection of 60 mg hyaluronan
University Hospital, Basel, Switzerlan d	N/A	Switzerland	1	Nasal cartilage is isolated, grown on collagen type I/III membrane and implanted in knee	One or two full- thickness cartilage defects	None (open-label, single- group safety study)
Hospital Znojmo	PRP	Czech Republic	N/A	9 PRP injections administered over a duration of 1 year	Grade II or III chondromalacia	None (open-label, single- group safety study)
Exactech, Inc	BiCRI	Taiwan	3	1 or 2 scaffolds were place in condyles	Focal Chondral and Osteochondral Lesions	MF
ISTO Inc	Revaflex	USA	3	Decellularized neo- cartilage scaffolds are implanted in defect	Articular cartilage lesions in the femur	MF
Tigenix	Chondrocel ect	Europe- mc	3	ACI performed along with Chondrocelect that isolated cartilage specific cells	Cartilage single lesion	ACI

Histogenics	Neocart	USA- mc	3	ACI performed and cells are seeded on scaffolds and re-implanted in knee	Articular cartilage defects	MF
University of Jordan	MSC and platelet lysate injection	Jordan	2	Intra-articular injection of MSC and/or platelet lysate	Moderate/severe articular injury	None (open-label, single-group safety study)
Istituto Ortopedico Rizzoli	PRP	Italy		PRP versus viscosupplementation with Hyalubrix	Early Knee Articular Degenerative Pathology	None (open-label, single-group safety study)
Fondren Orthopedic Group	N/A	USA	N/A	ASC isolated from fat pad and injected into defect site	arthritis	MF
University of Columbia-Missouri, Arthrex	Biocartilage	USA	FDA approved augmentation to microfracture	Microfracture and Biocartilage versus Microfracture	Defect of Articular Cartilage	MF
Tetec AG	NOVOCART 3D	Germany	3	Autologous cells are mixed with novocart and implanted into patients	Articular cartilage lesion	MF
Stempeutics Research Private Ltd	N/A	India	2	Ex- vivo cultured adult allogeneic MSCs	Osteoarthritis	Plasma Lysate
University Hospital, Montpellier	N/A	France, Germany	1	Autologous adipose derived stem cells administered for intra-articular use	Moderate or severe osteoarthritis	None (open-label, single-group safety study)
Cytori Inc.	Celution® device	USA-mc	1	Idiopathic osteoarthritic patients are administered an intra-articular administration of Celution processed Adipose Derived Regenerative Cells	Osteoarthritis	Placebo injection
StemGene x	SVF injection	USA- mc	N/A	Impact of Stromal Vascular Fat on joint pain and functionality due to osteoarthritis	Osteoarthritis	N/A - Observational study

Table 2.4: List of drug products under clinical trials for treating knee focal defects or osteoarthritis (Source: clinicaltrials.gov)

Company/ Institute Name	Product	Clinical Study Center(s)	FDA phase	Technology Overview	Treatment condition	Comparator Group
Shetty-Kim research foundation	PRP	UK	NA	Effectiveness of PRP injection	Early Cartilage Defects	Hyaluronic acid injection
Orthotrophix	TPX-100	USA	2	Intra-articular injection of TPX-100 (chondrogenic peptide)	Bilateral osteoarthritis	None (open- label, single- group safety study)
Merck kGaA	AS90233 0	EU- mc	1	AS902330 injection into knee defect	Primary osteoarthritis of the knee and Kellgren- Lawrence Grade 2 or 3	Placebo
Universidad Nacional de Rosario	12.5% dextrose injection	Argentina	2,3	Arthroscopic injection of 1 glucose injection at 1,2,3 months	Stage IV Knee Osteoarthritis	None (open- label, single- group safety study)
Hospital Universitario Dr. Jose E. Gonzalez	PRP	Mexico	N/A	PRP injection given every two weeks for 6 weeks	Mild knee osteoarthritis	None (open- label, single- group safety study)
Bioiberica	Condros an	Canada	3	Injection of chondroitin sulfate	Osteoarthritis	Placebo
Nantes University Hospital	Hydrogel with MSCs	France	NA	Blood, bone marrow and Hoffa's fat pad samplings during surgical intervention	Osteoarthritis	None (open- label, single- group safety study)
Genzyme	Synvisc	USA	Approve d	Hylan G-F 20 (Synvisc) is an FDA- approved hyaluronate derivative used to treat knee OA	Symptomatic knee osteoarthritis	Placebo
Novocart@3D Plus	Tetec AG	Germany	3	Combination of autologous cells in a biphasic 3D collagen- based matrix	Traumatic Articular Cartilage Defects	MF
The First Affiliated Hospital of Anhui University of Traditional Chinese Medicine	Xinfeng capsule	China	China Health Authorit y	Traditional chinese herbal medicine Xinfeng capsule	Osteoarthritis	Glucosamine Sulfate
Biomet	APDD- 33-00	USA	2	Autologous protein solution delivered as an intra-articular injection for patients who have failed at least one conservative OA therapy	Osteoarthritis	Placebo
Kyunghee University Medical Center	WIN-34B	Korea	Korean- FDA phase 2	Herbal drug used to treat inflammation	Osteoarthritis	Placebo

Table 2.5: Common inclusion and exclusion criteria to determine eligibility of the study cohort. The values are specific to osteoarthritis, focal lesions of the cartilage, osteoarthritis and osteochondritis dissecans disease pathology. (Source: clinicaltrials.gov)

Common Inclusion Parameters:

1. Age: Commonly 18-50
2. Approved and signed IRB consent of the subject (includes ability to read, understand and write)
3. Willingness to participate in post-op rehabilitation and clinical assays
4. Normal BMI (≤ 35)
5. Willingness to use more than 1 contraceptive device for childbearing aged women
6. Clinically normal hematology and serum values
7. Contralateral knee to be asymptomatic and functional
8. Intact meniscus on both the knees
9. Lesion region should be fillable by implant graft , if used
10. Defect grade: usually grade-III or grade- IV Kellergen Lawrence
11. Defect dimension requirements (size, diameter and depth) corresponding to a particular study

Table 2.5 (continued)**Common Exclusion Parameters:**

1. Pregnant or nursing women
2. History of malignancy or exposure to radiation
3. Autoimmune diseases (including rheumatoid arthritis) and immunocompromised patients
4. Allergy to drugs such as penicillin, acetaminophen, aspirin, ibuprofen, gentamycin, streptomycin, polymyxin B sulfate
5. Allergy to calcium phosphates, bovine serum or animal protein as described in the product
6. BMI > 35
7. Currently enrolled in other clinical studies
8. Current or history of alcoholism and/or drug abuse
9. Previous hyaluronic acid, PRP injection or microfracture technique.
10. Abnormal level of liver enzymes, thyroid level, hepatitis and anti-coagulant therapy
11. Hemoglobin level too low and a very low platelet count
12. Undergone ACL in the last one year or rehabilitation in the last 6 months
13. No history of knee fracture
14. Patellofemoral instability
15. Multiple or kissing lesions
16. For treating lesions: patients must not have previous OA conditions
17. Knee instability, bipolar articular cartilage defect, and axis alignment of tibial spines
18. Anything that restricts MRI imaging (metallic implants or pacemakers in body, gadolinium allergy)
19. Very high performance athletes who cannot ambulate for 20-30 minutes a day
20. No Amotrophic Lateral Sclerosis or Multiple Sclerosis

Table 2.6: Food and Drug Administration Approval Pathways for Cartilage Repair Products
(from McGowan et al. ¹⁶⁶)

FDA Classification	Responsible Center	Submission route	Clinical Trial category
1. Drug	Center for Drug Evaluation & Research (CDER)	New Drug Application (NDA)	Investigational New Drug (IND)
2. Device	Center for Devices and Radiological Health (CDRH)	Pre-Market Application (PMA)*	Investigational Device Exemption (IDE)
3. Biologic	Center for Biologics Evaluation and Research (CBER)	Biologics Licensing Application (BLA)	IND
4. Combination product	Lead center determined after request for designation (RFD)	Determined by Lead Center	IND/ or IDE

Table 3.1: List of the experimental groups and their abbreviations used in the manuscript

Group name	Abbreviation	Weight (per 100 g)
1. 50:50 PLGA + CS + NaHCO ₃	CS group	77.5:20:2.5
2. 50:50 PLGA	CS control	100
3. 75:25 PLGA + β -TCP	TCP group	90:10
3. 75:25 PLGA	TCP control	100

Table 4.1: Explanation of the different experimental groups used in the study and their abbreviations.

Study Group	Abbreviation	Control Group	Abbreviation
1. rBMSC		1. rBMSC	
10 million/mL aggregates (1-4)	10M LA (lower aggregates/ scaffold)	10 million/mL cell suspension (1-4)	10M LA CS
10 million/mL aggregates (5-7)	10M HA (higher aggregates/ scaffold)	10 million/mL cell suspension (5-7)	10M HA CS
20 million/mL aggregates (1-4)	20M LA	20 million/mL cell suspension (1-4)	10M LA CS
20 million/mL aggregates (5-7)	20M HA	20 million/mL cell suspension (5-7)	10M HA CS
2. hWJC		2. hWJC	
10 million/mL aggregates (1-4)	10M LA (lower aggregates/ scaffold)	10 million/mL cell suspension (1-4)	10M LA CS
10 million/mL aggregates (5-7)	10M HA (higher aggregates/ scaffold)	10 million/mL cell suspension (5-7)	10M HA CS
20 million/mL aggregates (1-4)	20M LA	Group not included	Group not included
20 million/mL aggregates (5-7)	20M HA	Group not included	Group not included

Table 4.2: Summary of the best performing groups for all the functional assays.

Desirable property	Cell type	Best performing group	Time point (weeks)
1. Cell viability	rBMSC	20M LA CS	0
	hWJC	20M LA CS	0
2. DNA per scaffold	rBMSC	20M HA	2
	hWJC	10M HA	0
3. GAG per DNA	rBMSC	20M HA	3
	hWJC	10M HA	2
4. Collagen per DNA	rBMSC	20M HA	3
	hWJC	20M HA	0
5. Collagen II and aggrecan gene expression	rBMSC	20M HA 10M LA	2 and 3
	hWJC	20M HA 20M LA 10M HA CS	3, 3, and 3
6. Collagen II and aggrecan antibody staining	rBMSC	10M LA 20M LA 10M HA	2, 2, and 3
	hWJC	10M LA 20M HA	0 and 0

Table 5.1: Description of the experimental group and time points.

Groups	Time points	Medium composition	Abbreviation
After hanging drop	NA	rBMSC medium (α MEM with 10% FBS) TGF β_3 (5 ng/mL) IGF (100 ng/mL) Aggrecan (40 μ g/mL) Chondroitin sulfate (40 μ g/mL)	rBMSC TGF IGF Aggrecan Chondroitin sulfate
Spheroids in HA coated 96 well-plate	(i) 24 h after plating (ii) 7 days after plating	rBMSC medium (α MEM with 10% FBS) TGF β_3 (5 ng/mL) IGF (100 ng/mL) Aggrecan (40 μ g/mL) Chondroitin sulfate (40 μ g/mL) TGF β_3 (5 ng/mL) for 3 days and IGF (100 ng/mL) for 4 days	rBMSC TGF IGF Aggrecan Chondroitin sulfate TGF/IGF
Spheroids in non-coated 96 well-plates	7 days after plating	rBMSC medium (α MEM with 10% FBS) TGF β_3 (5 ng/mL) IGF (100 ng/mL) Aggrecan (40 μ g/mL) Chondroitin sulfate (40 μ g/mL)	rBMSC TGF IGF Aggrecan Chondroitin sulfate

Table 5.2: Summary of the best performing groups for each assay

Desirable property	Best performing group(s)	Time point
Cell viability	TGF β_3 , aggrecan	Hanging drop
DNA content	rBMSC, IGF	Hanging drop
GAG/DNA content	IGF	7 days non-coated well plate
Collagen/DNA content	IGF	7 days non-coated well plate
Aggrecan gene expression	Aggrecan	Hanging drop
SOX9 gene expression	Chondroitin sulfate, TGF/IGF	Hanging drop and 7 day HA-coated well plated
Collagen I gene expression	IGF	7 day HA-coated well plated
Collagen II gene expression	Chondroitin sulfate	7 days non-coated well plate

Table 5.3: List of the antibodies and dilutions used for immunohistochemistry

Primary Antibody	Dilution	Vendor	Catalog number
Anti-collagen I, rabbit IgG polyclonal	1:200	Abcam	AB24133
Anti-collagen II, rabbit IgG polyclonal	1:200	Abcam	AB116142
Anti-aggrecan, rabbit IgG polyclonal	1:50	Abcam	AB36861

Table 6.1: List of primary antibodies with dilution and vendor information

Primary Antibody	Dilution	Vendor	Catalog number
Anti-collagen I, rabbit IgG polyclonal	1/200	Abcam	AB24133
Anti-collagen II, rabbit IgG polyclonal	1/200	Abcam	AB116142
Anti-aggrecan, rabbit IgG polyclonal	1/100	Abcam	AB36861

Table 6.2: Scoring card for morphological analysis of the retrieved implants

Gross morphological parameter	Scoring rubric
Repair tissue	Full=2, partial=1, none=0
Edge integration	Full=2, partial=1, none=0
Smoothness of repair tissue	Smooth=2, intermediate=1, rough/missing=0
Surface degree of filling	Flush=2, slight depression=1, depressed/overgrown=0
Color of cartilage	Opaque=2, translucent=1, missing=1
<u>Total morphological score</u>	Sum total of the above values
<u>Amount of repair tissue to total area (%)</u>	Amount of repair tissue relative to total area of defect % present in the defect

Table 6.3: Histology scoring parameters and associated numeric score. The grading system was modified from the previously reported system of O'Driscoll *et al.*¹⁹⁷.

Feature	Score
Safranin O staining	
Normal to nearly normal	3
Moderate	2
Slight	1
None	0
Cartilage thickness	
100% of normal adjacent cartilage	3
75%-100% of normal adjacent cartilage	2
50%-75% of normal adjacent cartilage	1
0%-50% of normal adjacent cartilage	0
Reconstruction of subchondral bone	
Normal	3
Reduced subchondral bone reconstruction	2
Minimal subchondral bone reconstruction	1
No subchondral bone reconstruction	0
Edge integration	
Smooth and intact	3
Superficial horizontal lamination	2
Fissures	1
Severe disruption, including fibrillation	0

Table 6.4: Animal ID and the weight of each animal at the time of implantation and after 8 weeks.

Animal ID	Weight in grams (time of surgery)	Weight in grams (time of death)
R01	248	527
R02	258	587
R03	230	397
R04	243	429
R05	268	575
R06	259	547
R07	258	550
R08	229	606
R09	254	470
R10	247	483